Book of Abstracts

Proceedings of the 2021 International Congress on Structural Integrity and Maintenance (SIM2021)

Preface

The first edition of the SIM 2021 congress gathers more than 90 participants from more than 10 nationalities, demonstrating the diversity of this new event. At this moment, the SIM 2021 1st edition will occur in a virtual format (April 08th and 09th, 2021) due to disorders caused by the COVID-19 pandemic situation. Hopefully, the conference 2nd edition will take place in person on 5 and 6 October 2021, in Belo Horizonte/Brazil.

The International Congress on Structural Integrity and Maintenance (SIM 2021) is organized by Federal University of Minas Gerais (UFMG, Brazil), Institute for R&D in Structures and Construction (CONSTRUCT, FEUP, Portugal) and University of São Paulo (USP, Brazil). The purpose of this conference is to bring together academic researchers and scholars, as well as engineers from the construction sector to exchange and share their innovative research results and practical experiences on all aspects of Structural Integrity, Design and Maintenance. Then, the participants will have the opportunity to view and share the recent advances related to the following themes: structural integrity, fatigue, fracture, damage mechanics, structural design, advanced construction materials, design of all civil engineering structures types, building information modelling (BIM), artificial intelligence applied to design, safety and risk analysis, structural retrofit and maintenance, probabilistic assessment of structures, management and life-cycle performance, and construction sector management. This event also covers subjects related to computational and numerical modelling of a wide range of infrastructures, such as engineer technical systems, transportation systems, bridges, buildings, dams, railways, underground constructions, wind and transmission towers, offshore platforms, pipelines, naval vessels and ocean structures. It is expected contributions from engineers, metallurgists, material scientists, and other professionals, allowing a significant multidisciplinary discussion.

The Organizing Committee of the SIM 2021 immensely acknowledges all members of the Advisory and Scientific Committees for their conference support, the Plenary Speakers and Sessions Chairmen for their knowledge and dedication, all the authors that contributed to the success of the event with their great presentations, and the sponsors for their important contributions. Finally, a word of appreciation for the Organizing Committee members as well as students and other UFMG/USP/FEUP staff for their tireless support.

Organization

Chair

Hermes Carvalho, Federal University of Minas Gerais, Brazil

Co-chairs

José António Correia, University of Porto, Portugal
Pedro Aires Montenegro, University of Porto, Portugal
Rui Calçada, University of Porto, Portugal
Tulio Nogueira Bittencourt, São Paulo University, Brazil
Tiago Fazeres Ferradosa, University of Porto, Portugal

Organizing Committee

Hermes Carvalho, Federal University of Minas Gerais, Brazil (Chairman)
José António Correia, University of Porto, Portugal (Chairman)
Pedro Aires Montenegro, University of Porto, Portugal (Chairman)
Rui Calçada, University of Porto, Portugal (Chairman)
Tulio Nogueira Bittencourt, São Paulo University, Brazil (Chairman)
Tiago Fazeres Ferradosa, University of Porto, Portugal (Chairman)
Rodrigo Barreto Caldas, Federal University of Minas Gerais, Brazil
Ana Lydia Castro e Reis, Federal University of Minas Gerais, Brazil
Paula Moura Leite Vilela, Federal University of Minas Gerais, Brazil
João Victor Fragoso Dias, Federal University of Minas Gerais, Brazil
José Guilherme Santos da Silva, State University of Rio de Janeiro, Brazil
João Paulo Correia Rodrigues, University of Coimbra, Portugal
Diogo Ribeiro, Porto School of Engineering, Portugal
José Miguel Castro, University of Porto, Portugal

Scientific Committee

A. Martín-Meizoso, University of Navarra, Spain
Abdul Rashid Dar, National Institute of Technology Srinagar, India
Abílio M.P. de Jesus, University of Porto, Portugal
Acir Mércio Loredo-Souza, Federal University of Rio Grande do Sul, Brazil
Adão da Fonseca, University of Porto, Portugal
Alain Nussbaumer, Swiss Federal Institute of Technology in Lausanne, Switzerland
Aleksandar Sedmak, University of Belgrade, Serbia

Alessio Pipinato, Pipinato & Partners, University of Padova, Italy
Alexandre Cury, Federal University Juiz de Fora, Brazil
Alexandre Queiroz Bracarense, Federal University of Minas Gerais, Brazil
Alfonso Fernández-Canteli, University of Oviedo, Spain
Alfredo P. C. Neto, University of São Paulo, Brazil
Andreas Schörghofer-Queiroz, Graz University of Technology, Austria
Andrei Kotousov, The University of Adelaide, Australia
António Reis, Grid International, University of Lisbon, Portugal
Ariel Rodriguez Arias, Federal University of Minas Gerais, Brazil
Arlene Maria Cunha Sarmanho, Federal University of Ouro Preto, Brazil
Armando Cesar Campos Lavall, Federal University of Minas Gerais, Brazil
Ayhan Ince, Concordia University, Canada
Behrooz Keshtegar, University of Zabol, Iran
Carlos Oliveira, Polytechnic Institute of Viana do Castelo, Portugal
Carlos Rebelo, University of Coimbra, Portugal
Chao Jiang, Hunan University, China
Chengwei Fei, Fudan University, China
Cristiana Reis, University of Trás os Montes e Douro, Portugal
Dariusz Rozumek, Opole University of Technology, Poland
David Ángel Cendón Franco, Universidad Politécnica de Madrid, Spain
David Greiner, SIANI/University of Las Palmas, Spain
Debiao Meng, University of Electronic Science and Technology of China, China
Dianyin Hu, Beihang University, China
Dimitrios Pavlou, University of Stavanger, Norway
Eduardo M. B. Campello, University of São Paulo, Brazil
Ehsan Noroozinejad, Graduate University of Advanced Technology, Iran
Elena Fedorova, ICT SB RAS, Krasnoyarsk Branch Office, Siberian Federal University, Russia
Elias Kassa, Norwegian University of Science and Technology, Norway
Estevam Barbosa de Las Casas, Federal University of Minas Gerais, Brazil
Evgeniia Georgievskaia, JSC NPO CKTI, Russia
Fabricio Longhi Bolina, Unisinos, Brasil
Filippo Berto, Norwegian University of Science and Technology, Norway
Francesco Lacoviello, University of Cassino e del Lazio Meridionale, Italy
Francisco Carlos Rodrigues, Federal University of Minas Gerais, Brazil
Gustavo de Souza Veríssimo, Federal University of Viçosa, Brazil
Grzegorz Lesiuk, Wroclaw University of Technology, Poland
Guian Qian, State Key Laboratory of Nonlinear Mechanics – Chinese Academy of Sciences, China
Haohui Xin, Delft University of Technology, Netherlands
Hermes Carvalho, Federal University of Minas Gerais, Brazil
Helena Gervásio, University of Coimbra, Portugal
Hermano Souza, University of Coimbra, Portugal
Hernán Pinto Arancet, Pontifical Catholic University of Valparaíso, Chile
Hojjat Adeli, Ohio State University, USA
Hryhoriy Nykyforchyn, Ukrainian Academy of Science, Ukraine
Humberto Varum, University of Porto, Portugal
Ian Burges, The University of Sheffield
Jian-Feng Wen, East China University of Science and Technology, China

Roberto Brighenti, University of Parma, Italy
Rodrigo Falcão Moreira, Porto School of Engineering, Portugal
Rui Liu, China Academy of Engineering Physics, China
Rui Martins, University of Nova de Lisboa, Portugal
Sabrina Vantadori, University of Parma, Italy
Sergio Blason, Federal Institute for Materials Research and Testing, Germany
Sergio Cicero Gonzalez, University of Cantabria, Spain
Shengchuan Wu, State Key Laboratory of Traction Power – Southwest Jiaotong University, China
Shun-Peng Zhu, University of Electronic Science and Technology of China, China
Stanislav Seitl, Czech Academy of Sciences, Czech Republic
Stéphane Sire, University of Brest, France
Sudath C. Siriwardane, University of Stavanger, Norway
Thomas Ummenhofer, Karlsruhe Institute of Technology, Germany
Tomasz Nowakowski, Wroclaw University of Science and Technology, Poland
Trayana Tankova, University of Coimbra, Portugal
Vinicius Alves, Federal University of Ouro Preto, Brazil
Vladimir Moskvichev, Institute of Computational Technologies SB RAS, Russia
Wojciech Błażejewski, Wroclaw University of Science and Technology, Poland
Xavier Romão, University of Porto, Portugal
Xiancheng Zhang, East China University of Science and Technology, China
Yury Matvienko, Institute of the Russian, Academy of Sciences, Russia
Yury Petrov, St-Petersburg State University, Russia
Zbigniew Marciniak, Opole University of Technology, Poland
Zacarias M. Chamberlain Pravia, University of Passo Fundo, Brazil
Zhongxiang Liu, Virginia Tech, USA

Institutional Supporters

Index

Notch and size effects in metal fatigue: recent advances

Shun-Peng Zhu [a]

[a] *University of Electronic Science and Technology of China, China*

ABSTRACT

Notch features commonly exist in engineering components, which generally act as stress raisers and thus present significant influences on the component strength and life, and are more remarkable under complex loading paths. Also, structural components with different scales normally show different fatigue behaviors. Accordingly, numerous theories and approaches have been developed to address both notch and size effects in metal fatigue as well as damage modelling and life predictions, which aim to provide theoretical support for structural optimal design and integrity evaluation. This speech recalls recent developments and achievements in notch fatigue modelling and analysis of metals under size effects. In particular, recent commonly used methods for fatigue evaluation of metallic notched parts under size effect are summarized and elaborated, including local stress-strain approaches, and critical distance theories as well as weighting control parameters-based approaches, which intend to provide a reference for further research on notch fatigue analysis and promote the integration and/or development among different approaches for practice.

Some modeling aspects for retrofitting and decommissioning activities in offshore environment

Nicholas Fantuzzi[a]

[a]*University of Bologna, Italy*

ABSTRACT

Offshore structures are known to be used for extracting natural gas and oil from the sea bed. However, when the underground source finishes, these structures should be moved to another location or removed if they have reached their design life.

Removal operations go under the name of decommissioning which is a multidisciplinary process by which a Company decides on how to shut down the field activities at the end of the structure life: plugging and abandoning the well(s), making the equipment/installation safe, remove some or all the facilities and restoring the area.

Decommissioning will occur at different stages of asset lifecycle and has wide relevance in terms of reputation, so it needs to be managed properly as a dedicated business process.

Nevertheless, another solution might be considered: change the future working life of these platforms by involving renewable energy and transforming them, for instance, into offshore wind towers.

This activity involves retrofitting activities in order to strengthen the original structural elements in order to carry new loads. All the aforementioned operations involve structural modeling which can be carried out at global and local scales. Such degrees of complexity might be time consuming for Companies that in general have limited time to make decisions in the initial phases of these operations and want to save money. Therefore, in this talk some modeling aspects for retrofitting and decommissioning activities will be discussed.

Structural Integrity Assessment of the Railway Infrastructure

Rui Calçada[a]

[a] *University of Porto, Portugal.*

ABSTRACT

Long-term operation of bridge steel and fatigue crack growth modelling based on energy approach

Grzegorz LESIUK[1]

[a] *Wroclaw University of Science and Technology, Department of Mechanics, Materials and Biomedical Engineering, Smoluchowskiego 25 St, PL-50370 Wrocław, Poland*
**Corresponding author: Grzegorz.Lesiuk@pwr.edu.pl*

Keywords: energy model, degradation, S355 steel, puddle iron, mixed-mode loading conditions, fatigue crack growth rate, crack closure phenomenon

ABSTRACT

Fatigue and fracture are the two main (more than 70% of all failures) phenomena responsible for the structural damage in steel structures subjected to cyclic loads. The main difficulty in describing of the fatigue crack growth rate in mathematical terms is the incomplete understanding the nature of this process in various material groups under different loading conditions (constant amplitude, random loads, single and multi-axial loads, etc.), One of the reasons for this inadequacy is the effect of mean stress expressed by e.g. by the R-stress ratio. The main goal of this lecture is to define new Crack Driving Force (CDF) as an invariant quantity in fatigue crack growth process. During the lecture, it will be proposed a method for description of fatigue crack growth regarding mixed-mode loading condition (I+II, I+III) in the range of elastic-plastic fracture mechanics based on new strain energy density parameter ΔS* (Fig.1.) expressed as a combination of J integral values. The fracture properties and fatigue crack growth results for 19th-century puddle iron are presented and compared with typical Kinetic Fatigue Fracture Diagram (KFFD) constructing methods. The presented results for fatigue crack growth rate description under mode I using $\Delta K_{applied}$ approach and $\Delta K_{effective}$ approach differs significantly using variable mean stress effect – R-ratio (0.05; 0.7). As it was demonstrated, the hysteresis loop analyses allow to obtain the estimated crack closure level. From the engineering point of view, there is a strong need for generalization of the KFFDs description using mean stress robust parameter involving local crack tip behavior for old puddle iron.

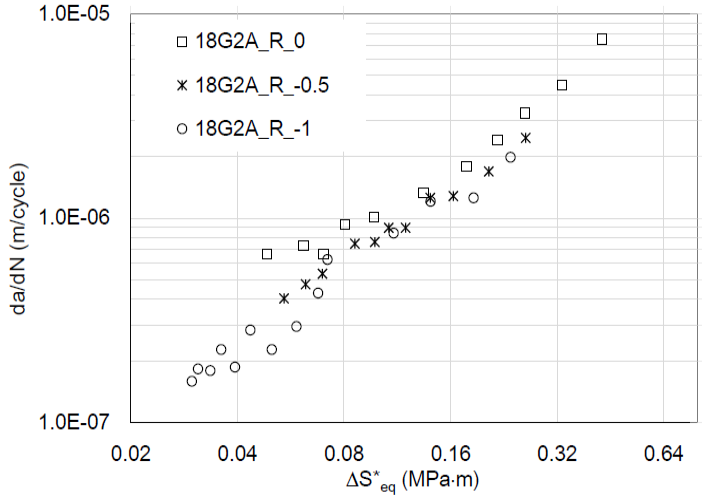

Fig.1. Kinetic Fatigue Fracture Diagram for S355 grade steel based on J-ΔS* strain energy density parameter

Recent advances on fatigue reliability of wind turbine: A review

Ding Liao[a, b], Shun-Peng Zhu[a, *], José Correia[b, *], Abílio De Jesus[b], Rui Calçada[b]

[a]*School of Mechanical and Electrical Engineering, University of Electronic Science and Technology of China, China*
[b]*Faculty of Engineering, University of Porto, Portugal*
**Corresponding author: zspeng2007@uestc.edu.cn, jacorreia@fe.up.pt*

Keywords: wind turbine; fatigue; reliability analysis; uncertainty; load variation.

ABSTRACT

Energy shortage and environmental degradation are two major crises facing human survival and social development. As reported in BP Statistical Review of World Energy 2019 [1], in the global structure of energy consumption today, renewable energy accounts for less than 20%. At present, fossil power, including coal, oil, and natural gas, is still dominant. However, they are after all non-renewable, and are gradually draining away with the long-term exploitation and utilization; in addition, a large amounts of greenhouse gases and certain harmful gases produce when they burn, which will cause greenhouse effect as well as great pollution to the environment.

To avoid problems such as energy depletion and environmental pollution, it's an imperative duty to find efficient and sustainable clean energies to replace traditional energies. Among new energy sources, wind energy which generates power from air flaw, holds superiorities of clean, pollution-free, and sustainable [2]. Compared with hydropower and photovoltaics, its installation is flexible and only requires a very short construction period with tiny environmental impacts; particularly, it has a huge reservation worldwide. However, the Global Wind Energy Outlook published by the Global Wind Energy Council shows that the utilization rate of wind resources is generally low, which is a burning question [3]. Vigorously developing wind power generation is of great significance to the promotion and application of clean energy and the sustainable development of the world.

With the increasing attention on sustainable development, energetic efforts were made by governments to promote and develop clean energies, industries of power generation with new energies is currently undergoing a long process of transition from a supporting role to a leading role. As a new energy source, wind energy is renewable energy with the most large-scale development and utilization prospects in the near future. In recent years, plenty of development plans and incentive policies have been formulated to accelerate technological improvement and market tapping in this field. The global installed gross capacity of wind power steadily increases year by year [4], see Fig. 1.

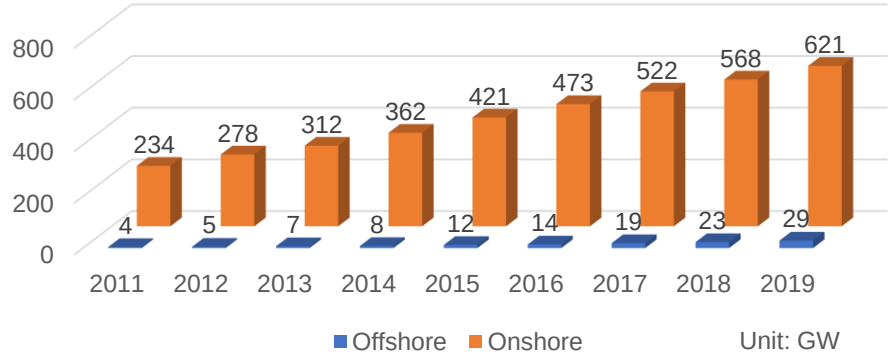

Fig. 1 Global installed gross capacity of wind power [4].

Note from Fig. 1, comparing with onshore wind turbines, offshore wind turbines only take a smaller percentage in gross capacity. But with the shortage of land sources as well as the situation that the locations with good wind fields are using up with the development of the wind power industry, it can be expected that more offshore wind turbines will be built in the foreseeable future [5].

However, wind power is not the only option, which also faces competition with other renewable energy branches. Consequently, the main focus for wind turbine manufacturers and operators is how to increase the reliability of wind turbines and to decrease their cost. Probabilistic fatigue design of wind turbines is a new approach to optimize the design by reducing in reliability- and cost-optimal ways the total cost of manufacturing, operation, and maintenance, ultimately reducing the cost of energy [6, 7]. This paper systematically reviews the state-of-the-art on fatigue reliability of wind turbines, elaborates the method evolution in wind load uncertainty modeling, and the fatigue reliability analysis techniques on three typical components, intending to provide references for future development in this field.

REFERENCES

[1] B. Dudley, "BP Statistical Review of World Energy 2019: An unsustainable path," London, 2019.
[2] J. Firestone, "Wind energy: A human challenge," Science, vol. 366, no. 6470, pp. 1206–1206, 2019.
[3] S. Sawyer, S. Teske, S. Shukla, and L. Fried, "Global Wind Energy Outlook 2014," Brussels, 2014.
[4] Wind Energy Professional Committee of Chinese Renewable Energy Society, Wind Machinery Branch of China Agricultural Machinery Industry Association, and China National Renewable Energy Centre, "Statistics Briefing on Wind Power Hoisting Capacity in China, 2019," Beijing, 2019.
[5] P. Tavner, Offshore wind turbines: Reliability, availability and maintenance. London: The Institution of Engineering and Technology, 2012.
[6] P. S. Veers, H. J. Sutherland, and T. D. Ashwill, "Fatigue life variability and reliability analysis of a wind turbine blade," Albuquerque, 1991.
[7] W. B. Dong, T. Moan, and Z. Gao, "Fatigue reliability analysis of the jacket support structure for offshore wind turbine considering the effect of corrosion and inspection," Reliab. Eng. Syst. Saf., vol. 106, pp. 11–27, 2012.

ACKNOWLEDGMENTS

Financial support of the National Natural Science Foundation of China (No. 11972110 and 11672070), Sichuan Provincial Key Research and Development Program (No. 2019YFG0348), Science and Technology Program of Guangzhou, China (No. 201904010463) and Fundamental Research Funds for the Central Universities (No. ZYGX2019J040) are acknowledged. This research was also supported by the project grant (UTA-EXPL/IET/0111/2019) SOS - Wind Energy - Sustainable Reuse of Decommissioned Offshore Jacket Platforms for Offshore Wind Energy by national funds (PIDDAC) through the Portuguese Science Foundation (FCT/MCTES).

Recent knowledge on rip-rap scour countermeasures for offshore structures

Tiago Fazeres-Ferradosa[a,b*], Francisco Taveira-Pinto[a,b], Paulo Rosa-Santos[a,b], Hermes Carvalho[c]

[a]*Hydraulics, Water Resources and Environment Division, Civil Engineering Department, Faculty of Engineering, University of Porto, Portugal.*
[b]*Marine Energy and Hydraulic Structures Group, Interdisciplinary Centre of Marine and Environmental Research, Portugal*
[c] *Department of Structural Engineering, Federal University of Minas Gerais, Brazil*
**Corresponding author: tferradosa@fe.up.pt*

Keywords: Scour Protections; Offshore Structures and Foundations; Marine Energy; Optimisation.

ABSTRACT

Marine foundations often experience severe scour phenomena, which may have a considerable impact in the natural frequency of the structure [1]. This problem has remarkable importance when designing particularly slender structures at rather reduced water depths, *e.g.* up 30 m for monopiles or 50 m for structures with larger footprints, such as jackets or gravity-based foundations, all of these being commonly used in offshore wind and oil & gas investments. Avoiding scour at the foundations is often achieved by means of the installation of a scour protection system, which prevents the generalized lowering of the seabed near the foundations' vicinity.

Rip-rap scour protections are the most common countermeasure used in practical cases, due the availability and reduced costs of rubble-mound material [2]. However, the capital expenditures and operation and maintenance costs related to the scour protection, represent a considerable portion of the foundation's costs, which for instance in offshore wind turbines may easily be above 30% of the overall costs [3]. Therefore, optimising the costs of the solutions implemented as scour protection remains as a key aspect to tackle towards competitive levelized costs of energy in different marine energy structures. Such optimizations become particularly important for marine renewables, namely, in offshore wind, waves and tidal-current energy [4].

Recently, a number of optimisations have been proposed to the design of rip-rap scour protections, with the most relevant ones being the design based on the dynamic stability and the wide-graded single layer configuration, recently reviewed in [1]. In physical modelling studies, these optimisations have been shown to contribute with reductions of the median diameter of the rubble mound material, thus leading to lower transport, installation and capital costs. The present research provides a brief review on the most recent findings related to such optimisations, with a strong focus on the discussion of their benefits for the numerous marine structures that are now becoming a trend in the marine renewable energy sector, including the application of hybrid structures, which are used to combine different energy harvesting technologies, *e.g.* offshore wind and wave energy.

The results indicate that these optimisations contribute the reduce the median stone diameter that may vary between 20% to 80% when compared to the statically stable design, commonly applied. Additionally, it is shown that the reduction of protection's costs is a crucial aspect to answer to some of the design challenges related to the cyclic motion of energy converters in offshore hybrid structures.

REFERENCES

[1] Fazeres-Ferradosa T, Chambel J, Taveira-Pinto F, Rosa-Santos P, Taveira-Pinto FVC, Giannini G, Haerens P. Scour Protections for Offshore Foundations of Marine Energy Harvesting Technologies: A Review. *Journal of Marine Science and Engineering*. 9(3):297 (2021). https://doi.org/10.3390/jmse9030297.

[2] Fazeres-Ferradosa, T., Welzel, M., Schendel, A., Baelus, L., Santos, P.R., Pinto, F.T. Extended characterization of damage in rubble mound scour protections. Coastal Engineering, 158, art. no. 103671 (2020). https://doi.org/10.1016/j.coastaleng.2020.103671.
[3] Fazeres-Ferradosa, T., Taveira-Pinto, F., Rosa-Santos, P., Chambel, J. A review of reliability analysis of offshore scour protections. Proceedings of the Institution of Civil Engineers: Maritime Engineering, 172 (3), pp. 104-117 (2019). https://doi.org/10.1680/jmaen.2019.11
[4] Taveira-Pinto, F., Rosa-Santos, P., Fazeres-Ferradosa, T. Marine renewable energy. Renewable Energy, 150, pp. 1160-1164 (2020). https://doi.org/10.1016/j.renene.2019.10.014

ACKNOWLEDGMENTS

This work is supported by the project POCI-01-0145-FEDER-032170 (ORACLE project), funded by the European Fund for Regional Development (FEDER), through the COMPETE2020, the Programa Operacional Competitividade e Internacionalização (POCI) and FCT/MCTES through national funds (PIDDAC).

Advanced research on marine renewable energies and ocean systems

Tiago Fazeres-Ferradosa[a,b*], Francisco Taveira-Pinto[a,b], Paulo Rosa-Santos[a,b]

[a]*Hydraulics, Water Resources and Environment Division, Civil Engineering Department, Faculty of Engineering, University of Porto, Portugal.*
[b]*Marine Energy and Hydraulic Structures Group, Interdisciplinary Centre of Marine and Environmental Research, Portugal*
**Corresponding author: tferradosa@fe.up.pt*

Keywords: Marine renewable energy; Physical modelling; Numerical modelling; Marine structures.

ABSTRACT

Marine renewable energy has gathered a wide range of attention from different research fields, due to the high expectations in its future significant role in the World's low carbon economy and counteracting climate change effects. Just looking at the offshore wind, wave and tidal energy, the theoretical potential available exceeds the 300,000 TWh/yr, which compares to about 162,500 TWh/yr of primary energy consumption in 2017 world-wide [1]. Therefore, the vast and untapped energy resources placed at sea are a vital contribution to the growing population and growing electricity demands, which are estimated to grow by over 25% until 2040 reaching circa 206,000 TWh/yr of primary energy consumption [1].

The challenges related to the design and installation of different harvesting technologies at sea imply a deep knowledge on the complex interaction between supporting structures, energy converters, soil, hydrodynamics among several other aspects.

Therefore, advanced research on marine renewable energy is a multidisciplinary field which encompasses a broad range of topics, commonly studied by means of physical and numerical modelling activities that provide insights on the most efficient way to design, build and implement ocean systems for energy harvesting purposes [2].

The Marine Energy and Hydraulic Structures group is a leading group in the advanced research on marine renewable energy, which devotes its activity towards the development of such multidisciplinary studies. This includes, for instance, the fields of wave energy, tidal-current energy and offshore wind, which are also combined with broader topics, such as the reconversion of former oil and gas platforms into renewable energy structures or the use of sea energy converters to provide energy supply for remote systems related to aquaculture, monitoring equipment and other similar applications [3].

The present work provides a broad review on the recent advanced research performed under group's activities and projects, while focusing challenges and opportunities related to the design of ocean systems and coastal or offshore structures for marine energy exploitation. Additionally, synergies with different related fields of research, are identified, discussed and framed into the most recent trends of the European Sea Economy. This study shows and highlights that novel research on marine renewable energy looking for applied results that can be combined with different economical activities in coastal and offshore regions is a vital aspect to reach the commercialization of less mature energy sources, such as waves or tidal-current energy.

REFERENCES

[1] Taveira-Pinto, F., Rosa-Santos, P., Fazeres-Ferradosa, T. Marine renewable energy. Renewable Energy, 150, pp. 1160-1164 (2020). https://doi.org/10.1016/j.renene.2019.10.014.

[2] Fazeres-Ferradosa, T., Rosa-Santos, P., Taveira-Pinto, F., Vanem, E., Carvalho, H., Correia, J. Editorial: Advanced research on offshore structures and foundation design: Part 1. Proceedings of the Institution of Civil Engineers: Maritime Engineering, 172 (4), pp. 118-123 (2019). https://doi.org/10.1680/jmaen.2019.172.4.118.
[3] Fazeres-Ferradosa, T., Rosa-Santos, P., Taveira-Pinto, F., Pavlou, D., Gao, F-P., Carvalho, H., Oliveira-Pinto, S. Preface: Advanced Research on Offshore Structures and Foundation Design: Part 2. Proceedings of the Institution of Civil Engineers: Maritime Engineering, 173 (4), pp. 96-99 (2020). https://doi.org/10.1680/jmaen.2020.173.4.96.

ACKNOWLEDGMENTS

This work is supported by the project POCI-01-0145-FEDER-032170 (ORACLE project), funded by the European Fund for Regional Development (FEDER), through the COMPETE2020, the Programa Operacional Competitividade e Internacionalização (POCI) and FCT/MCTES through national funds (PIDDAC).

Analysis of Wind Speed and Assessment of Wind Energy Potential on the Coast of Dar es Salaam Region, Tanzania using Weibull Distribution Method

Enock Michael, Dominicus Danardono Dwi Prija Tjahajana*, Aditya Rio Prabowo*

[a] *Department of Mechanical Engineering, Universitas Sebelas Maret, Surakarta 57126, Indonesia*
** Corresponding author: ddanardono@staff.uns.ac.id (D.D.D.P.T.); aditya@ft.uns.ac.id (A.R.P.)*

Keywords: Mean Wind Speed; Weibull distribution; Wind energy potential; Dar es Salaam-Tanzania.

ABSTRACT

Renewable energy is an environmental friendly source of energy, which is regarded as the most favorable and useful form of energy [1]. There are different types of renewable energy resources available all over the world [2]. Among those, wind energy is one of the fastest heighten and cost-effective form of renewable energy technology [3].

This study aimed to analyze the wind speed of the coast of Dar es Salaam region, Tanzania and concluded by determining the suitable wind turbine that's cost effective for a study location. The wind energy potential and wind speed characteristics of the coast region of Dar es Salaam Tanzania were studied by using a recorded three-hourly interval, monthly wind speed data that collected in a period of one year (2019) by rotating cup anemometer at a height of 10 m. The Weibull probability distribution function was used to investigate the wind power density and energy density of the coast of Dar es Salaam region in Tanzania as it is expressed in equations 1 and 2 respectively [4], [5].

$$P_D = \frac{P(V)}{A} = \frac{1}{2}\rho V^3{}_m \quad (1)$$

Where $P(V)$ is the power of the wind (in watt), P_D is the power density of the wind (watt per square meter), ρ = the site density of air that's assumed to be 1.225 kg/m3 in this study and A = the rotor blades swept area (in square meter).

$$E_D = \frac{1}{2}\rho c^3 \Gamma\left(1+\frac{3}{k}\right)T \quad (2)$$

Where E_D is the mean energy density, $\Gamma(x)$ is the gamma function, T is the specific period of time, c and k are the Weibull scale parameter and shape parameter respectively.

The mean annual values Weibull shape c and scale k parameters of a study location are 2.71 and 5.76 m/s respectively, and the annual mean wind power density and annual total energy density are 84.53 $\mathrm{w/m^2}$ and 1128.086 $\mathrm{kWh/m^2}$ respectively as it shown in Table 1. The five commercial wind turbine models were used to simulate their performances and Polaris P50-500 wind turbine model recommended as a suitable due to its good performance with a capacity factor of 49.35% as it shown in Fig 1.

Table 1. Monthly Weibull parameters (k and c), mean wind power density and energy density

Month	V_m	k	c (m/s)	V_F (m/s)	V_E (m/s)	P_D (w/m^2)	E_D(kWh/m^2)
Jan	6.29	3.35	7.01	6.31	8.01	152.43	150.735
Feb	5.87	3.14	6.57	5.81	7.69	123.89	126.902
Mar	5.12	2.76	5.83	4.95	7.10	82.21	93.906
Apr	5.09	2.42	5.74	4.61	7.36	80.77	97.071
May	4.94	2.77	5.56	4.73	6.77	73.84	81.301
Jun	5.27	2.58	5.93	4.90	7.41	89.65	102.642
Jul	4.86	2.80	5.46	4.66	6.62	70.31	76.573
Aug	4.67	2.82	5.25	4.49	6.35	62.38	67.833
Sep	4.77	2.58	5.36	4.43	6.69	66.48	75.798
Oct	4.86	2.54	5.48	4.50	6.89	70.31	81.790
Nov	4.38	2.36	4.94	3.91	6.41	51.47	63.011
Dec	5.29	2.38	5.97	4.75	7.71	90.67	110.524
Annual	5.12	2.71	5.76	4.84	7.09	84.53	1128.086

Where V_m, mean wind speed; k, Weibull shape parameter; c, Weibull scale parameter; V_F, most probable wind speed;V_E, wind speed carrying maximum energy;P_D, mean wind power density;E_D, mean wind energy density

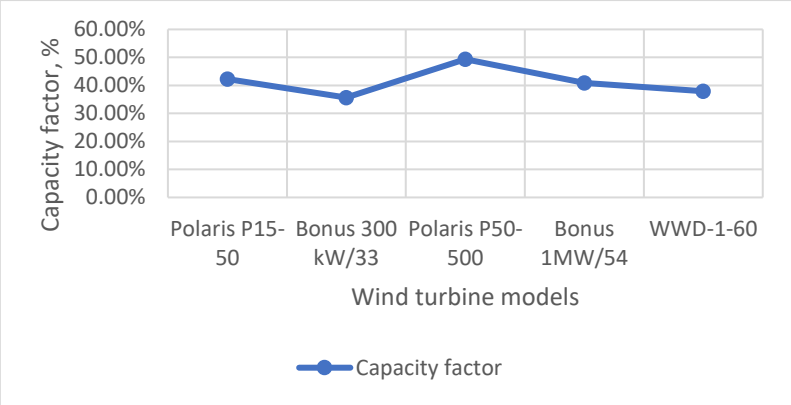

Fig 1. Capacity factor

REFERENCES

[1] K. Azad, M. Rasul, P. Halder, and J. Sutariya, "Assessment of wind energy prospect by weibull distribution for prospective wind sites in Australia," Energy Procedia, vol. 160, no. 2018, pp. 348–355, 2019.

[2] C. Ilkiliç, "Wind energy and assessment of wind energy potential in Turkey," Renew. Sustain. Energy Rev., vol. 16, no. 2, pp. 1165–1173, 2012.

[3] F. H. Mahmood, A. K. Resen, and A. B. Khamees, "Wind characteristic analysis based on Weibull distribution of Al-Salman site, Iraq," Energy Reports, vol. 6, no. September 2019, pp. 79–87, 2020.

[4] P. K. Chaurasiya, S. Ahmed, and V. Warudkar, "Study of different parameters estimation methods of Weibull distribution to determine wind power density using ground based Doppler SODAR instrument," Alexandria Eng. J., vol. 57, no. 4, pp. 2299–2311, 2018.

[5] S. H. Pishgar-Komleh, A. Keyhani, and P. Sefeedpari, "Wind speed and power density analysis based on Weibull and Rayleigh distributions (a case study: Firouzkooh county of Iran)," Renew. Sustain. Energy Rev., vol. 42, pp. 313–322, 2015.

ACKNOWLEDGMENTS

The authors are thankful to the Tanzania Meteorological Agency (TMA), Dar es Salaam, Tanzania, for providing wind data for this study.

Simplified fatigue damage assessment based on the hot-spot stress approach using numerical and analytical solutions of an offshore tubular KT joint

Bianca Vieira Ávila[a*], Hermes Carvalho[a], José A.F.O. Correia[b], António Mourão[b], Ali Aidibi[c], Paulo Mendes[b], Nicholas Fantuzzi[c]

[a]*Structural engineering department, Federal University of Minas Gerais, Brazil.*
[b]*Department of Civil Engineering, Faculty of Engineering, University of Porto, Porto, Portugal.*
[c]*DICAM Department, University of Bologna, Italy*
**Corresponding author: biancavieiraavila@gmail.com*

Keywords: Simplified accumulated damage approach, Hot-spot stress, Numerical analysis.

ABSTRACT

Jacket-type structures are support structures for offshore platforms or wind tur-bines composed of welded steel tubular trusses. Due to the cyclical nature of the environmental loads to which they are subjected, the offshore structures suffer damage over time, generating cracks in the structure that can evolve to its collapse. The connections are critical regions due to the joining of one or more members welded on the same chord. The design life of a truss-type support structure is, therefore, determined by the fatigue life of the structure joints [1,2].

Nominal stresses have long been used in the assessment and study of fatigue strength; however, this approach is limited and does not consider the effects of geometric discontinuities and stress concentration. On the other hand, the hot-spot stress approach has been proposed in codes and recommendations as in IIW [3] and DNVGL [4] for presenting more reliable results.

For this reason, this study aims to assess the fatigue damage of a tubular KT-joint of a jacket-type offshore support structure. For this, the joints were studied analytically and numerically using the ABAQUS software by the hot-spot method described in DNVGL [4]. In the numerical method, the influence of the weld geometry is evaluated. The models are shown in fig. 1.

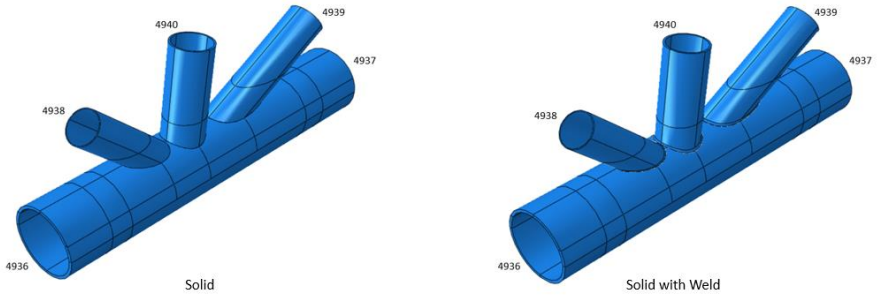

Fig. 1. Numerical models.

The hot-spot stress was also calculated using the analytical method proposed by DNVGL-RP-C203 [3] derived from Efthymiou's analytical equations for the stress concentration factor combined with the superposition of stresses method. Finally, the damage was calculated using the simplified damage accumulation method proposed by DNVGL. The results are shown in Tab. 1.

Brace	Analysis	Point 1	Point 2	Point 3	Point 4	Point 5	Point 6	Point 7	Point 8
	Solid	1.05E-03	3.21E-04	1.60E-04	3.80E-04	3.83E-04	1.44E-03	1.10E-03	1.30E-03
4938	Solid with Weld	8.72E-04	2.89E-04	1.61E-04	6.23E-04	2.66E-04	1.01E-03	9.35E-04	1.07E-03
	Analytical Solution	5.75E-04	3.14E-04	2.37E-04	2.26E-04	4.01E-04	8.29E-04	1.17E-03	1.00E-03
	Solid	3.27E-06	1.30E-05	8.31E-04	3.25E-05	4.43E-06	1.57E-05	1.24E-03	2.50E-05
4940	Solid with Weld	2.91E-05	1.24E-09	1.11E-04	3.64E-06	3.58E-06	1.52E-06	4.10E-04	1.79E-07
	Analytical Solution	2.78E-07	3.29E-04	6.65E-04	1.55E-04	1.30E-07	3.32E-04	6.90E-04	1.87E-04
	Solid	5.49E-05	1.33E-05	1.60E-05	2.63E-05	2.00E-04	2.66E-05	9.24E-06	4.02E-05
4939	Solid with Weld	3.28E-04	3.21E-05	1.63E-05	2.54E-05	2.08E-04	2.98E-05	2.02E-05	2.37E-04
	Analytical Solution	1.07E-04	6.73E-06	5.74E-06	1.61E-06	3.69E-05	3.69E-04	6.74E-04	4.79E-04

As noted, the solid model without weld geometry of DNV was more conservative with maximum damage of 1.44 x 10^{-3} against 1.07 x 10^{-3} of the model with weld representation and 1.17 x 10-3 for the analytical solution presented in DNV. Once the damage has been calculated for an expected useful life of 50 years, it is possible to conclude that in none of the adopted approaches does the assessed wave cause dangers to the structure, and without a doubt, it is possible that the life of this structure is much longer than expected.

REFERENCES

[1] Hammerstad, B. H.; Schafhirt. S.; Muskulus, M. On Fatigue Damage Assessment for Offshore Support Structures with Tubular Joints. Energy Procedia (94), 339-346 (2016).
[2] Böker C. Load simulation and local dynamics of support structures for offshore wind turbines. Hannover: Institut für Stahlbau, Gottfried Wilhelm Leibniz Universität Han-ner; 2010.
[3] IIW. Hobbacher A. INTERNATIONAL INSTITUTE OF WELDING (IIW). Recommendations for fatigue design of welded joints and components, 2nd ed. Ed. Springer, (2014).
[4] DNV GL Group. DNV-RP-C203: Fatigue Design of Offshore Structures, Noruega, 2016.

ACKNOWLEDGMENTS

The authors are grateful for the financial support in the form of support for research granted by CAPES, FAPEMIG, CNPq and UFMG.

Feasibility Study for the Reuse of a Steel Offshore Platform as the Support Base of a Wind Tower

V.M. Quissanga[a], J.G. Santos da Silva[a*]

[a]*Civil Engineering Postgraduate (PGECIV), State University of Rio de Janeiro (UERJ), Brazil.*
**jgss@uerj.br*

Keywords: fixed steel offshore platform; wind tower; structural verification.

ABSTRACT

The Brazilian offshore industry began with the installation of its first platform in the Guaricema Field, state of Sergipe, in 1968, 53 years ago. Considering that most of the platforms, already installed, were designed for a 30 year service life, it is easy to understand that there are a large number of fixed Brazilian structures that should have already been decommissioned. Brazil has already built about 100 fixed platforms, of which only 4 have been removed. There are, however, a large number of these platforms, whose production has been practically depleted, so the only reason for not having been removed is their high decommissioning cost [1].

The reuse of fixed offshore platform jackets in fields, that are no longer productive, is an alternative that has been mentioned frequently by the offshore wind industry, but which has not been used at all in Brazil and very scarcely elsewhere. Brazil has a large number of fixed offshore platforms, mainly in the northern part, which are producing very poorly. Those, however, in which the field is exhausted, continue to generate costs, but were only added to the list of platforms "to be decommissioned". In that order, the article published in 2017 [2], evaluated and suggested the possibility of transforming a typical Brazilian structure into an offshore wind tower. In this study they have investigated the wind conditions along the Brazilian coast, the structural conditions of this typical offshore platform and the financial conditions for its reuse. Based on these results they have concluded that this small typical Brazilian platform can be used to install a 5MW wind tower, which at that time, was the one most frequently used for offshore purposes.

Only 3 years after that paper has been published (4 or 5 years after the paper was written) [2], however, the 5MW wind tower is no longer used for offshore purposes. It is still available for the onshore market, but for offshore purposes, almost all platforms being installed have 10MW towers and those that are still being planned are considering 12 and even 15MW wind towers. Considering that the 5MW tower can no longer be purchased for offshore purposes, the question which must be answered is if this same typical Brazilian offshore platform, used in [2], can resist a present day 10MW tower without having to go through huge reinforcements these days. Answering this question is the object of this paper.

In Brazil there are over 50 of these typical small wellhead platforms, so the structural model of these platforms was considered to perform the analyses required in order to answer the question asked above, taking into account the excellent wind conditions on the Brazilian coast, especially in the Northeast from the country, that as we know; 9m/sec. is an excellent average wind speed for the implementation of wind towers, this means also that the entire Northeast region, which has 7.85m/sec. speeds at 50m, will have 9m/sec. speeds at 150m high. Additionally, it is worth mentioning that approximately 75% of the Brazilian fixed offshore platforms were installed more than 25 years ago.

Hence, this research aims to evaluate the behaviour of the structural system of a typical Brazilian fixed offshore platform (jacket) when subjected to the loading of a 10MW (Fig. 1) wind tower and new operating conditions without the need for a major reinforcement that makes its reuse meaningless. The jacket presents a height of 26 m (from the mudline), eight legs, is composed of five decks, with the lower area (deck) of 9.97 x 9.97 m^2 and the upper area of 6.10x6.10 m^2. The loading related to the 10MW wind tower was considered and distributed on top of the four legs of the jacket (see Fig. 1).

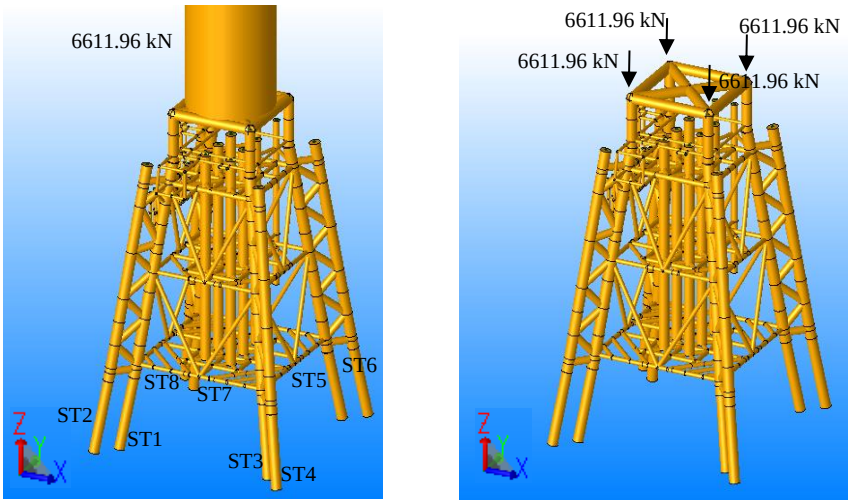

Fig. 1. Offshore platform jacket under environmental and wind turbine tower load.

However, it is worth reiterating that this paper focuses on the possibility of reusing of a fixed offshore platform, with the purpose to understand whether the removal of the deck from the platform would be considered including the replacement for a wind tower. Thus, the present research aims to verify the structural behaviour of a fixed offshore platform (jacket) when subjected to the loading of a 10 MW wind tower. However, in addition to the static loading coming from the wind tower, the environmental forces (waves and wind) acting on the platform was pondered.

The numerical model was developed based on the use of the SACS V12.0 [4] computational software, and via the use of the Finite Element Method (MEF). Initially, the analysed members of the jacket demonstrate an adequate structural behaviour, as their stress ratios result in values obtained from the project perspective. On the other hand, the piles present results of undue stress ratios, as well as deflections, when considering the overturning moments of the structure.

This way, based on the resistance structural analysis performed on the fixed offshore platform (jacket), considering the influence of static and variable loads, the results obtained throughout this investigation pointed out to the fact that the assessed jacket does not meet the design criteria to support 10 MW wind towers under operating conditions.

REFERENCES

[1] Quissanga, V. M.: Descomissionamento de plataforma offshore fixa e utilização para base de unidade de geração de energia eólica. Masters Dissertation, Federal Fluminense University (UFF), Rio de Janeiro/RJ, Brazil (2018).
[2] Barros, J. C., FERNANDES, G. C., SILVA, M. M., SILVA, R. P., SANTOS, B.: Fixed platforms at ageing oil fields: feasibility study for reuse to wind farms. Offshore Technology Conference (OTC), Houston, USA (2017).
[3] Atlas do Potencial Eólico Brasileiro, Ministério de Minas e Energia, Brasília (2001).
[4] SACS V12.0: Structural Analysis Computer System. Engineering Dynamics, Inc-Kenner, Louisiana, USA (2019).

ACKNOWLEDGMENTS

The authors gratefully acknowledge the financial support for this research work provided by the Brazilian Science Foundation's CNPq, CAPES and FAPERJ.

Horizontal and Vertical Axis Wind Turbines on Existing Jacket Platforms: A Comparative Study

P. Mendes[a*], J. Correia[a], J.M. Castro[a], N. Fantuzzi[b], D. Haselibozchaloee[a], L. Manuel[c]

[a]*CONSTRUCT/Faculty of Engineering, University of Porto, Portugal*
[b]*DICAM Department, University of Bologna, Italy*
[c]*University of Texas, Austin, USA*
**Corresponding author: pjmendes@fe.up.pt*

Keywords: Offshore structure; Wind turbines; Dynamic analysis; Wind and wave analysis;

ABSTRACT

The wind resource offshore is generally outstanding due to a higher potential for power generation due to faster and more constant winds, also providing energy at a more stable rate. Also, there are no visual or noise pollution disadvantages as those caused by onshore wind farms. A jacket is made up of four legs of more than 1 m diameter connected to each other with bracings and its design is commonly applied by the oil and gas industry for supporting rigs offshore. When the offshore resources run out, these structures must be displaced to another area containing underground resources or removed in the case of reaching their design life. Therefore, one possible procedure to reduce the carbon footprint on the planet, allowing society to rely on promising sources of 'clean' energy while salvaging these oil and gas platforms, is to consider the transformation of these oil and gas platforms into offshore wind turbine support structures. The present research focuses on the possibility of converting such structures for gas extraction into offshore platforms for wind turbines. In this study, a comparison between the behaviour of horizontal and vertical axis wind turbines on the same old offshore platform is presented. Also, two different software programs were used in this comparison: MATLAB and SAP. The model proposed is a new simplified tool used to study the structural analysis of the jacket structure, developed and summarized in 10 steps, adopted to evaluate the behaviour of the platform with the wind tower configurations. Figures 1 and 2 display the first vibration modes as example of the 18-DOF model associated to the corresponding undamped natural structural frequencies ω_n with n = 1 taken from SAP and MATLAB, respectively.

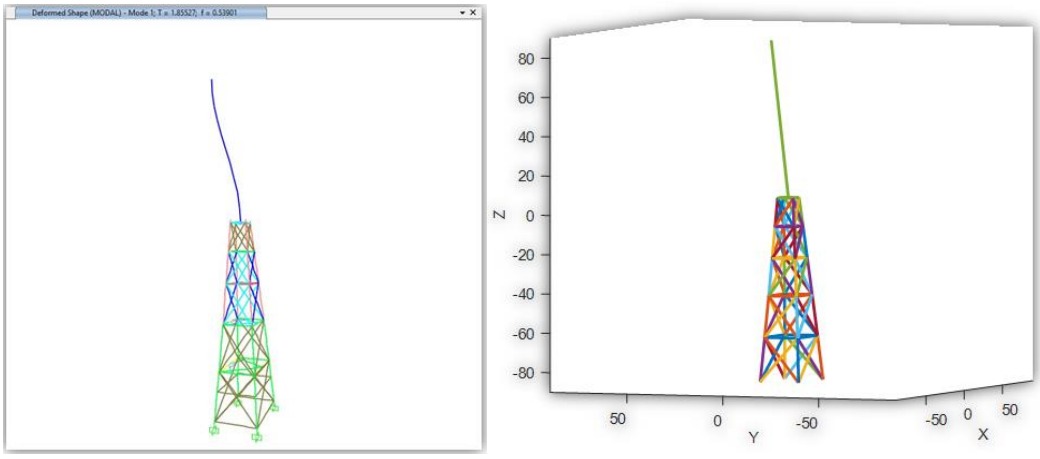

a) b)

Fig. 1**.** Mode 1 for the horizontal-axis wind turbine developed in both softwares a) SAP b) MATLAB

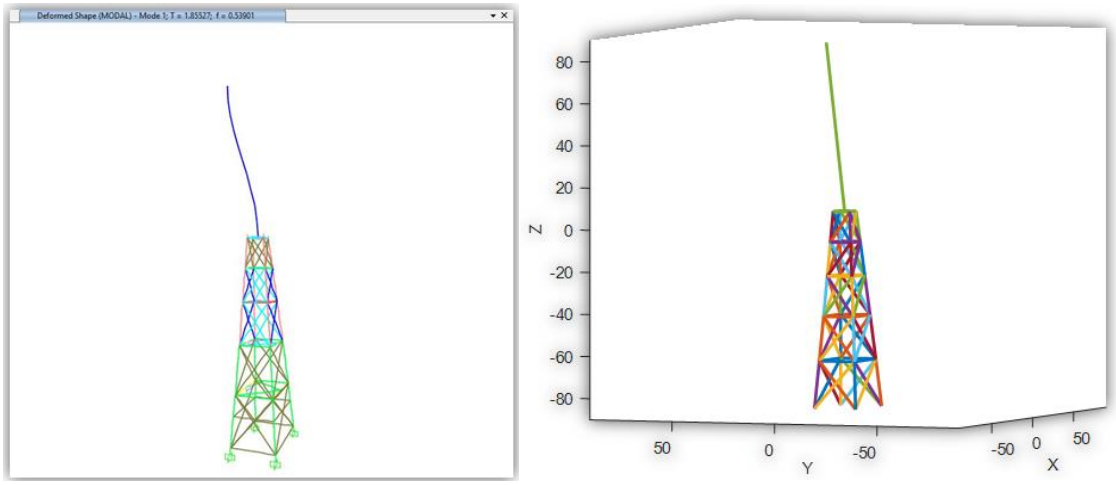

a) b)

Fig. 2**.** Mode 1 for the vertical-axis wind turbine developed in both softwares a) SAP b) MATLAB

ACKNOWLEDGMENTS

The authors want to acknowledge Marziyeh Zarifkar and Sadegh Takavar for their important contribution to the simulations for this work. Also, the authors want to acknowledge "Fondazione Flaminia" (Ravenna, Italy) for supporting the present research.

Additionally, this research was also supported by the project grant (UTA-EXPL/IET/0111/2019) SOS-WindEnergy - Sustainable Reuse of Decommissioned Offshore Jacket Platforms for Offshore Wind Energy by national funds (PIDDAC) through the Portuguese Science Foundation (FCT/MCTES); and, base funding - UIDB/04708/2020 and programmatic funding - UIDP/04708/2020 of the CONSTRUCT - Instituto de I\&D em Estruturas e Construções - funded by national funds through the FCT/MCTES (PIDDAC). The authors would also like to thank all support by UT Austin Portugal Programme and UT-Austin Portugal grants - UTA18-001217 and UTA-EXPL/IET/0111/2019.

Methodologies for Fatigue Life Assessment based on Analytical and Numerical Local Strains using Hot-spot Concept applied to Welded Details

C.O. Viana[a,*], H. Carvalho[a], J.A.F.O. Correia[b]

[a] *Department of Structural Engineering, Federal University of Minas Gerais, Brazil*
[b] *CONSTRUTC & Department of Civil Engineering, Faculty of Engineering, University of Porto, Portugal*

**Corresponding author: crisoviana94@gmail.com*

Keywords: Fatigue; Sub-modelling; Elastoplastic Local Strain; Neuber; Ramberg-Osgood; Hot-spot Concept.

ABSTRACT

Several research works have deepened in the local approaches for the study of the metallic structures behaviour submitted to the fatigue process [1] [2] [3] [4]. This paper presents different elastoplastic local strain methodologies using the hot-spot concept applied to welded joints for the fatigue process evaluation. The first methodology is based on the estimation of elastoplastic stresses from the Neuber equation and then obtaining the elastoplastic strains from the Ramberg-Osgood equation. The second methodology obtains such parameters from numerical simulation [1] [2]. Both use hot-spot elastoplastic strain as a damage parameter for the fatigue life estimation.

After selecting the detail to be studied, it is necessary to define the considerations of the numerical analysis: type of dynamic analysis to be applied, loading model, use of global-local model, among others. The global-local approach is a good choice to refine the structure in the region of interest and for the optimization of results quality and computational simulation time. [5]. It is proposed a dynamic simulation performed on the global model considering modal superposition analysis and loading by moving loads, and several static local analysis applying the different methodologies described.

Boundary conditions are extracted from the global to the local model, then it is possible to obtain the elastic stresses and strains for the first methodology and the elastoplastic stresses and strains for the second methodology, both using the hot-spot concept. The elastoplastic curve on the second methodology is estimated from the multilinear kinematic hardening model [6] and experimental results are used as input [7]. In the ANSYS software it is advisable to select the material model based on the Besseling model, which is considered the Bauschinger effect [6] [8].

REFERENCES

[1] Correia, J. et al. A generalization of the fatigue Kohout-Veˇchet model for several fatigue damage parameters. Fract Eng Fract Mechanics. 284-300. DOI: http://dx.doi.org/10.1016/j.engfracmech.2017.06.009. (2017)
[2] Horas, C. et al. Application of the modal superposition technique combined with analytical elastoplastic approaches to assess the fatigue crack initiation on structural components. Fract Eng Fract Mechanics. 271-283. DOI: http://dx.doi.org/10.1016/j.engfracmech.2017.06.001. (2017)
[3] Karunananda, K. et al. New Combined High and Low-Cycle Fatigue Model to Estimate Life of Steel Bridges Considering Interaction of High and Low Amplitudes Loadings. Advances in Structural Engineering 15-2. 287-302. (2012)
[4] Siriwardane, S. et al. Application of new damage indicator-based sequential law for remaining fatigue life estimation of railway bridges. Journal of Constructional Steel Research 64 228–237 (2008).
[5] Viana, C. et al. Fatigue assessment based on hot-spot stresses obtained from the global dynamic analysis and local static sub-model. International Journal of Structural Integrity. DOI: 10.1108/IJSI-03-2019-0021. (2019)
[6] ANSYS INC. Release 18.2 – Documentation for ANSYS. Canonsburg, Estados Unidos. (2017)
[7] Pereira, H. Comportamento à Fadiga de Componentes Estruturais sob a Acção de Solicitações de Amplitude Variável. FEUP Departamento de Engenharia Mecânica e Gestão Industrial. Dissertação de Mestrado. 225 p. (2006)

[8] Correia, J. et al. Fatigue Crack Propagation Rates Prediction Using Probabilistic Strain-Based Models. Chapter 11: Fracture Mechanics – Properties, Patterns and Behaviours. Web of Science Core Collection, IntechOpen. (2016)

Notch fatigue life prediction under size effect using critical distance theory

Jin-Chao He[a], Shun-Peng Zhu[a*], Xiao-Peng Niu[a], Ding Liao[a]

[a]*School of Mechanical and Electrical Engineering, University of Electronic Science and Technology of China, Chengdu 611731, China*
**Corresponding author: zspeng2007@uestc.edu.cn*

Keywords: fatigue; size effect; critical distance; Weibull model.

ABSTRACT

For engineering components with notches, cracks and other defects, accurate fatigue life prediction is critical for ensuring the structural integrity. Therefore, it is of vital importance to accurately interpret the detrimental effect of notches during fatigue analysis. Until now, various methods have been explored to describe the notch effect, including nominal stress approaches [1], hot spot methods [2], weighting control parameters-based approaches [3] and critical distance theories [4]. Considering the superior advantages of the critical distance theories, it is adopted in this analysis.

In addition, a significant scatter in fatigue life for material testing also creates barriers for fatigue life predictions, which results in the necessity of advanced probabilistic fatigue models. In this regard, Weibull model [5] is adopted in the present study for describing uncertainties. In the present study, a probabilistic framework coupling critical distance theory with Weibull model is established for fatigue life prediction of notched components, as illustrated in Fig. 1.

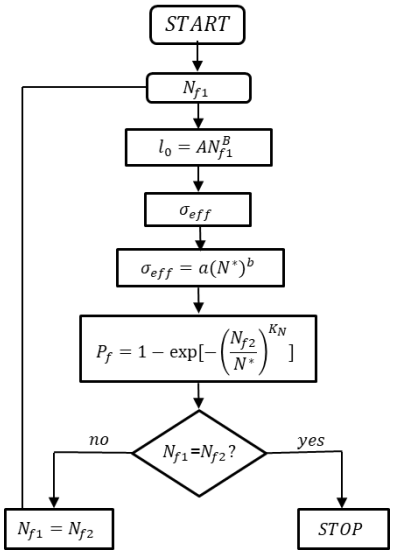

Fig. 1 Recursive procedure to predict fatigue life.

Utilizing experimental data of Al 2024-T351 notched specimens, the proposed model was compared with the traditional method, as illustrated in Fig. 2.

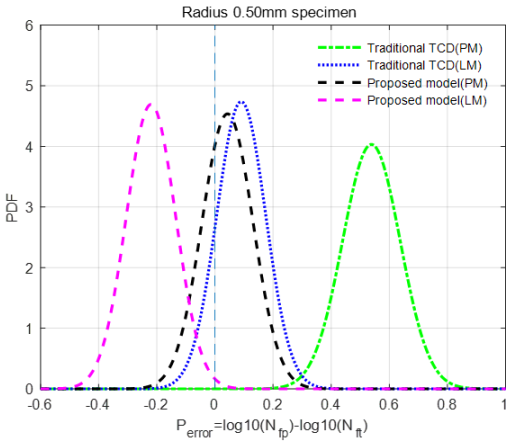

Fig. 2 Comparison of model prediction errors.

REFERENCES

[1] Q. Hu and H. Xu, "Two-parameter nominal stress approach," *Int. J. Fatigue*, vol. 17, no. 5, pp. 339–341, 1995.

[2] G. A. Qian, M. T. Wang, and L. Wang., "High cycle fatigue life prediction by local stress-strain method.," *J. Mech. Strength*, vol. 26, no. S, pp. 275–277, 2004.

[3] D. Liao, S. P. Zhu, J. A. F. O. Correia, A. M. P. De Jesus, and F. Berto, "Recent advances on notch effects in metal fatigue: A review," *Fatigue Fract. Eng. Mater. Struct.*, 2020.

[4] L. Susmel, "A unifying approach to estimate the high-cycle fatigue strength of notched components subjected to both uniaxial and multiaxial cyclic loadings," *Fatigue Fract. Eng. Mater. Struct.*, vol. 27, no. 5, pp. 391–411, 2004.

[5] Y. Ai *et al.*, "Probabilistic modeling of fatigue life distribution and size effect of components with random defects," *Int. J. Fatigue*, vol. 126, pp. 165–173, 2019.

Strain energy-based approach for probabilistic fatigue life prediction of notched components

Xue-Kang Li[a], Sijia Chen[b], Shun-Peng Zhu[a, b, *], Ding Liao[a], Jie-Wei Gao[a]

[a]*School of Mechanical and Electrical Engineering, University of Electronic Science and Technology of China, China*
[b]*Center for System Reliability & Safety, University of Electronic Science and Technology of China, Chengdu, China*
**Corresponding author: zspeng2007@uestc.edu.cn*

Keywords: notch; fatigue; strain energy density; life prediction; compressor disk.

ABSTRACT

In the design of engineering structures, geometrical discontinuities are commonly introduced due to various functional demands. Among them, compressor disks of aero engines hold complex cross-sectional patterns to meet the requirements of heat dissipation, connection, transmission, and weight reduction [1]. However, these discontinuous features would raise local stress concentration under external loadings, which inclines to trigger crack initiation. In practice, it is generally unrealistic to directly perform large amounts of fatigue tests on full-scale components because of time and costs, as well as the limitation of experimental equipment [2]. As a result, for ensuring structural integrity and achieving anti-fatigue design, it is vital to develop robust and effective methods for fatigue analysis of notched components [3]–[5].

To meet various functional requirements, engineering components are usually designed with geometrical discontinuities, which raise stress concentrations undergoing external loadings. Comparing with other locations, these regions with high levels of stress incline to initiate cracks under cyclic loadings, which determine fatigue strength of the whole part. Accordingly, a novel strain energy density-based model for notch fatigue life prediction is developed, and a P–W–N_f curve is raised to consider the fatigue life scatter originating from material dispersity. see Fig. 1. Experimental data of different notched specimens made with TC4 alloys are used for model validation and comparison. Results indicate that the proposed model predictions show higher accuracy than the SWT, Liu, HSV and TCD models. Finally, fatigue life assessment of a compressor disk considering material and load uncertainties is conducted.

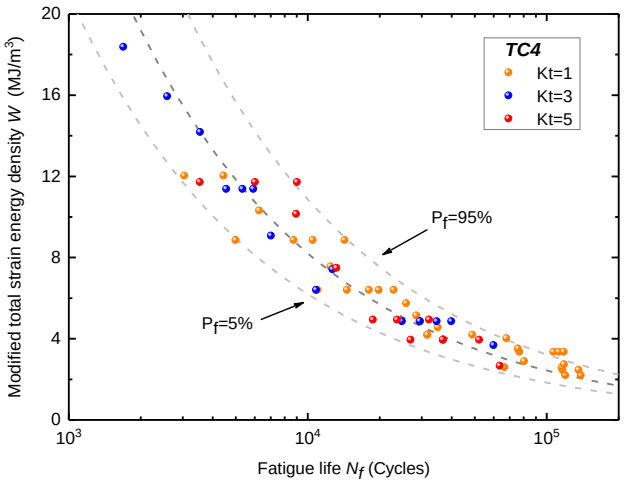

Figure 1 The fitted P–W–N_f curve of TC4 alloy.

Table 1 Predicted compressor disk lives using different models.

Models	Evaluated lives (Cycles)		
	0–450r/s–0	230r/s–450r/s–230r/s	431r/s–450r/s–431r/s
Proposed	2.5870×10^5	3.2063×10^6	$>10^{12}$
TCD [6]	2.2323×10^5	2.9255×10^6	$>10^{12}$
HSV [7]	2.1856×10^5	2.5864×10^6	$>10^{12}$

REFERENCES

[1] D. Liao, S. P. Zhu, J. A. F. O. Correia, A. M. P. De Jesus, and R. Calçada, "Computational framework for multiaxial fatigue life prediction of compressor discs considering notch effects," *Eng. Fract. Mech.*, vol. 202, pp. 423–435, 2018.

[2] D. Liao, S. P. Zhu, B. Keshtegar, G. Qian, and Q. Wang, "Probabilistic framework for fatigue life assessment of notched components under size effects," *Int. J. Mech. Sci.*, vol. 181, p. 105685, 2020.

[3] S. P. Zhu, S. Foletti, and S. Beretta, "Probabilistic framework for multiaxial LCF assessment under material variability," *Int. J. Fatigue*, vol. 103, pp. 371–385, 2017.

[4] D. Liao, S. P. Zhu, J. A. F. O. Correia, A. M. P. De Jesus, and F. Berto, "Recent advances on notch effects in metal fatigue: A review," *Fatigue Fract. Eng. Mater. Struct.*, vol. 43, pp. 637–659, 2020.

[5] J. A. F. O. Correia, A. M. P. De Jesus, and A. Fernández-Canteli, "Local unified probabilistic model for fatigue crack initiation and propagation: Application to a notched geometry," *Eng. Struct.*, vol. 52, pp. 394–407, 2013.

[6] L. Susmel and D. Taylor, "A novel formulation of the theory of critical distances to estimate lifetime of notched components in the medium-cycle fatigue regime," *Fatigue Fract. Eng. Mater. Struct.*, vol. 30, pp. 567–581, 2007.

[7] Y. Ai, S. P. Zhu, D. Liao, J. A. F. O. Correia, A. M. P. De Jesus, and B. Keshtegar, "Probabilistic modelling of notch fatigue and size effect of components using highly stressed volume approach," *Int. J. Fatigue*, vol. 127, pp. 110–119, 2019.

ACKNOWLEDGMENTS

Financial support of the National Natural Science Foundation of China (No. 11672070 and 11972110), Sichuan Provincial Key Research and Development Program (No. 2019YFG0348), Science and Technology Program of Guangzhou, China (No. 201904010463), and Fundamental Research Funds for the Central Universities (No. ZYGX2019J040) are acknowledged.

A modified energy field intensity approach for notch fatigue analysis under size effect

Yan-Lai Wu[a], Shun-Peng Zhu[a,b,*], Wen-Long Ye[a]

[a]*School of Mechanical and Electrical Engineering, University of Electronic Science and Technology of China, Chengdu 611731, China*
[b]*Center for System Reliability & Safety, University of Electronic Science and Technology of China, Chengdu 611731, China*
**Corresponding author: zspeng2007@uestc.edu.cn*

Keywords: notch fatigue; life prediction; size effect; energy field intensity.

ABSTRACT

Notched components with complex configurations are normally designed for engineering functional requirements. Geometrical discontinuities generally result into stress concentration and multiaxial stress states and eventually lead to fatigue failure[1]. For a notched specimen under uniaxial loadings, a complex multiaxial stress field appears near the notch root region or geometrical discontinuities Accordingly, numerous theories and approaches have been developed to address notch effect in metals fatigue as well as damage modelling and life predictions. In addition, size effect is still vital for studying the fatigue behavior of actual components/structures, fatigue strength of material/component normally decreases with the sample size of interest [2][3]. However, highly efficient methods for notch fatigue analysis considering size effect of engineering components are still lacking.

Among the existing fatigue failure criteria, energy-based criteria have shown superior ability to unify microscopic and macroscopic experimental evidences and formulate multiaxial life prediction models [4][5]. In this work, by adopting the elastic-plastic FE analysis, a novel model for notch fatigue life prediction considering the size effect was developed based on the energy field intensity (EFI) concept [6]. A modified weight function considering inhibition effect, which characterize the influence of strain energy gradient better. In addition, a novel concept of the fatigue effective damage zone was proposed:

$$W_{FI} = \frac{1}{V_W}\int_{\Omega_w} \Delta W_i \varphi(\chi_w, r)\, dv \tag{1}$$

which the effective damage zone Ω_w can be defined accurately by introducing a characteristic strain energy density (SED) W_c:

$$\Omega_w = \left\{ \int dv | \Delta W_i \geq W_c \right\} \tag{2}$$

It should be noted that the initial characteristic SED should be chosen for calculations of the energy field intensity of a given notched component using Eq. (2). Then, the characteristic stress W_c should be corrected using the fatigue failure data of notched components (see Fig. 1).

A specific mathematical quantification of the relationship between specimen scales and characteristic SED was proposed in the present study to account for influence of size effect on effective damage zone:

$$\frac{W_c}{W_{c,0}} = \frac{S}{S_0} \tag{3}$$

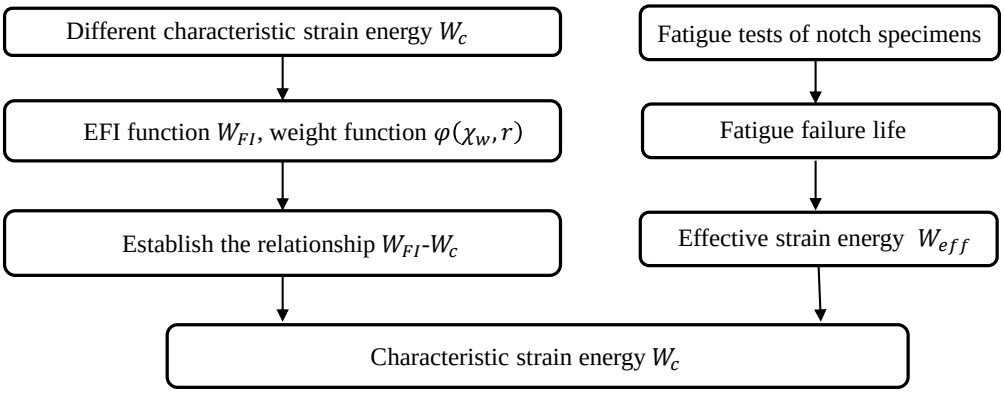

Fig. 1. Procedure for determination of the characteristic SED of the component.

Through determining aforementioned items (i.e. the weight function and the effective damage zone), to predict fatigue lives of notched specimens, a simple recursive procedure is employed. Finally, experimental data of low carbon steel GH4169 and TA19 [7] notch specimens are utilized for model validation and application, results show that the proposed model yields acceptable correlations with the experimental results.

REFERENCES

[1] D. Liao, S. P. Zhu, J. A. F. O. Correia, A. M. P. De Jesus, and F. Berto, "Recent advances on notch effects in metal fatigue: A review," Fatigue Fract. Eng. Mater. Struct., vol. 43, no. 4, pp. 637–659, 2020.
[2] K. H. Kloos, A. Buch, and D. Zankov, "Pure Geometrical Size Effect in fatigue tests with constant stress amplitude and in programme tests," Materwiss. Werksttech., vol. 12, no. 2, pp. 40–50, 1981.
[3] Y. Ai et al., "Probabilistic modeling of fatigue life distribution and size effect of components with random defects," Int. J. Fatigue, vol. 126, pp. 165–173, 2019.
[4] A. Fatemi and N. Shamsaei, "Multiaxial fatigue: An overview and some approximation models for life estimation," Int. J. Fatigue, vol. 33, no. 8, pp. 948–958, 2011.
[5] F. Ellyin, "A Strain Energy Based Criterion for Multiaxial Fatigue Failure," in Proceedings of the 9th international conference on multiaxial fatigue and fracture, 2010, pp. 167–174.
[6] D. Liao and S. P. Zhu, "Energy field intensity approach for notch fatigue analysis," Int. J. Fatigue, vol. 127, pp. 190–202, 2019.
[7] R. Wang, D. Li, D. Hu, F. Meng, H. Liu, and Q. Ma, "A combined critical distance and highly-stressed-volume model to evaluate the statistical size effect of the stress concentrator on low cycle fatigue of TA19 plate," Int. J. Fatigue, vol. 95, pp. 8–17, 2017.

ACKNOWLEDGMENTS

Financial support of the National Natural Science Foundation of China (No. 11972110), Sichuan Provincial Key Research and Development Program (No. 2019YFG0348), Science and Technology Program of Guangzhou, China (No. 201904010463), Fundamental Research Funds for the Central Universities (No. ZYGX2019J040) and Opening funds of Key Laboratory of Deep Earth Science and Engineering (Sichuan University), Ministry of Education (No. DESE201901) are acknowledged.

Probabilistic fatigue evaluation of notched components using critical distance theory under size effect

Wen-Long Ye[a], Zlling Zhang[a], Shun-Peng Zhu[a,b,*], Xue-Kang Li[a]

[a]*School of Mechanical and Electrical Engineering, University of Electronic Science and Technology of China, Chengdu 611731, China*
[b]*Center for System Reliability & Safety, University of Electronic Science and Technology of China, Chengdu 611731, China*
**Corresponding author: zspeng2007@uestc.edu.cn (S.P. Zhu)*

Keywords: relative stress gradient; size effect; effective stress; critical distance; fatigue life.

ABSTRACT

Fatigue life analysis has come to the foreground in modern engineering field, and has been widely used in engineering. In practical engineering applications, complex engineering parts are usually subject to Irregular stress, moreover, geometric discontinuity of notches overwhelmingly raises stress concentrations, further leads to more complex fatigue problems [1]. Meanwhile, fatigue behaviors of complex engineering components are generally evaluated based on mechanical properties of materials collected from tests on standardized small-scale specimens. In addition, achieving the transformation between fatigue properties of small-scale laboratory specimens to the structural strength of large-scale engineering components has become an increasingly urgent task in this field nowadays [2]. Among factors impeding the fatigue life analysis, notch and size effects are two dominant elements, which in the necessity of an effective approach considering size effect in notch fatigue life prediction.

Notch and size effects generally show great influence on the fatigue behaviour of engineering structures, which plays a vital role on their structural integrity and life evaluations [3]. Meanwhile, the critical distance is not only related to fatigue life, but also affected by size effect. In this work, by adopting the combination of the theory of critical distance and the Weibull distribution, fatigue life evaluation of notch components considering size effect is investigated. In addition, the modified critical distance is proposed considering size effect, in which the relationship between critical distance and size and life is modified by using relative stress gradient (s) which is a physical quantity to measure the size effect to address insufficient accuracy of the theory of critical distance in notch fatigue analysis [4]. A specific mathematical quantification of the relationship between relative stress gradient and critical distance was proposed in the present study to account for influence of notch size effect on critical distance:

$$\frac{l}{l_0} = \left(\frac{S_0}{S}\right)^n \tag{1}$$

Based on abovementioned, critical distance can be modified as follow:

$$l = a * S^r \left(N_f\right)^b \tag{2}$$

And an effective stress concept is introduced to characterize the fatigue life of notch components [ ]:

$$\sigma_{eff} = \frac{1}{l}\int_0^l \sigma(x, \theta = 0)dx \tag{3}$$

From the abovementioned points, a general probabilistic framework based on relative stress gradient for notch fatigue life assessment considering size effects is investigated. Finally, experimental data of Al-2024-T351 central circular holes specimens with different radii are utilized for model validation and application, results show that the proposed model yields acceptable correlations with the experimental results, see Table 1. And the flow chart of notch fatigue life prediction based on modified critical distance is shown in Figure 1.

Table 1. Comparison between average absolute errors using proposed model and Susmel model (%).

Hole radius (mm)	1.50	0.50	0.25	0.12
Susmel model	26.24	18.76	19.57	35.43
Proposed model	3.65	5.32	6.74	9.08

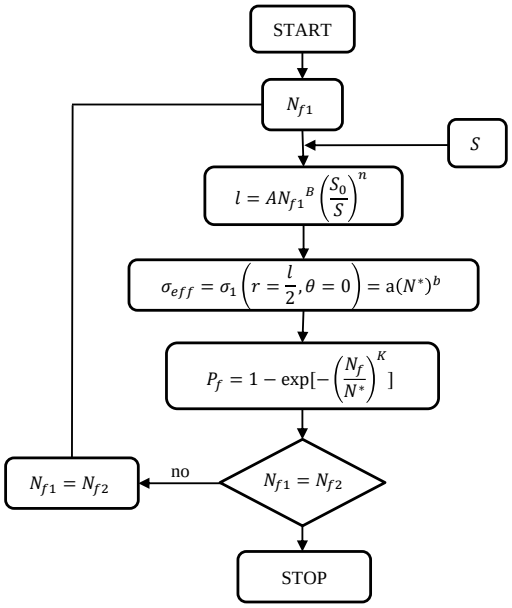

Figure 1. Modified iterative procedure accounting for notch size effect.

REFERENCES

[1] L. Mäde, S. Schmitz, G. Rollmann, H. Gottschalk, T. Beck, "Probabilistic LCF risk evaluation of a turbine vane by combined size effect and notch support modelling," *Proceedings of the ASME Turbo Expo*, 2017.

[2] D. Liao, S. P. Zhu, J. A. F. de O. Correia, A. M. P. De Jesus, and F. Berto, "Recent advances on notch effects in metal fatigue: A review," *Fatigue Fract. Eng. Mater. Struct.*, vol. 43, no. 4, pp. 637–659, 2020.

[3] J. C. He, S. P. Zhu, D. Liao, and X. P. Niu, "Probabilistic fatigue assessment of notched components under size effect using critical distance theory," *Eng. Fract. Mech.*, vol. 235, p. 107150, 2020.

[4] R. Q. Wang, D. Li, D. Y. Hu, F. C. Meng, H. Liu, and Q. H. Ma, "A combined critical distance and highly-stressed-volume model to evaluate the statistical size effect of the stress concentrator on low cycle fatigue of TA19 plate," *Int. J. Fatigue*, vol. 95, pp. 8–17, 2017.

ACKNOWLEDGMENTS

Financial support of the National Natural Science Foundation of China (No. 11972110), Sichuan Provincial Key Research and Development Program (No. 2019YFG0348), Science and Technology Program of Guangzhou, China (No. 201904010463), Fundamental Research Funds for the Central Universities (No. ZYGX2019J040) and Opening funds of Key Laboratory of Deep Earth Science and Engineering (Sichuan University), Ministry of Education (No. DESE201901) are acknowledged.

Notch fatigue analysis of metals using CPZ and TCD theories

Anteneh Tilahun Taddesse[a], Shun-Peng Zhu[a,b,*], Ding Liao[a]

[a] *School of Mechanical and Electrical Engineering, University of Electronic Science and Technology of China, Chengdu 611731, China*
[b] *Center for System Reliability & Safety, University of Electronic Science and Technology of China, Chengdu 611731, China*
**Corresponding author: zspeng2007@uestc.edu.cn*

Keywords: Notch; Fatigue life; Cyclic plastic zone; Theory of critical distance; Life prediction.

ABSTRACT

Notch fatigue analysis is vital for ensuring structural integrity and reliability of engineering components. Consequently, ensuring the fatigue strength of regions with stress concentration is of considerable importance in safe structural design and operational reliability of engineering components [1]. Recently, notch fatigue analysis has been studied by different approaches. Amongst them, continuum damage mechanics methods [2], strain energy density-based approaches [3] and theory of critical distance (TCD) [4] are mentioned frequently. Furthermore, for notched structures, the presence of the cyclic plastic zone (CPZ) is one of commonly mentioned cause and controlling factor of failure due to crack initiation and growth near notch vertex [5]. Note that the presence of CPZ alters the notch shape, and which is assumed to be longer than its physical size under fatigue loadings [6]. Particularly, the influence of the CPZ is more significant in a low cycle fatigue (LCF) regime.

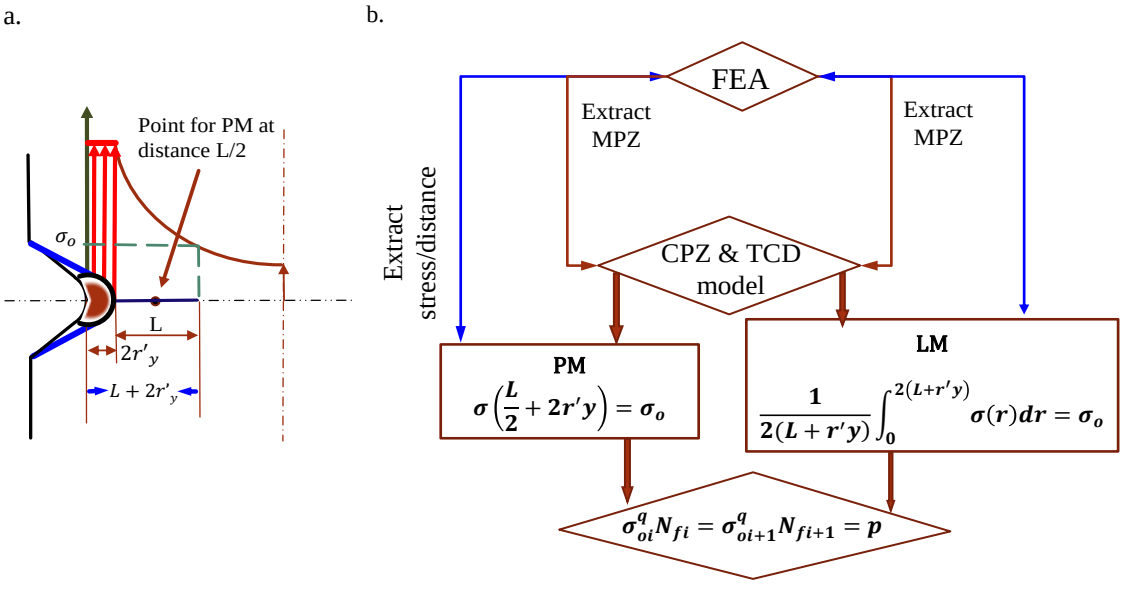

Fig. 1. (a). the presence of CPZ shifts the critical distance location in TCD methods and (b). Procedure for employing the proposed model

Accordingly, a new model is proposed by coupling TCD with CPZ concepts for LCF analysis as shown in Fig. 1 to take in to account the formation of plasticity to employ classic TCD method under elasto plastic fracture mechanics analysis.

Experimental data of En3B low carbon steel and 6082 Aluminium alloy are introduced for model validation and correlation. Results indicate that the proposed model provides better correlations of predicted fatigue lives with tested results than classic TCD and Susmel and Taylor models as illustrated in Fig. 2

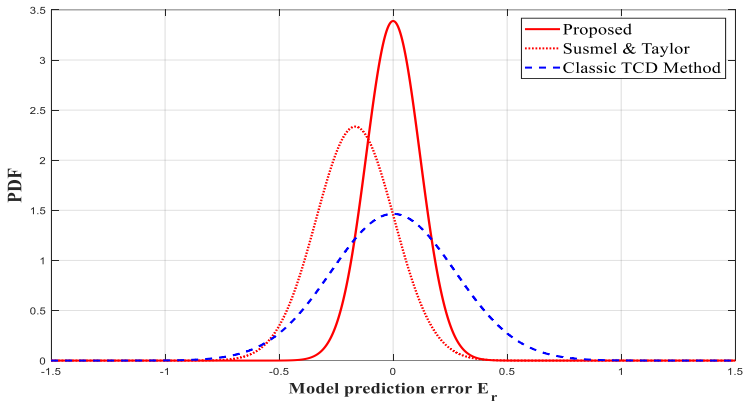

Fig. 2 Probabilistic distribution function plots of model prediction errors for: En3B low carbon steel

REFERENCES

[1] D. Liao, S. P. Zhu, J. A. F. de O. Correia, A. M. P. De Jesus, and F. Berto, "Recent advances on notch effects in metal fatigue: A review," *Fatigue Fract. Eng. Mater. Struct.*, vol. doi.org/10, pp. 1–23, 2020.

[2] J. L. Chaboche, "Continuum Damage Mechanics: Part II—Damage Growth, Crack Initiation, and Crack Growth," *J. Appl. Mech.*, vol. 55, pp. 65–72, 1988.

[3] S.-P. Zhu, Y. Liu, Q. Liu, and Z.-Y. Yu, "Strain energy gradient-based LCF life prediction of turbine discs using critical distance concept," *Int. J. Fatigue*, vol. 113, pp. 33–42, 2018.

[4] L. Susmel and D. Taylor, "A critical distance/plane method to estimate finite life of notched components under variable amplitude uniaxial/multiaxial fatigue loading," *Int. J. Fatigue*, vol. 38, pp. 7–24, 2012.

[5] G. S. Wang, "The plasticity aspect of fatigue crack growth," *Eng. Fract. Mech.*, vol. 46, pp. 909–930, 1993.

[6] G. R. Irwin, "Plastic zone near a crack and fracture toughness," in *Proc. 7th Sagamore Conf.*, 1960, pp. 63–78.

Probabilistic Fatigue Life Prediction of a Rail Vehicle Axle Based on Small-Scale Fatigue Data

Pedro Costa[a,*], José Correia[a], Shun-Peng Zhu[b], Sheng-Chuan Wu[c], Abílio De Jesus[a]

[a] *CONSTRUCT & INEGI, Faculty of Engineering, University of Porto, Portugal*
[b] *School of Mechanical and Electrical Engineering, University of Electronic Science and Technology of China, China*
[c] *State Key Laboratory of Traction Power, Southwest Jiaotong University, China*
**Corresponding author: up201404682@fe.up.pt*

Keywords: Rail Vehicle Axle; Fatigue; Numerical Analysis; Stress Concentration Factor; Probabilistic Analysis

ABSTRACT

This paper presents a probabilistic approach for fatigue life prediction of a rail vehicle axle with outside axle boxes based on small-scale fatigue data. The fatigue crack initiation stage was analysed. This study was based on a numerical analysis using the finite element method as well as analytical solutions. A local stress approach based on the Neuber rule and the Ramberg-Osgood relation was also considered. Special attention was paid to the stress relief groove between the wheel and the gearbox of the axle, as this region is one of the critical areas in terms of stress. The stress concentration factor, K_t, was evaluated in this region. Fatigue design standards for railway vehicle axles, such as EN 13103 and EN 13104, were reviewed. Rotating bending fatigue S-N curves were obtained based on the numerical-analytical procedure for the EA4T steel which is typically used in railway vehicle axles in Europe. Experimental data, from rotating bending high cycle fatigue experiments, were also collected for fatigue strength characterization of steel grade EA4T. Then, the probabilistic fatigue life fields were generated for both small-scale and derived full-scale EA4T specimens based on the ASTM E739 standard. The fatigue S-N curves obtained with the numerical-analytical procedure were compared with the probabilistic fatigue fields acquired with ASTM E739 standard for derived full-scale specimens.

ACKNOWLEDGMENTS

This work was financially supported by: Base Funding - UIDB/04708/2020 and Programmatic Funding - UIDP/04708/2020 of the CONSTRUCT - Instituto de I&D em Estruturas e Construções - funded by national funds through the FCT/MCTES (PIDDAC).

Probabilistic Fatigue Strength Modelling based on various statistical approaches for a Double-Side Welded Connection

P. Mendes[a*], R. Dantas[a], J. Correia[a], N. Fantuzzi[b], G. Lesiuk[c], A. Jesus[a], L. Manuel[d], F. Berto[e]

[a] *CONSTRUCT/Faculty of Engineering, University of Porto, Portugal*
[b] *DICAM Department, University of Bologna, Italy*
[c] *Department of Mechanics, Materials Science and Biomedical Engineering, Wroclaw University of Science and Technology, Poland*
[c] *University of Texas, Austin, USA*
[e] *Department of Mechanical and Industrial Engineering Faculty of Engineering, Norwegian University of Science and Technology, Norway*
**Corresponding author: pjmendes@fe.up.pt*

Keywords: S355 steel; S-N curve; Bayesian inference; hot-spot stress; nominal stress.

ABSTRACT

S355 steel is currently used in the fabrication of most wind turbine monopile support structures and offshore structures. In this type of structures, most fatigue failures occur in the welded connections where cyclic loading is the main responsible for this phenomenon. Similar to high cycle fatigue analysis, the stress life method utilizing stress-cycle curves (S-N curves) can be used to determine the strength of a welded joint under fatigue loading. In this research, the evaluation of design S-N curves for a double side welded connection made of S355 steel is proposed. This study concludes with a comparison between the experimental fatigue curves obtained and the design S-N curves proposed in design codes for offshore structures and general steel structures. For the specimens under investigation, the hot spot and nominal stress approaches are taken into consideration. The characteristic fatigue curve of the double-side welded connection is obtained using statistical analyses based either presented in the ASTM E739 standard or ISO 12107 standard. The hot-spot and nominal stress approaches yield very similar S-N results considering the specimens under study. A comparison between these fatigue curves at 5% of probability of failure provided by standards and the probabilistic fatigue strength curves based on Bayesian inference and Weibull distribution is done.

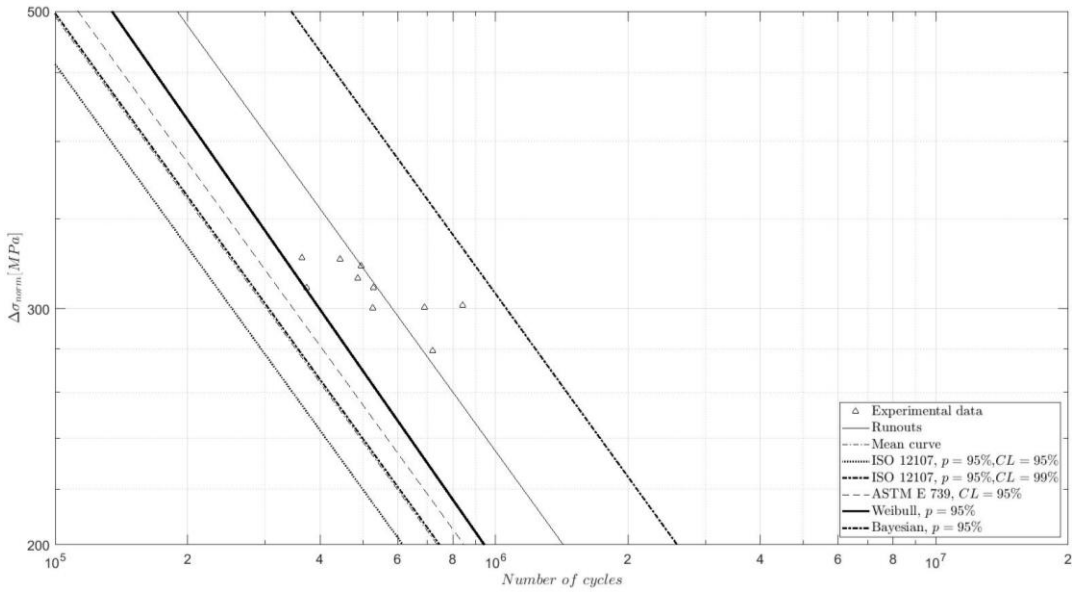

Figure 1 - Comparison of the pf = 5% P-S-N curves from different methodologies for the hot-spot stress case

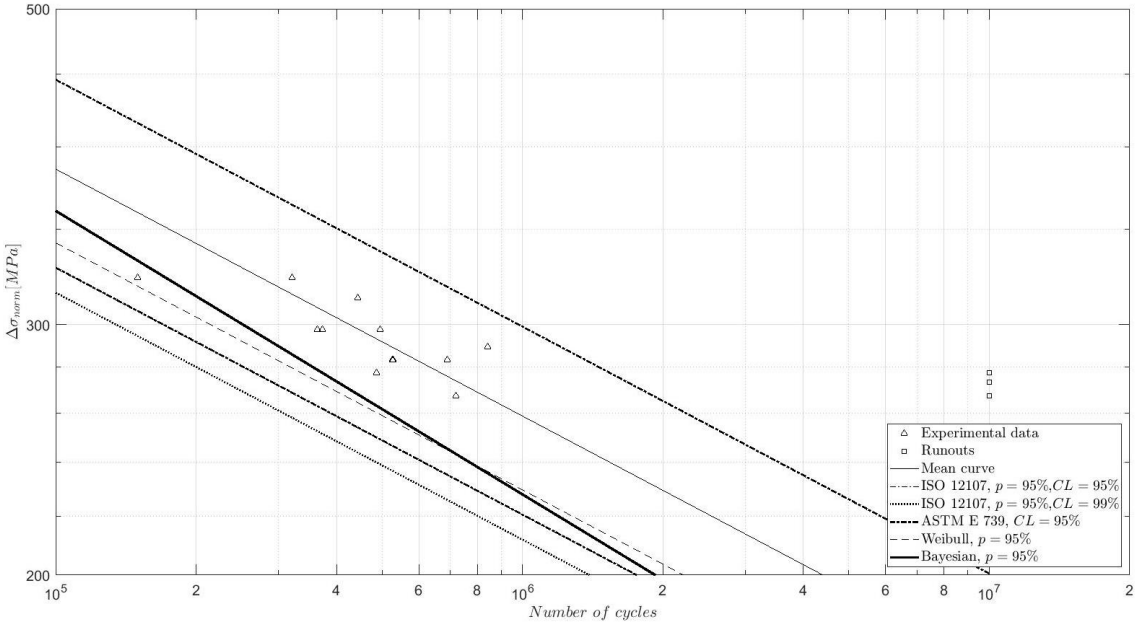

Figure 2 - Comparison of the pf = 5% P-S-N curves from the different methodologies for the nominal stress case

ACKNOWLEDGMENTS

This research was supported by the project grant (UTA-EXPL/IET/0111/2019) SOS-WindEnergy - Sustainable Reuse of Decommissioned Offshore Jacket Platforms for Offshore Wind Energy by national funds (PIDDAC) through the Portuguese Science Foundation (FCT/MCTES); and, base funding - UIDB/04708/2020 and programmatic funding - UIDP/04708/2020 of the CONSTRUCT - Instituto de I\&D em Estruturas e Construções - funded by national funds through the FCT/MCTES (PIDDAC). The authors would also like to thank all support by UT Austin Portugal Programme and UT-Austin Portugal grants - UTA18-001217 and UTA-EXPL/IET/0111/2019.

The effect of the amount of fatigue data sample on the estimation of P-S-N fields with the Weibull distribution

J.F. Barbosa[a*], A.N. Sirokyb[b], J.A.F.O. Correia[c], M. Calvente[d], R.C.S. Freire Júnior[a]

[a] *UFRN, Technology Center, Federal University of Rio Grande do Norte, Natal, Brazil.*
[b] *CIDACS-FIOCRUZ, Bahia, Salvador, Brazil*
[c] *CONSTRUCT and Faculty of Engineering, University of Porto, Porto, Portugal.*
[d] *Dep. of Construction and Manufacturing Engineering, University of Oviedo, Campus de Viesques, Gijón, Spain.*
**Corresponding author: jbarbosa@ct.ufrn.br*

Keywords: Fatigue data; Sample size; Statistical analysis; Estimation methods; Monte Carlo simulation.

ABSTRACT

The stochastic behaviour of life due to the fatigue of metallic materials promoted the development of probabilistic models capable of predicting failures resulting from damage caused by dynamic loading, coupled with the need to improve the safety and reliability protocols of project engineering. *P-S-N* curves are a widely used tool to assess the relationship between the probability of failure due to fatigue, stress range, and the number of cycles to failure. The *P-S-N* curve developed by Castillo & Fernández-Canteli [1] is being widely used by researchers for its statistical robustness and general application capacity in fatigue problems of mechanical/structural components and different materials, regardless of the failure mechanism. This model is the basis for using the Weibull distribution of three parameters and there are no reports in the literature on the performance of this model when subjected to small fatigue samples [2]. The purpose of this work is to develop a comparative study based on the Monte Carlo simulation of the Weibull parameter estimation models, maximum likelihood (EMV), Weighted least squares (WLS), maximum product spacing (MPS), probability-weighted moment (PWM), and Castillo, subject to estimates of small experimental fatigue samples. This will provide information on which model has a better estimation performance based on bias and mean square error as a function of the sample size and therefore a better fit on the P-S-N curve. Preliminary results show that the Castillo model presents a better performance for the β (shape parameter) in terms of mean square error when applied to samples of size between 9 and 30, for samples larger than 30, the maximum likelihood brings a better adjustment.

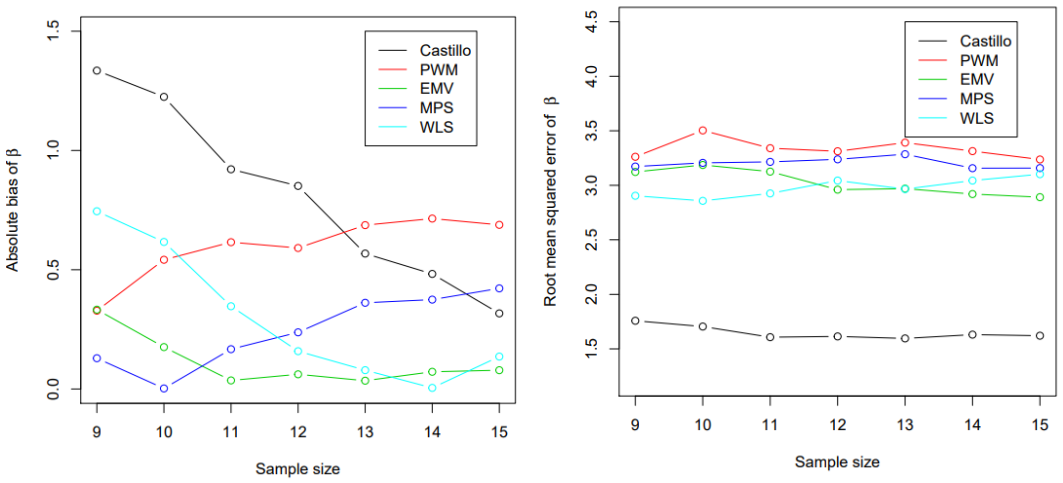

Fig. 1. Bias and RMSE of Castillo, PWM, EMV, MPS and WLS methods for small sample size

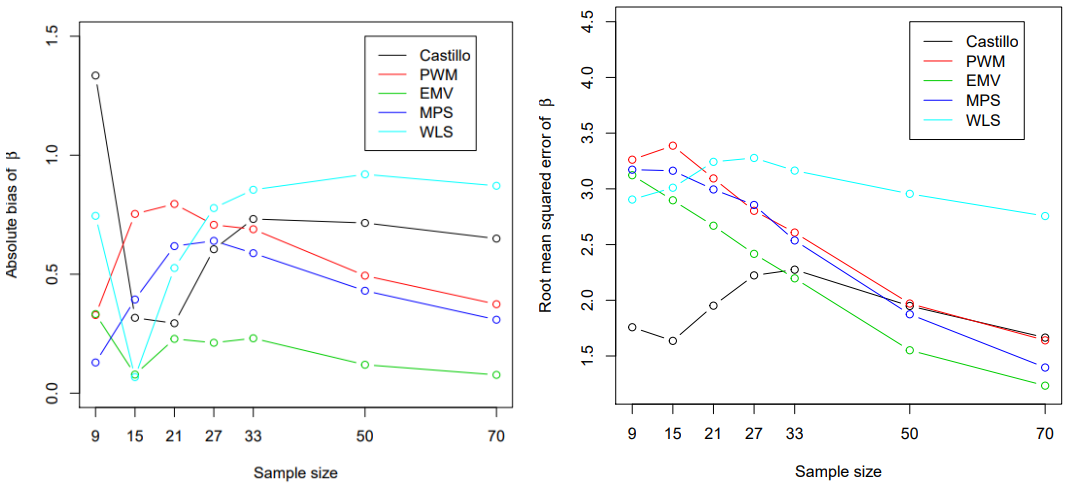

Fig. 2. Bias and RMSE of Castillo, PWM, EMV, MPS and WLS methods

REFERENCES

[1] Castillo E, Fernández-Canteli A. A unified statistical methodology for modeling fatigue damage. Springer Science & Business Media; 2009.
[2] Li, Cunhai, et al. "Determination of the fatigue PSN curves–A critical review and improved backward statistical inference method." International Journal of Fatigue 139 (2020): 105789.

ACKNOWLEDGMENTS

This research was supported by the base funding - UIDB/04708/2020 and programmatic funding - UIDP/04708/2020 of the CONSTRUCT - Instituto de I&D em Estruturas e Construções - funded by national funds through the FCT/MCTES (PIDDAC).

Elastic Critical Moment of Lateral-Distortional Buckling of Steel-Concrete Composite Beams under Non-Uniform Hogging Moment

L. S. Nery[a*]; J. V. F. Dias[a]; R. B. Caldas[a]; R. H. Fakury[a]

[a]*Department of Structural Engineering, Universidade Federal de Minas Gerais, Brazil*
**Corresponding author: leticias.nery@outlook.com*

Keywords: steel-concrete composite beam; lateral-distortional buckling; elastic critical moment; non-uniform hogging moment.

ABSTRACT

Lateral-distorsional buckling, an instability mode characterized by a horizontal displacement and twist of the bottom flange of the steel profile with distortion of the web, may occur in continuous and semicontinuous composite beams close to the internal supports, where hogging bending moments and developed.

The current Brazilian standard [1] for verification of composite structures adopts the formulation proposed by [2] to determine the critical moment of lateral-distortional buckling. In this formulation, the influence of bending moment distribution is taken into account by an equivalent uniform moment factor (C_{dist}). Recent research indicates imprecisions in this procedure. [3] demonstrated that this equation leads to unsatisfactory results for the calculation of the critical moment of beams subjected to uniform bending moment diagram. The authors also proposed a new procedure for the calculation of this moment.

Since the formulation of [2] shows inconsistencies for the case of uniform moment diagram and the equation of [3] is more appropriate in this case, the present work presents new values for the C_{dist} coefficients, to extend the formulation of [3] for linear bending moment diagrams.

First, the influence of adjacent spans was evaluated to determine which boundary conditions of the numerical models would be most appropriate for the analyses, comparing 46 complete models with three and two spans with respective simplified models developed in the software *ANSYS Mechanical APDL*. It was concluded that the bending moment of the adjacent span has little influence on the value of the critical moment, generating only a warping restriction effect that reduces with increasing length of the span. Thus, as observed by [4], there is no prejudice to safety and accuracy when adopting a simplified model consisting of a single span, as long as adequate boundary conditions are imposed.

Then, 144 simplified models with the most diverse geometric parameters were developed for each of the 9 linear moment diagrams described in the Brazilian standard, including the uniform negative moment diagram, obtaining a total of 1,296 models. Next, $C_{dist,num}$ values were obtained from the ratio between the elastic critical moment of each beam subjected to each bending moment diagram and the beam of the same geometry under uniform hogging moment. It was observed that the value of the $C_{dist,num}$ coefficient, and consequently of the critical moment, depends not only on the bending moment distribution but also on the ideal number of half-waves, n_{id}, calculated as presented in [3] (Fig. 1).

Therefore, to reproduce the variation observed, exponential equations are proposed for the calculation of C_{dist} as a function of the n_{id} parameter, in which the coefficients of these functions depend on the shape of the bending moment diagram. These equations are also represented as continuous lines in Fig. 1.

Conservatively, when n_{id} tends to infinity, these proposed equations tend to a minimum value and, therefore, this value can be used for a simplified determination of the critical moment.

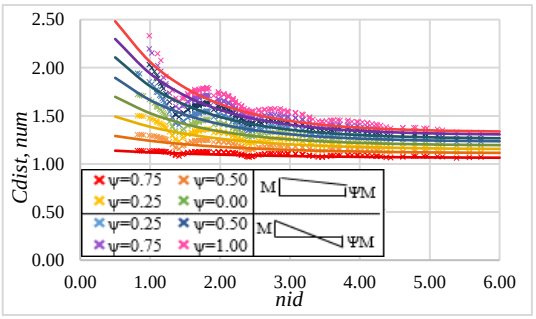

Fig. 1. $C_{dist,num}$ x n_{id}

The ratios between numerical and analytical moment values obtained by the proposed procedure and by [2] are presented in Fig. 2. It is noticeable that the proposed procedure leads to great precision when compared to numerical values, presenting an average ratio between analytical and numerical results equal to 0.98. As expected, it is also observed that when using only the minimum value of the equations, conservative values are obtained. Finally, it is noticeable that the formulation described in the Brazilian standard is imprecise and, in the majority of cases, it leads to a critical moment greater than that obtained numerically, leading to values up to two times greater than the numerical, especially for larger spans.

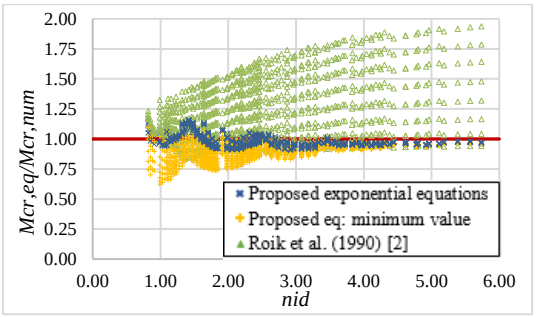

Fig. 2. Comparison between numerical and analytical results in relation to n_{id}: proposed exponential equations; the minimum value of the proposed equations and formulation presented by [2].

REFERENCES

[1] Associação Brasileira de Normas Técnicas. ABNT NBR 8800:2008 Projeto de estrutura de aço e de estrutura mista de aço e concreto de edifícios. (Rio de Janeiro, Brazil, 2008).
[2] Roik, K., Hanswille, G. e Kina, J.: Solution for the lateral torsional buckling problem of composite beams. Stahlbau 59(11), 327 - 333 (1990).
[3] Dias, J. V. F., et al.: Elastic Critical Moment of Lateral-Distortional Buckling of Steel-Concrete Composite Beams under Uniform Hogging Moment. International Journal of Structural Stability and Dynamics 19(7). (2019).
[4] Amaral, T. V., et al.: Lateral-distortional buckling of continuous steel-concrete composite beam. Revista IBRACON de Estruturas e Materiais 11(4). 719 – 756 (2018).

ACKNOWLEDGMENTS

The authors gratefully acknowledge the support provide by the Brazilian public agencies CNPq, CAPES, FAPEMIG and UFMG.

Study on the lateral distortional buckling sensitivity to geometrical imperfections in steel-concrete composite beams

N. C. F. Filla[a*], J. V. F. Dias[b], R. B. Caldas[c], R. H. Fakury[d]

[a] *Department of Mechanical Engineering, Federal University of Minas Gerais, Av. Presidente Antônio Carlos, 6627, Belo Horizonte, Brazil*

[b, c and d] *Department of Structural Engineering, Federal University of Minas Gerais, Av. Presidente Antônio Carlos, 6627, Belo Horizonte, Brazil*

**Corresponding author: nicolasfilla@ufmg.br*

Keywords: Lateral-distortional buckling, composite beams, numerical simulation, geometric imperfections.

ABSTRACT

Lateral distortional buckling (LDB) is an ultimate limit state that may occur in continuous and semi-continuous composite beams near the hogging moment regions. Due to the significant restriction imposed to the top flange of the steel profile by the concrete slab, the only way the bottom flange can buckle is by bending (distortion) of the web. The LDB phenomenon has been studied mainly with support of computational simulations, due to the high cost and difficulty on the execution of physical tests. The commonly used software (based on the finite element method in general), enable reasonable control over the initial conditions of the models, which provides the means to high fidelity simulation, as long as those conditions are properly defined [1, 2, 3].

An important aspect that impacts directly on the response of the simulations of beams subjected to LDB is the presence, shape and magnitude of initial geometric imperfections. Thanks to the randomness of manufacturing defects, the shape of the imperfections can usually be considered in a simplified manner, as equal to the most critical *eigenmode* found in linear buckling analyses (LBA) and its magnitude may be determined as fractions of the dimension of the studied element [4, 5]. Research points to a suitability in the use of LBAs, however, proper imperfection magnitudes may be of hard determination for several instability phenomena [6].

The present study examines LDB's sensitivity to different types and formats of geometrical imperfections. Initially, a numerical model was developed on the Ansys commercial code and doubly symmetric I-shaped beams with restrictions imposed to the top flange, subject to uniform hogging moment were simulated. In these beams, the buckling mode was adopted as initial imperfection shape with a maximum imperfection amplitude of L/1000. This configuration was called mode "0".

Results showed that an increase in the length of the beams resulted in a change of the buckling mode, which presented more than one half-wave, without variation of the critical moment. This observation is in agreement with the literature [2]. As a consequence, for models with larger span, the first eigenmode presented multiple half-waves and, due to the fact that the amplitude of the imperfections is based on the whole length of the piece, the final curvatures stablished became greater (Fig. 1). This increase can lead to excessive conservatism in the results of simulations when the mode "0" is adopted.

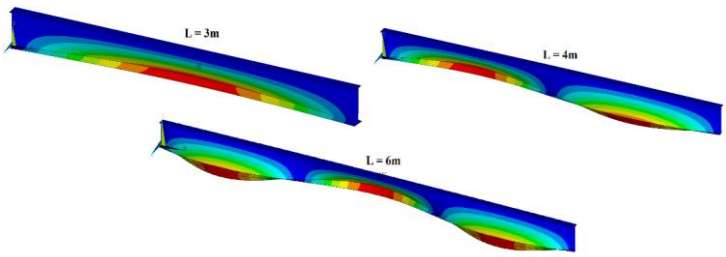

Fig. 1. Increase in half-wave numbers due to beam length increase.

To evaluate the suitability of utilizing mode “0” imperfections, models with the imperfection shapes that are normally found in steel beams that are relevant to the studied buckling mode, i.e., bending about the minor axis of inertia and bending of the web as well as combinations of these modes, were simulated. A preliminary analysis was made to determine which of these common manufacturing imperfection shapes produced the most critical value for the resistant moment. The imperfection amplitude was also varied from 60%, 100%, 140%, until 180% of the commonly observed values (obtained from [7], which measured imperfections of real beams). Besides that, combinations of global and local modes were tested. It was observed that the existence of the imperfection mode “1” did not conduct to a great reduction in the resistant moment with an increase in the span. This observation is consistent with standard’s prescriptions for determination of the resistant bending moment [8] but leads to a different behavior when compared to models with imperfection of mode “0”.

A method based on using the buckling mode, but with a reduced imperfection size was proposed and it led to less conservative results than the ones obtained with mode “0”, with better agreement with mode “1” imperfection and with the trend observed from [8].

REFERENCES

[1] Couto, C.; Vila Real, P.: Numerical investigation on the influence of imperfections in the lateral-torsional buckling of beams with slender I-shaped welded sections. Thin-Walled Structures 145, 106429 (2019).

[2] Dias, J. V. F.; Fakury, R. H.; Oliveira, J. P. S.; Calenzani, A. F. G.: Elastic critical moment of lateral-distortional buckling of steel-concrete composite beams under uniform hogging moment. International Journal of Structural Stability and Dynamics 19(07), 1950079 (2019).

[3] Gérard, L.; Li, L.; Kettler, M.; Boissonnade, N.: Recommendations on the geometrical imperfections definition for the resistance of I-sections. Journal of Constructional Steel Research 162, 105716 (2019).

[4] European Committee for Standardization – EN-1993-1-1:2005. Eurocode 3: Design of steel structures – Part 1-1: General rules and rules for buildings. Brussels (2005).

[5] European Committee for Standardization – EN-1993-1-5:2006. Eurocode 3: Design of steel structures – Part 1-5: Plated structural elements. Brussels (2006).

[6] Teixeira, F. B.: Análise numérica de perfis alveolares de aço. Master of science’s thesis. Universidade Federal de Minas Gerais. Belo Horizonte (2017). (In Portuguese)

[7] Shi, G., Zhang, Z., Zhou, L., Yang, L., Zhou, W.: Experimental and numerical investigation on Local-Overall interactive buckling behavior of welded I-section steel columns. Thin-Walled Structures 151, 106763 (2020).

[8] European Committee for Standardization – EN-1994-1-1:2004. Eurocode 4: Design of composite steel and concrete structures – Part 1-1: General rules and rules for buildings. Brussels (2004).

ACKNOWLEDGMENTS

The authors gratefully acknowledge the support provided by the Brazilian public agencies CNPq, CAPES, FAPEMIG and UFMG.

Design Resistant Axial Force calculation based on NBR-14762

L. Mapa*, D. Resende, A. Miranda

Graduate Program in Civil Engineering, Federal University of Ouro Preto, Brazil
**Corresponding author: lidianne.pinto@aluno.ufop.edu.br*

Keywords: Resistant axial force, NBR 14762, cold-formed steel section

1.INTRODUCTION

The Cold-formed steels are light and easy to transport highly used in steel structures. These can be manufactured in different and desirable forms (Kaleeswaran et al., 2020; Vy et al., 2020).

In order to calculate the compressive strength of cold formed profiles, it is necessary to take into account the local buckling (Winter Equation) and the overall buckling of the element. Traditionally, cold-formed steel projects in Brazil are carried out based on ABNT NBR 14762, which is based on the Effective Width Method and the Effective Section Method. The latter was recently included in the standard (Batista, 2009; Batista, 2010; Couto et al., 2014).

In this work, the resistant calculation force N,rcd, of cold hardened steel U and Z is investigated by the ABNT NBR 14762 standard considering the effective section method. As it includes include different configurations.

2. METHODOLOGY

Referring to the ABNT NBR 14762 standard, the effects of global buckling and the effects of local buckling were calculated including the interaction with global buckling, the equations are described in the previous section. For calculation purposes, the lengths of L = 2.0 m, L = 3.0 m, L = 4.5 m and L = 6 were considered.

The Z series profiles were initially considered asymmetrical, but in this profile the centroid O coincides with the torsion center (x0, y0), this causes the torsion centers to be x0 = 0 and y0 = 0 in the equation item 9.7.2.3 . (ABNT NBR 14762). Thus, specifically for the stiffened Z profiles analyzed, the analysis as an asymmetrical or symmetrical profile at one point, generates the same results for resistant axial force of calculation (NcRd), according to the procedure indicated in item 9.7.2.3 of NBR 14762.

The hardened U series profiles are symmetrical in relation to the x axis. Therefore, the calculation methodology indicated in item 9.7.2.2 of the aforementioned standard was followed.

3. RESULTS

With the results obtained, it was observed that the profile calculation resistance decreases as the bar length increases. As the strength of the stiffened profile is increased, the resistant design force increases. This is because, in addition to the gain of inertia, the local buckling coefficient kl increases and causes the axial strength of local elastic buckling to increase, which in turn decreases the slenderness value.

When considering the same profile series and the increase in thickness, the resistant calculation force, Nc, rd, is increased, indicating greater profile stability.

Analyzing series of Z profiles that differ only in terms of the bw dimension (larger dimension of the Z profile), it is observed that there was a small reduction in the resistant axial force of calculation, Nr, cd. This is because despite the fact that profiles with a larger bw dimension have greater inertia, there is a reduction in the axial strength of elastic buckling Nl which causes the buckling slenderness to increase.

It appears that the axial flexural buckling axial force in relation to the main y axis is always the lowest for the calculation of the Ze profile, while for the Ue profile the Nexz is predominantly smaller (flexural-torsion global buckling).

In general, it can be concluded that the greater the length of the profile, the lower the axial force of global elastic buckling. This causes the reduced slenderness to be increased, which in turn, makes the reduction factor of the resistant axial compression force smaller. This factor is directly proportional to the resistant axial force of calculation. For short columns the axial force reduction factor tends to approach 1 (2 m), for long columns (6 m) this value is less than 1, and the resistance strength value decreases considerably. For greater lengths, an increase in the effective area was also observed, however, the decrease in the reduction factor was decisive.

The comparative analysis between the Ue and Ze profiles indicated that as the profile thickness and the length of the bar increases, the resistance of the stiffened Z-type profile approaches the resistance of the stiffened U-profile and, in some cases, is even higher.

REFERENCES

[1] C. Kaleeswaran, R. Saravanakumar, D. Vivek, K.S. Elango, R. Gopi, D. Balaji,A study on cold formed steel compression member - a review, Materials Today: Proceedings, 2020,ISSN 2214-7853.

[2] Son Tung Vy, Mahen Mahendran, Thananjayan Sivaprakasam, Built-up back-to-back cold-formed steel compression members failing by local and distortional buckling, Thin-Walled Structures, 2020, 107224.

[3] Eduardo de Miranda Batista, Local–global buckling interaction procedures for the design of cold-formed columns: Effective width and direct method integrated approach, Thin-Walled Structures, Volume 47, Issue 11, 2009, Pages 1218-1231.

[4] Carlos Couto, Paulo Vila Real, Nuno Lopes, Bin Zhao, Effective width method to account for the local buckling of steel thin plates at elevated temperatures, Thin-Walled Structures,mVolume 84, 2014,Pages 134-149.

[5] Eduardo de Miranda Batista, Effective section method: A general direct method for the design of steel cold-formed members under local–global buckling interaction,Thin-Walled Structures, Volume 48, Issues 4–5, 2010, Pages 345-356.

Constraint on the local buckling of the steel plate, provided by the concrete component in composite steel-concrete sections under pure compression

D. A. Barbosa[a*], R.B. Caldas[a], Hermes Carvalho[a], Ana Lydia Reis de Castro e Silva[a] and Jorge Fernando dos Reis[a]

[a]*Structural engineering department, Federal University of Minas Gerais, Brazil*
**Corresponding author: engdenisebarbosa@gmail.com*

Keywords: buckling; steel-concrete composite; rigid medium, compression.

ABSTRACT

The local elastic buckling force of a steel plate in contact with a rigid medium constrained, such as concrete, is invariably higher than without the presence of a rigid medium, as concrete constrains the free formation of buckling waves, forcing them to move away from the concrete (Fig. 1 (a)). (Uy and Bradford [3]).

In addition, previous research (Wright [6] and Uy [5]) has shown that each wall of a box section filled with concrete can be treated as an internal plate element with all edges set in contact with the concrete (Fig 1 (b) (c)), and that the minimum local elastic buckling force of a steel plate with all the edges clamped and under pure compression occurs for an aspect ratio equal to 1.0.

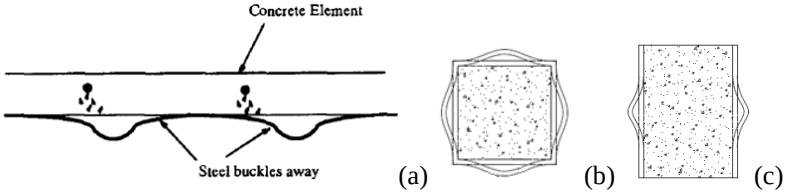

Fig. 1. Buckling mode: of the steel plate constrained by concrete (Uy and Bradford, 1996) (a); transversal in a box section (b) and longitudinal in a box section (c)

The most recent research (Huang et al. [1], Song et al. [2]) considers in the computational modeling of sections steel box with concrete component, the contact interaction (non-linear) between the steel plate and the concrete component (solid element).

Thus, static post-critical analysis using the Riks Method often presents convergence problems, and quasi-static analysis is used to obtain the solution to the problem, which increases computational time. Therefore, the objective of the present work is to validate the simulation of transversal (Fig. 1 (b)) and longitudinal (Fig. 1 (c)) constraints to the local buckling of the steel plate, provided by the concrete component, by means of clamped supports, in composite steel-concrete sections under pure compression.

The columns in steel box section filled with concrete studied by Uy [4], Uy [5], Huang et al. [1] and Song et al. [2] were adopted in the present study, and then analyzed numerically in the Abaqus program by the Riks Method, using clamped supports (Fig. 2) with the objective of forming plates with the four edges set and an aspect ratio equal to 1.0, and simulate the constraints provided by the concrete to the local buckling of the steel plate.

The numerical results obtained ("force versus deformation" curves) in the present study were compared with the numerical, experimental and theoretical results of the cases studied in the literature, including the standard EN 1993-1-5:2006. Fig. 3, for example, shows the "force versus deformation" curve for the FB80-2 specimen studied by Huang et al. [2], which shows the agreement between the numerical results of the

present study (blue curve) with those obtained by Huang et al. [2]. With regard to the amount of cases studied, the average of the "numerical of the present study / experimental of the previous research" and "numerical of the present study / numerical of the previous research" is approximately 1.0, and the standard deviation (SD) is less than 0.1.

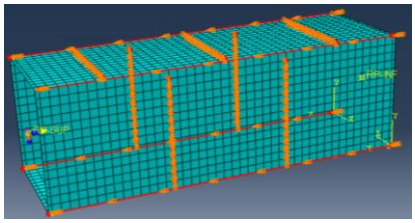

Fig. 2**.** Clamped supports constraints - Specimen FB80-2

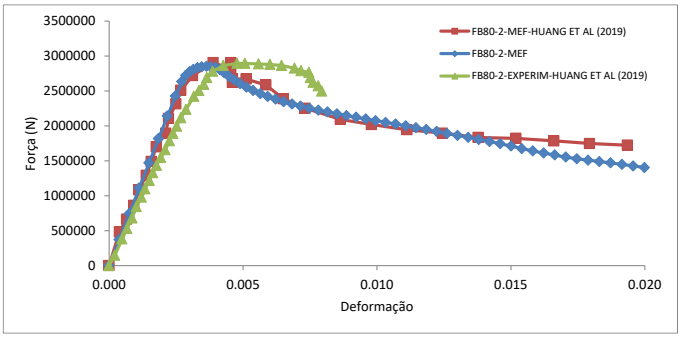

Fig. 3**.** Numerical results versus experimental and numerical results - Huang et al. [2] - Specimen FB80-2

Therefore, the consideration of clamped supports in nodal lines to simulate the local buckling constraints in the steel plate, provided by the concrete component, has been validated numerically.

REFERENCES

[1] HUANG, Zhichao; LI, Dongxu; UY, Brian; THAI, Huu-Tai ; HOU, Chao. Local and post-local buckling of fabricated high-strength steel and composite columns. Journal of Constructional Steel Research, v. 154, p. 235-249, 2019.

[2] SONG, Yuchen; LI, Jie; CHEN, Yiyi. Local and post-local buckling of normal/high strength steel sections with concrete infill. Thin-Walled Structures, v. 138, p. 155-169, 2019.

[3] UY, Brian; BRADFORD, M. A. Elastic local buckling of steel plates in composite steel-concrete members. Engineering Structures, v. 18, n. 3, p. 193-200, 1996.

[4] UY, Brian. Local and post-local buckling of concrete filled steel welded box columns. Journal of Constructional Steel Research, v. 47, n. 1-2, p. 47-72, 1998.

[5] UY, Brian. Local and postlocal buckling of fabricated steel and composite cross sections. Journal of Structural Engineering, v. 127, n. 6, p. 666-677, 2001.

[6] WRIGHT, H. D. Buckling of plates in contact with a rigid medium. Structural Engineer, v. 71, n. 12, 1993.

ACKNOWLEDGMENTS

The authors are grateful for the financial support in the form of support for research granted by CAPES, FAPEMIG, CNPq and UFMG.

Behavior of clothoidal longitudinal stiffeners on elastic stability of steel plates

J. F. Reis[a*], R. B. Caldas[b]

[a]*Departamento de Engenharia de Estruturas, Universidade Federal de Minas Gerais, Brasil*
[b]*Departamento de Engenharia de Estruturas, Universidade Federal de Minas Gerais, Brasil*
**Corresponding author: jorgereis@ufmg.br*

Keywords: stiffened plate; elastic stability; plate bukling.

ABSTRACT

The use of structural elements characterized as slender steel plates is very appropriate associated with the fact that it provides high mechanical strength and efficient material consumption. These elements are traditionally used by the naval and aeronautical industry, but also significantly in civil construction, in this case especially in structural designs with the need to overcome long-spans, such as bridges and overpasses.

A large amount of theoretical work is found in the literature regarding longitudinal stiffened plate buckling. Calculating the critical stress for simply supported plates submitted to uniform compression or pure shear [1] and later for cases of plates submitted to bending and different stiffener distributions [2-4]. Other authors have continued studies in the area of stiffened plate stability by means of theoretical, experimental and numerical analyses covering a great diversity of parameters and complex cases, analyzing the stress distribution, position, number and forms of stiffeners [5-13].

Therefore, the objective of this work is to develop a numerical study analyzing the stability of longitudinally stiffened plates with Clothoidal shape stiffeners, an efficient geometry used as a connector in steel-concrete mixed structures. The study compares the behavior of plates stiffened with the Clothoidal and the conventional flat section stiffener considering the load distribution (from pure bending to uniform compression), stiffener position and influence on stiffness.

The study was developed using the ABAQUS software [14] which uses the finite element method (FEM), through its function of linear perturbation analysis oriented to buckling problems. It was considered a symmetrical load, i.e. the load is applied on both sides of the plate in opposite directions and the boundary conditions were adopted in order to simulate a supported plate along its edges. A finite quadrilateral shell element with 8 nodes and 6 degrees of freedom per node and a mesh with width equal to b/40, where b is the height of the plate, has been adopted.

The study revealed that the models with Clothoidal stiffeners demonstrates similar behavior to the conventional flat type, presenting the same convergence in the optimum stiffness, and in adition, the behavior is identical when considering the use in this range of optimum stiffness between the two types, there are no significant differences associated on the parameters of the stiffener position and load distribution. Although, analyzing the variation in the buckling coefficient for stiffeners of both types with equal flat parts, it is identified that there are stiffness gains as a function of the clothoidal part, as shown in Figure 1.

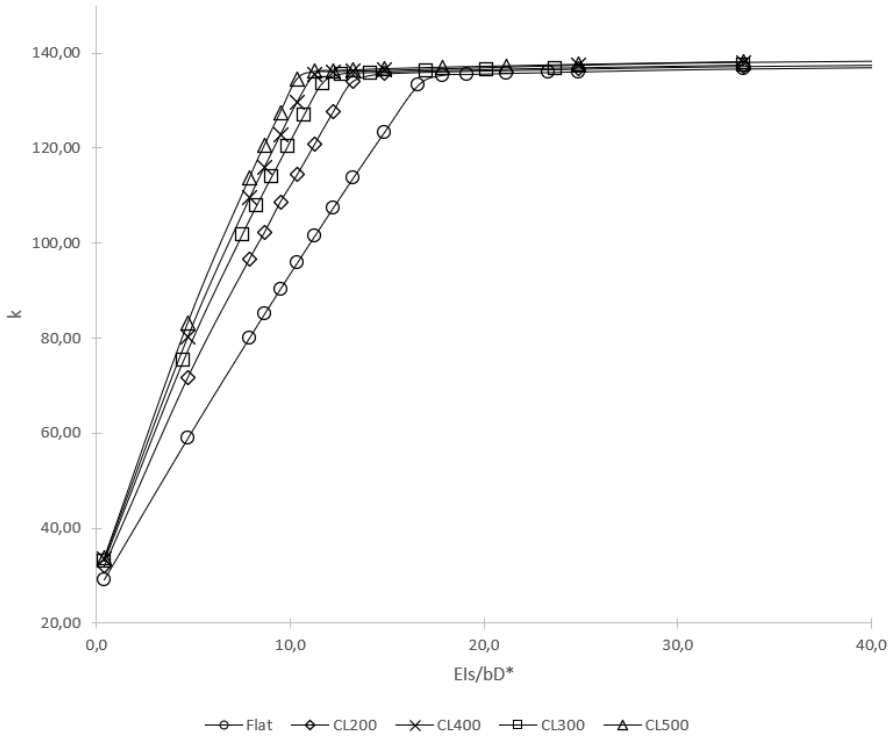

Fig. 1. K vs EI_s/bD^* for longitudinally stiffened plates under pure bending with a stiffener located at 0.2b.

REFERENCES

[1] TIMOSHENKO, S. P. Über die Stabilität versteifter Platten. Der Eisenbau, v. 12, p. 147-163, 1921.
[2] CHWALLA, E. Die Bemessung der Waagerecht ausgesteiften Stegbleche vollwandiger Träger. In: Kongress der Intern. Vereinig. fur Bruckenbau und Hochbau, 2., 1936, Berlim-Munich. Prelim Publ. IABSE, p. 957.
[3] LOKSHIN, A. S. On the calculation of plates with ribs. Journal of Applied Math. and Mech., v. 2, p. 225, 1935.
[4] BARBRÉ, R. Stability of rectangular plates with longitudinal or transverse stiffeners under uniform compression. Washington: National Advisory Committee for Aeronautics, 1939
[5] C. Dubas, Contribution to the study of buckling of stiffened plate, in: 3rd Congr. Int. Assoc. Bridg. Struct. Eng, 1948.
[6] K.C. Rockey, Web buckling and the design of web-plates, Struct. Eng. 36 (1958) 45–60.
[7] P.B. Cooper, Strength of longitudinally stiffened plate girders, J. Struct. Div. 93 (1967).
[8] K.C. Rockey, I.T. Cook, Optimum reinforcement by two longitudinal stiffeners of a plate subjected to pure bending, Int. J. Solids Struct. 1 (1965) 79–92.
[9] K.C. Rockey, I.T. Cook, The buckling under pure bending of a plate girder reinforced by multiple longitudinal stiffeners, Int. J. Solids Struct. 1 (1965) 147–156.
[10] M. Azhari, M.A. Bradford, Local buckling of I-section beams with longitudinal web stiffeners, Thin-Walled Struct. 15 (1993) 1–13.
[11] K.H. Frank, T.A. Helwig, Buckling of webs in unsymmetric plate girders, Eng. J. Second Quart. (1995) 43–53.
[12] M.M. Alinia, S.H. Moosavi, A parametric study on the longitudinal stiffeners of web panels, Thin-Walled Struct. 46 (2008) 1213–1223.
[13] E. Maiorana, C. Pellegrino, C. Modena, Influence of longitudinal stiffeners on elastic stability of girder webs, J. Constr. Steel Res. 67 (2011) 51–64.
[14] SIMULIA, D. S. ABAQUS 6.14 User's Manual. Dassault Systems, 2014.

ACKNOWLEDGMENTS

The authors are grateful for the financial assistance in the form of support for research granted by CAPES, FAPEMIG, CNPq and UFMG.

Numerical study of the Shear Lag effect in welded connections with channel cross section steel profiles

J.F. Reis[a*], B.M.S. Melo[a], A.L.R.C. Silva[a]

[a]*Structural engineering department, Federal University of Minas Gerais, Brazil*
**Corresponding author: reisjorgef@gmail.com*

Keywords: shear lag; steel structure; channels.

ABSTRACT

In structural steel designs it is very usual to use laminated bars under tensile with angle, channel and tee cross sections. These sections can be connected by means of welds or bolts, arranged in a variety of different combinations. It is particularly common to make connections by parts of the cross-section, which can lead to non-uniform stress distributions associated with the shear lag effect, which can be defined as a phenomenon that causes the loss of strength of a pulled bar connected only by parts of the cross-section [1].

The Brazilian standard ABNT NBR 8800:2008[2] and the American ANSI/AISC 360[3] approach this phenomenon by applying reduction coefficients depending on the cross section and the type of connection, applied in the cross-section area resulting in a reduced strength.

In addition, the literature contains a substantial number of studies on the effect of shear lag, but due to the different usable cross-sections and their dimensions and a wide variety of possible connections, it is difficult to precisely generalize reduction coefficients. In this sense, as there is no significant number of studies with welded channel connections, this study aims to analyze a range of channels pulled and connected by weld and to evaluate their behavior in relation to the already established propositions.

The study consists of 120 models (Fig. 1), considering 3 cross sections usual in structural projects, each with an eccentricity of connection, e_c. The analysis was carried out considering the following parameters: connection lengths, l_c; bar and connection length ratio, L/l_c; and use of transverse or non-transverse welding in conjunction with longitudinal welding.

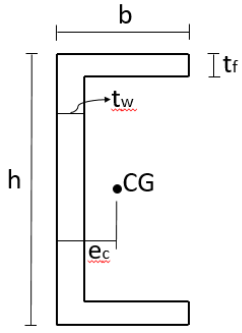

Section	h (mm)	b (mm)	t_w (mm)	t_f (mm)	e_c (mm)
A	70	40	5	7	13.83
B	100	50	5	7.5	16.86
C	125	65	6	8	21.11

Fig. 1. Sections used in the analyses

Validation was performed by comparison with experimental results obtained by Gonzalez [4], according to Table 1. Four double tensioned channels models were reproduced which presented a relative difference between 5-9% in comparison with the reduction coefficients obtained by Gonzalez [4].

Table 1. Validation of numerical models with [4]

Model	C_t - numeric	C_t [4]	Difference (%)
C-L-1b	0.972	0.89	9.17
C-L-2b	0.971	0.9	7.92
C-L-3b	0.973	0.91	6.88
C-B-1	0.967	0.92	5.07

Based on the results obtained, the influence of the length of the connection on the reduction coefficient for the three sections was evaluated (Fig. 2). For short connection lengths, the reduction coefficient exhibits smaller values, which increase as the length of the connection increases, reaching a plateau and remaining constant from a certain point forward. It is noticeable that for the class A profile, with the smallest dimensions, the coefficient remains constant with a value above 0.96 for the whole range of variation, unlike for larger profiles, such as class C which presents great variation, starting with values of 0.75 for a connection length of 50 mm until stability is reached approaching 0.94.

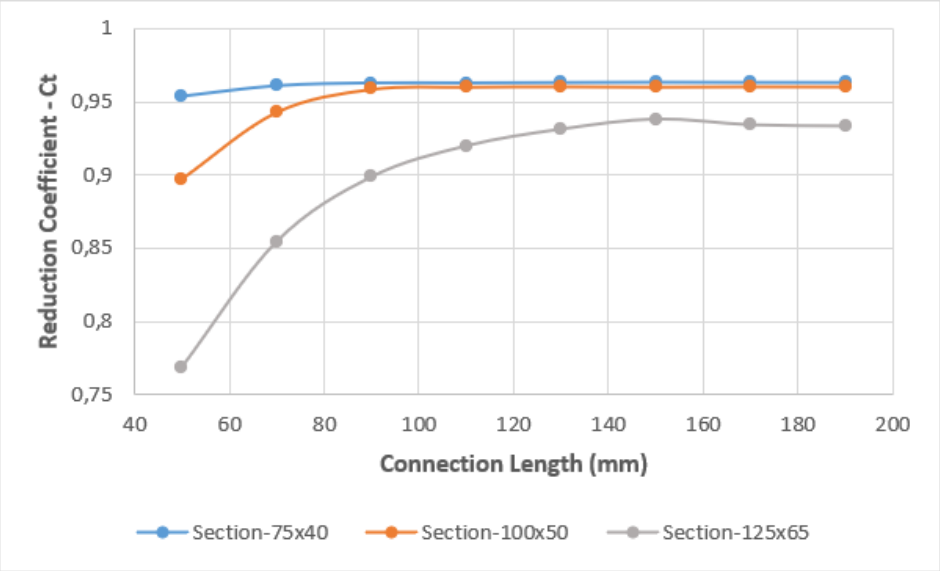

Fig. 2. Reduction coefficient as a function of connection length

REFERENCES

[1] Abi-Saad, G., Bauer. D. Analytical approach for shear lag in welded tension members. Canadian Journal of Civil Engineering(33), (2006).
[2] ABNT NBR 8800. Projeto de estruturas de aço e de estruturas mistas de aço e concreto de edifícios. Associação Brasileira de Normas Técnicas (2008).
[3] ANSI/AISC 360-10, Specification for steel buildings, American Institute of Steel Construction, Chicago, II, USA (2010).
[4] Easterling. W.S., Gonzalez. L. Shear lag effects in steel tension members. AISC Engineering Journal(3), 77-89, (1993).

ACKNOWLEDGMENTS

The authors are grateful for the financial support in the form of support for research granted by CAPES, FAPEMIG, CNPq and UFMG.

Numerical study for optimization of the buckling behavior of longitudinally stiffened plates under pure bending

B.M.S. Melo[a*], H. Carvalho[a], A.L.R. Castro e Silva[a], D.A. Barbosa[a], J.O. Ferreira Filho[b], R.B. Caldas[a]

[a]*Structural engineering department, Federal University of Minas Gerais, Brazil*
[b]*Institute for Sustainability and Innovation in Structural Engineering, University of Coimbra, Portugal*
**Corresponding author: bernardodematossilva@gmail.com*

Keywords: buckling; optimal position; minimum flexural rigidity; stiffeners.

ABSTRACT

Welded steel girders are used in bridges, whose main objective is to overcome large spans. Generally, these girders have slender web, so that the buckling of this element tends to occur before phenomena such as lateral torsional buckling and yielding. In these cases, although the web buckling does not represent the strength limit of the element, which still has considerable post-buckling reserve strength, it is common and important to use efficient stiffeners that ensure greater strength to the structure.

Several studies have been developed to evaluate the improvement of the buckling strength provided by longitudinal stiffeners in plates simply supported under pure bending. Alinia and Moosavi [1] and Vu et al. [2] used numerical analyses to study the optimum position of the longitudinal stiffener and to propose equations to determine the minimum flexural rigidity of this element in order to obtain a higher local buckling strength.

Although the elastic buckling behavior of longitudinally stiffened plates under pure bending was widely explored by researchers, most of the numerical analyses do not evaluate the influence of the slenderness of the web, do not consider panels with multiple stiffeners, and adopt for the height of the plate a value lower than that observed in practice. In this sense, the objective of the present paper is to evaluate, by means of the Finite Element Method (FEM), the elastic buckling behavior of a stiffened plate with simply supported edges when subjected to pure bending, in relation to the influence of the aspect ratio of the plate and the positions and flexural rigidity of 1, 2 and 3 stiffeners. Finally, the results of the minimum flexural rigidities are compared with the equations proposed by Alinia and Moosavi [1], Vu et al. [2], and the American standard, AASHTO LRFD [3].

The numerical model elaborated in the ABAQUS program (version 6.14) [4] was validated from the study developed by Vu et al. [5], according to Table 1.

Table 1. Validation of the numerical model with Vu et al. [5].

Aspect ratio, α	Stiffener dimensions	Buckling coefficient, k		Difference (%)
		Present study	Vu et al. [5]	
1.00	Unstiffened plate	25.610	25.650	0.156
1.00	35 x 5 (mm)	150.568	152.630	1.370
1.00	40 x 5 (mm)	152.576	154.080	0.986
1.00	45 x 5 (mm)	154.110	157.900	2.460

Forces varying linearly along the two transverse edges were applied to represent pure bending. Regarding the simply supported conditions of the plate edges, specific nodal constraints were considered in the displacements and rotations of the model, as illustrated in Fig. 1.

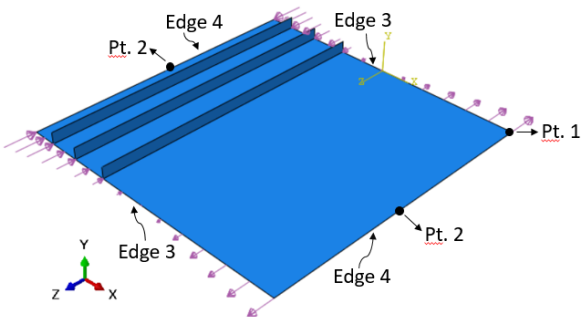

Point/Edge	U_x	U_y	U_z	θ_x	θ_y	θ_z
1	R	F	F	F	F	F
2	F	F	R	F	F	F
3	F	R	F	F	R	R
4	F	R	F	R	R	F

F - Free R - Restrained

Fig. 1**.** Boundary conditions.

Based on the results, the elastic buckling behavior of a plate stiffened by one stiffener was analyzed, considering the influence of the aspect ratio and flexural rigidity. It is observed that the greater the stiffness of the stiffener, the greater the buckling coefficient of the plate. However, the increase in this coefficient reaches a level, in which there is a transition from the global to the local buckling mode (Fig. 2). In relation to the aspect ratio, it can be concluded that plates with greater lengths require more rigid stiffeners to achieve higher values of this coefficient.

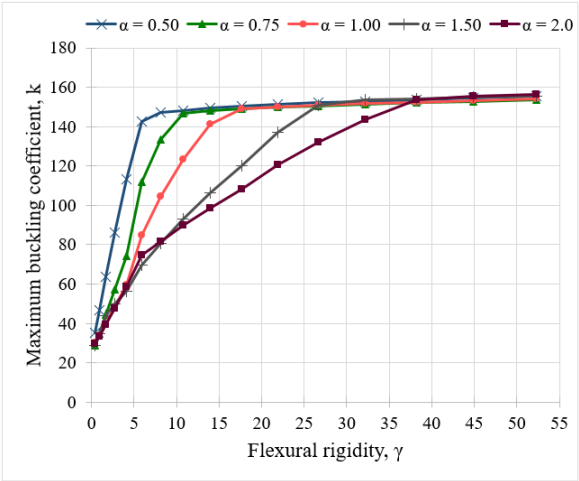

Fig. 2. Buckling coefficient as a function of flexural rigidity

REFERENCES

[1] Alinia, M.M., Moosavi, S.H. A parametric study on the longitudinal stiffeners of web panels. Thin-Walled Structures(46), 1213-1223 (2008).
[2] Vu, Q.V., Truong, V. H., Papazafeiropoulos, G., Graciano, C., Kim, S.G. Bend-buckling strength of steel plates with multiple longitudinal stiffeners. Journal of Constructional Steel Research(158), 41-52 (2019).
[3] AASHTO LRFD, Bridge design specifications. 6th edn. Washington, DC (2012).
[4] Simulia. Abaqus/CAE user's guide (2014).
[5] Vu, Q.V., Papazafeiropoulos, G., Graciano, C., Kim, S.G. Optimum linear buckling analysis of longitudinally multi-stiffened steel plates subjected to combined bending and shear. Thin-Walled Structures(136), 235-245 (2019).

ACKNOWLEDGMENTS

The authors are grateful for the financial support in the form of support for research granted by CAPES, FAPEMIG, CNPq and UFMG.

Review: Optimizing Magnetorheological Brake Model and Characteristics to Achieve Braking Torque

Agus Lutanto[a], Ubaidillah[b], Aditya Rio Prabowo[c*], Zainal Arifin[d]

[a,b,c,d]*Department of Mechanical Engineering, Universitas Sebelas Maret, Indonesia*
**Corresponding author: aditya@ft.uns.ac.id*

Keywords: Magnetorheological Fluid, Magnetorheological Brake, Magnetorheological Brake Model, Braking Torque.

ABSTRACT

Magnetorheological brake (MRB) is a brake by wire technology that utilizes the unique properties of magnetorheological fluid (MRF). MRF is composed of three particles, namely micro-ferromagnetic particles, base fluid, and additives. When the MRF is affected by a magnetic field (on-state), in a matter of milliseconds, the viscosity of the MRF will increase and form chain-like structures. Meanwhile, when it is not affected by the magnetic field (off state), the viscosity of MRF decreases and returns in the form of rheological properties [1]. Because the particle structure can be changed by adjusting the magnetic field and is responsive as well, MRF in the last two decades has been widely researched and applied as MRB. In the medical and robotic fields, low torque MRB is used in surgical aids [2], [3], haptic arms [4], and knee prostheses [5], [6]. Whereas in the automotive industry, high torque MRB is applied to clutches and brakes with torque ranging from 400 - 1400 Nm [7], [8]. Torque is an important parameter in MRB in addition to dimensions, response time, and working temperature. When the condition is on state, MRB must produce high braking torque but conversely, when it is off-state, the braking torque is expected to be zero [9]. Many designs and characteristics were developed to achieving goals. Table 1 shows some of the MRBs and their braking torque achievements. More details in this article will discuss the various designs, characteristics, and torque achievements of the MRB.

Table 1. Design and characteristic of the proposed MRB

Publication	Design MRB	Characteristic	Maximum Brake Torque (Nm)
Hidayatullah et al. [10]	Disc	Serpentine flux path	2.1
Nam and Ahn [1]	Disc	Double disc waveform	160
Yu et al. [11]	Disc	Multi path magnetic	1400
Ma et al. [12]	Disc	Multi disc	1000
Sayyaadi and Zareh [5]	Drum/cyinder	T-shaped	17
Wu et al. [13]	Drum/cyinder	Multi pole, multi layer	133
Wang et al. [14]	Drum/cyinder	Shear – squeeze mode	241
Nguyen et al. [15]	Hybrid	Inverted	155
Saini et al. [16]	Vane	Bypass rotary	73

REFERENCES

[1] T. H. Nam and K. K. Ahn, “A new structure of a magnetorheological brake with the waveform boundary of a rotary disk,” *Smart Mater. Struct.*, vol. 18, no. 11, p. 115029, Nov. 2009, doi: 10.1088/0964-1726/18/11/115029.

[2] A. M. Okamura, “Haptic feedback in robot-assisted minimally invasive surgery,” *Curr. Opin. Urol.*, vol. 19, no. 1, pp. 102–107, Jan. 2009, doi: 10.1097/MOU.0b013e32831a478c.

[3] D. Senkal and E. I. Konukseven, “Passive Haptic Interface with MR-Brakes for Dental Implant Surgery,” *Presence Teleoperators Virtual Environ.*, vol. 20, no. 3, pp. 207–222, Jun. 2011, doi: 10.1162/PRES_a_00045.

[4] X. Yin, S. Guo, and Y. Song, “Magnetorheological Fluids Actuated Haptic-Based Teleoperated Catheter Operating System,” *Micromachines*, vol. 9, no. 9, p. 465, Sep. 2018, doi: 10.3390/mi9090465.

[5] H. Sayyaadi and S. H. Zareh, “Prosthetic knee using of hybrid concept of magnetorheological brake with a T-shaped drum,” in *2015 IEEE International Conference on Mechatronics and Automation (ICMA)*, Aug. 2015, pp. 721–726, doi: 10.1109/ICMA.2015.7237574.

[6] J. Kim, “Development of an Above Knee Prosthesis using MR Damper and Leg Simulator,” pp. 3686–3691, 2001.

[7] C. Sarkar and H. Hirani, “Development of a magnetorheological brake with a slotted disc,” *Proc. Inst. Mech. Eng. Part D J. Automob. Eng.*, vol. 229, no. 14, pp. 1907–1924, 2015, doi: 10.1177/0954407015574204.

[8] K. Karakoc, E. J. Park, and A. Suleman, “Design considerations for an automotive magnetorheological brake,” *Mechatronics*, vol. 18, no. 8, pp. 434–447, 2008, doi: 10.1016/j.mechatronics.2008.02.003.

[9] F. Imaduddin, S. A. Mazlan, and H. Zamzuri, “A design and modelling review of rotary magnetorheological damper,” *Mater. Des.*, vol. 51, no. April, pp. 575–591, 2013, doi: 10.1016/j.matdes.2013.04.042.

[10] F. H. Hidayatullah, Ubaidillah, E. D. Purnomo, D. D. D. P. Tjahjana, and I. B. Wiranto, “Design and simulation of a combined serpentine T-shape magnetorheological brake,” *Indones. J. Electr. Eng. Comput. Sci.*, vol. 13, no. 3, pp. 1221–1227, 2019, doi: 10.11591/ijeecs.v13.i3.pp1221-1227.

[11] L. Yu, L. Ma, and J. Song, “Design, testing and analysis of a novel automotive magnetorheological braking system,” *Proc. Inst. Mech. Eng. Part D J. Automob. Eng.*, vol. 231, no. 10, pp. 1402–1413, 2017, doi: 10.1177/0954407016674394.

[12] L. Ma, L. Yu, J. Song, W. Xuan, and X. Liu, “Design, Testing and Analysis of a Novel Multiple-Disc Magnetorheological Braking Applied in Vehicles,” in *SAE Technical Papers*, Apr. 2015, vol. 2015-April, no. April, doi: 10.4271/2015-01-0724.

[13] J. Wu, H. Hu, Q. Li, S. Wang, and J. Liang, “Simulation and experimental investigation of a multi-pole multi-layer magnetorheological brake with superimposed magnetic fields,” *Mechatronics*, vol. 65, no. November 2019, p. 102314, Feb. 2020, doi: 10.1016/j.mechatronics.2019.102314.

[14] H. Wang and C. Bi, “Study of a magnetorheological brake under compression-shear mode,” *Smart Mater. Struct.*, vol. 29, no. 1, p. 017001, Jan. 2020, doi: 10.1088/1361-665X/ab5162.

[15] Q. H. Nguyen, J. C. Jeon, and S. B. Choi, “Optimal Design of an Hybrid Magnetorheological Brake for Middle-Sized Motorcycles,” *Appl. Mech. Mater.*, vol. 52–54, pp. 371–377, Mar. 2011, doi: 10.4028/www.scientific.net/AMM.52-54.371.

[16] R. S. T. Saini, S. Chandramohan, S. Sujatha, and H. Kumar, “Design of bypass rotary vane magnetorheological damper for prosthetic knee application,” *J. Intell. Mater. Syst. Struct.*, p. 1045389X2094257, Jul. 2020, doi: 10.1177/1045389X20942577.

Automatic detection of exposed steel rebars based on deep-learning techniques and Unmanned Aerial Vehicles

P. Lopes [a,*], D. Ribeiro [b,*], R. Santos [b], R. Cabral [c], R. Calçada [c]

a School of Engineering, Polytechnic of Porto, Porto, Portugal
b CONSTRUCT - LESE, School of Engineering, Polytechnic of Porto, Porto, Portugal
c CONSTRUCT - LESE, Faculty of Engineering, University of Porto, Porto, Portugal
** Corresponding author: 1090431@isep.ipp.pt*

Keywords: Remote inspection, Reinforced Concrete (RC), concrete structures, exposed steel rebars, Unmanned Aerial Vehicles (UAVs), Convolutional Neural Network (CNN).

Reinforced concrete is one of the most common materials used worldwide on the construction of civil engineering infrastructures. However, over time, reinforced concrete buildings inevitably begin to suffer from anomalies that compromise their durability and functionality. Continuous monitoring, maintenance and rehabilitation of civil engineering infrastructures are of paramount importance to ensure their structural integrity [1]. Researchers and engineers have been developing several methodologies to perform automatic and lower cost inspection procedures for engineering infrastructures using remote and contactless technologies.

Advances in Unmanned Aerial Vehicle (UAV) technologies have produced low-cost and high-mobility UAVs which are rapidly expanding their applications on real-world civil engineering [2]. UAVs allow to perform the structural health monitoring and surface inspections, both based on high-resolution images, on large-scale civil engineering structures, facilitating the anomalies identification [3]. Convolutional Neural Networks (CNNs) are a deep learning neural network sketched for processing structured arrays of data. This technique has revolutionized autonomous image classification and object identification in the last decade. Applications of deep CNNs in UAV assisted inspections has begun to attract researchers for a more robust non-contact damage detection [4]. Although studies have shown the successful application of deep learning techniques to detect damage on concrete structures, namely cracks identification, the literature have rarely shown its application on exposed steel rebars. Having this in mind, this article presents the development and implementation of computational tools for automatic detection of exposed steel rebars using CNNs and UAVs.

The process of creating an efficient CNN follows two essential steps. First, the constitution of a database of images and second the algorithm's training and validation. The database should cover the most varied scenarios that can be found in a real-world environment and involved capturing images in real context as well as images online. Then, the images were divided in a 227×227 pixels resolution format for the pre-trained network. Two categories were created for training: i) positive label, for exposed steel rebars, and ii) negative label for intact concrete surface. A data augmentation technique was applied to the positive label images to enlarge the size of the database based on heuristic image transformations (lightning, contrast, blur, etc.). In total 40 000 images were used for training and validation, equally divided by the two categories. Using the pre-trained network *AlexNet*, 80% of the original database was used for training and 20% for validation. The training took about 8 hours in a mid-range desktop, obtaining an accuracy of 96.6%. A dedicated algorithm was also developed to apply the trained CNN on images of any size, based on regions division approach (R-CNN), as well as highlighting the regions where the exposed steel rebars were detected.

The tool was applied to the remote inspection of *Monte da Virgem* telecommunications tower, which is the tallest building of its type in Portugal with a total height of 177 m. Using an UAV, several proximity photographs were taken of the structure, which were processed by the developed tool based on an R-CNN.

Fig. 1 presents two of the captured images, the original and the processed by R-CNN computational tool.

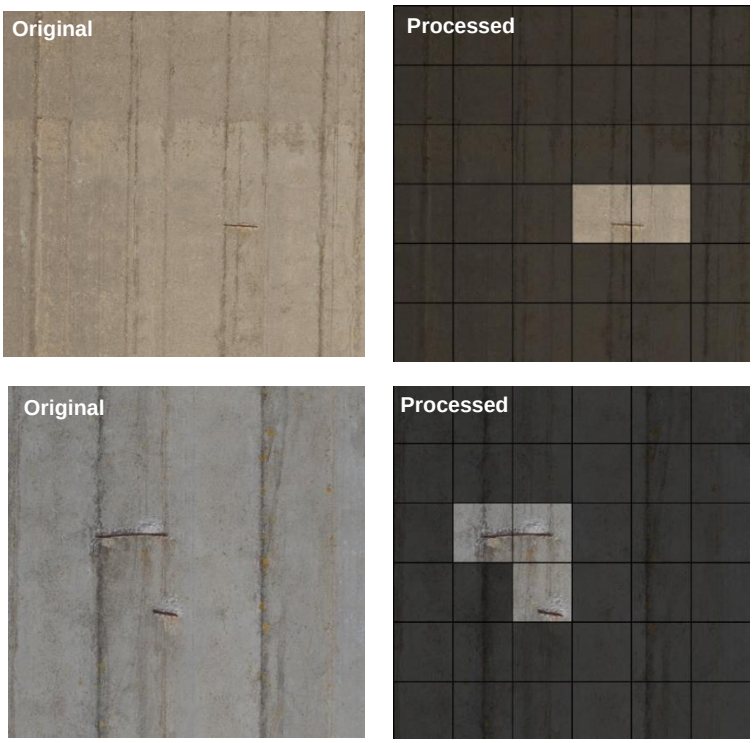

Fig. 1. Images captured on the remote inspection of Monte da Virgem Tower: original versus processed by R-CNN algorithm.

As can be seen in Fig. 1, the application of the R-CNN was fully successfully in the precise detection of the exposed steel rebars. In several detections performed the only few false positives were related to local corrosion spots as well as cracks associated with delamination. The high accuracy achieved demonstrates how the CNNs can be a promising technique in supporting the inspection of structures in the upcoming future.

REFERENCES

[1] H.-N. Li, L. Ren, Z.-G. Jia, T.-H. Yi, and D.-S. Li, State-of-the-art in structural health monitoring of large and complex civil infrastructures, Civil Structural Health Monitoring 6 (1) (2016) 3-16, DOI: 10.1007/s13349-015-0108-9.

[2] S. Sreenath, H. Malik, N. Husnu, and K. Kalaichelavan, Assessment and Use of Unmanned Aerial Vehicle for Civil Structural Health Monitoring, Procedia Computer Science 170 (2020) 656-663, DOI: 10.1016/j.procs.2020.03.174.

[3] D. Ribeiro, R. Santos, A. Shibasaki, P. Montenegro, H. Carvalho, and R. Calçada, Remote inspection of RC structures using unmanned aerial vehicles and heuristic image processing, Engineering Failure Analysis 117 (2020), DOI: 10.1016/j.engfailanal.2020.104813.

[4] K. Chaiyasarn, Crack Detection in Historical Structures Based on Convolutional Neural Network, International Journal of GEOMATE 15 (51) (2018), DOI: 10.21660/2018.51.35376.

ACKNOWLEDGMENTS

This work was financially supported by: Base Funding - UIDB/04708/2020 and Programmatic Funding - UIDP/04708/2020 of the CONSTRUCT - Instituto de I&D em Estruturas e Construções.

Nonlinear Analysis of Storage Tanks Assisted by Laser Scan Dimensional Inspection Techniques.

M.A. Lopes[a], F.J.C.P. Soeiro[a,b], J.G. Santos da Silva[a,b*]

[a]*Mechanical Engineering Postgraduate Programme (PPG-EM), State University of Rio de Janeiro, Brazil.*
[b]*Civil Engineering Postgraduate Programme (PGECIV), State University of Rio de Janeiro, Brazil.*
**Corresponding author: jgss@uerj.br*

Keywords: storage tanks; integrity assessment; nonlinear structural analysis.

ABSTRACT

An analysis methodology for assessment of atmospheric storage tanks integrity is developed in this investigation. The analysed tank presents 45 m diameter and 14 m height, approximately, and is constructed based on the use of ASTM A-283 steel plates. The laser scan technique is used for dimensional inspection of a damaged surface of the actual storage tank, which presents deformations on its shell. The results of the laser scan inspection are used to build a finite element model, considering the damages measured and precisely representing the imperfections. Fitness-For-Service criteria from API 579 design code are used to evaluate if the tank is suitable for operation, through finite element analysis considering geometric and material nonlinearities. Wind buckling behaviour is investigated and the structural steel shapes as wind girders are shown to be the best way aiming to prevent collapse from buckling. The main results of this study, see Figs. 1 to 3, show that the developed analysis methodology is very effective in order to assess the storage tanks integrity and to reduce maintenance costs.

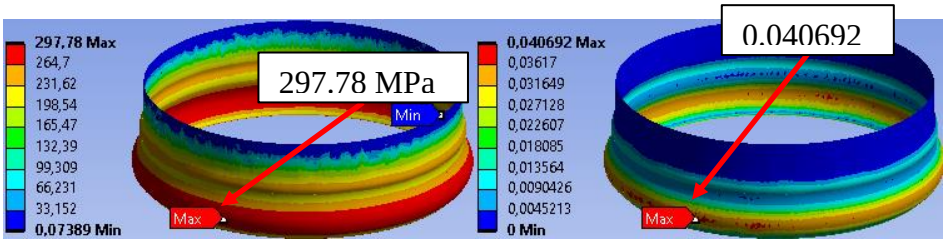

Fig. 1. Membrane plus bending stresses (left) and equivalent plastic strains (right) for plastic collapse assessment of the studied storage tank.

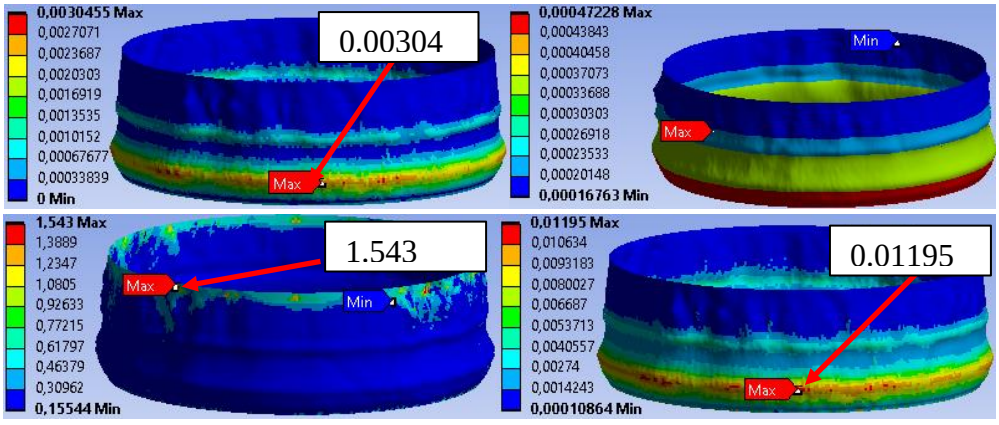

Fig. 2. Equivalent plastic (upper left) and cold forming (upper right) strains; strain limit (lower left) and local failure criterion (lower right) for local failure assessment of the investigated tank.

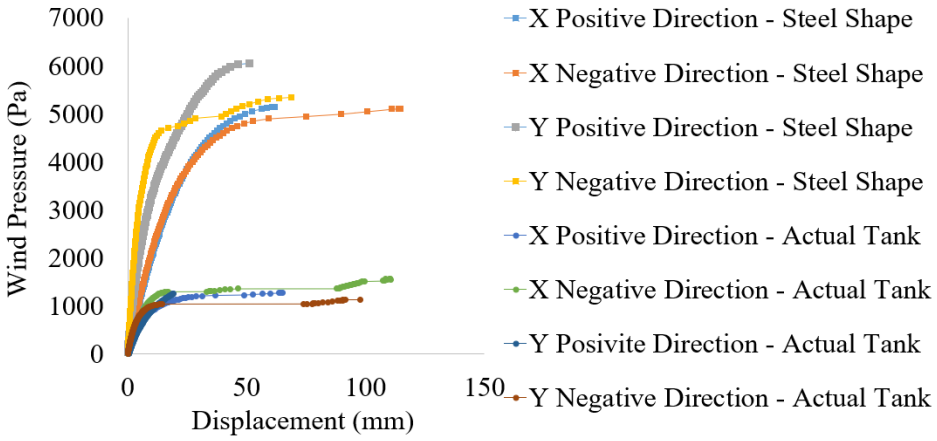

Fig. 3. Geometric and material with imperfection nonlinear buckling analyses results.

REFERENCES

[1] Lopes, M. A.: "Integrity Assessment: A Real Storage Tank Study Case". PhD Thesis (In Portuguese/In development), State University of Rio de Janeiro (2020).
[2] API 650: "Welded Tanks for Oil Storage". American Petroleum Institute, 12th ed. (2013).
[3] API 653: "Tank Inspection, Repair, Alteration, and Reconstruction". American Petroleum Institute, 5th ed. (2014).
[4] API 579-1/ASME FFS-1: "Fitness-for-service". American Petroleum Institute, The American Society of Mechanical Engineers (2016).
[5] Arumugam, U., Tandon, S., Gao, M., Krishnamurthy, R., Hanson, B., Rehman, H., Fingerhut, M.: "Portable Laserscan for In-Ditch Dent Profiling and Strain Analysis: Methodology and Application Development". In: Proceedings of the 2010 8th International Pipeline Conference, Volume 1, pp. 519-527. Alberta, Canada (2010).
[6] Nelson, G., Bradley, I., Fingerhut, M., and Yu, D.: "Application of Laser Profilometry for Fitness-for-Service Assessment on Pressure Vessel External Corrosion". In: Proceedings of the 2012 9th International Pipeline Conference, Volume 1, pp. 359. Alberta, Canada (2012).
[7] Allard, P. H., Fraser, J. S.: "Application of 3D Laser Method for Corrosion Assessment on a Spherical Pressure Vessel". In: The British Institute of Non-destructive Testing (BINDT) Material Testing Conference. Telford, United Kingdom (2013).
[8] Allard, P. H., Mony, C.: "Pipeline External Corrosion Analysis Using a 3D Laser Scanner". In: 18th World Conference on Nondestructive Testing, pp. 16-20. Durban, South Africa (2012).
[9] ASME B31G: "Manual for Determining the Remaining Strength of Corroded Pipelines". The American Society of Mechanical Engineer (2009).
[10] Samman, M., Tinoco, E. B., Marangone, F. C.: "Comparison of Stress and Strain Analysis Techniques for Assessment of Bulges in Coke Drums". In: Proceedings of the ASME 2014 Pressure Vessels and Piping Conference. Volume 3. California, USA (2014).
[11] A283/A283M-18: "Standard Specification for Low and Intermediate Tensile Strength Carbon Steel Plates". American Society for Testing and Materials (2018).
[12] ABNT NBR 6123: "*Forças devidas ao vento em edificações*". *Associação Brasileira de Normas Técnicas*, 66p. (1988).
[13] ASME PCC-2: "Repair of Pressure Equipment and Piping". The American Society of Mechanical Engineers (2016).

ACKNOWLEDGMENTS

The authors gratefully acknowledge the financial support for this research work provided by the Brazilian Science Foundation's CNPq, CAPES and FAPERJ.

Optimized FORM for accurate reliability assessment of concrete gravity dams

S. Ohadi[a], J. Jafari-Asl[a], M. Ben Seghier[b,c*], Hermes Carvalho[d], Jose A. F. O. Correia[e]

[a]*Department of Civil Engineering, University of Sistan and Baluchestan, Zahedan, Iran.*
[b]*Department, University, Country Division of Computational Mathematics and Engineering, Institute for Computational Science, Ton Duc Thang University, Ho Chi Minh City, Vietnam*
[c] *Faculty of Civil Engineering, Ton Duc Thang University, Ho Chi Minh City, Vietnam*
[d] *Department of Structural Engineering, Federal University of Minas Gerais, Belo Horizonte, Brazil*
[e]*INEGI, Faculty of Engineering, University of Porto, Rua Dr. Roberto Frias, 4200-465 Porto, Portugal*
**Corresponding author: benseghier@tdtu.edu.vn*

Keywords: FORM; Concrete gravity dam; Slime mould algorithm; Sliding Failure; Monte Carlo simulation.

ABSTRACT

Dams are one of the most important infrastructures in any country, which in case of failure may cause inevitable financial damages and human losses to the society. Among the major causes of dam failure is sliding failure that occurs under the influence of the reservoir water level. Reliability analysis methods allow the designer to provide an estimation of the safety levels and the most probable state of the failure by considering the different water levels of the reservoir that may occur. First Order Reliability Method (FORM) is one of the most common methods of the reliability analysis that is widely used to assess the reliability of structures. In this paper, a new method based on the first order reliability method (FORM) and Slime mould algorithm (SMA) for evaluating the reliability of concrete gravity dams is presented under the uncertainty of the inherent parameters of strength and load. The proposed method was first evaluated to solve several benchmark reliability problems and then used to assess the reliability of the sliding failure of the Sariyar dam in Turkey. The results of comparing the FORM-SMA method with the Monte Carlo simulation (MCS) and FORM showed that the proposed method, in addition to reducing the number of calls the limit state function, also has a high accuracy for calculating the probability of failure of concrete dams under sliding failure.

Use of the box-behnken method to decrease measurement uncertainty in the PIG MFL inspection technique

H.A. Costa Júniora, J.F. Barbosab, J.J. Oliveira Júniora, Carvalho, Hermes

[a]*Postgraduate in Mechanical Engineering, Federal University of Rio Grande do Norte, Natal, Brazil*
[b]*Technology Center, Federal, University of Rio Grande do Norte, Natal, Brazil*
[c]*Department of Structural Engineering, Federal University of Minas Gerais, 31270-901 Belo Horizonte MG, Brazil*
**Corresponding author: jbarbosa@ct.ufrn.br, hermes@dees.ufmg.br*

Keywords: pipeline inspection gauge; Box-Behnken; Magnetic Flux Leakage, in -line inspection;

ABSTRACT

The Pipeline Inspection Gauge (PIG) is widely used to carry out automatic inspections of the coating with non-destructive testing (NDT), the Magnetic Flux Leakage (MFL) technology is able to identify metallic losses caused by corrosion in long-distance cartons [1, 2]. Although the technique is widespread in the industry, it brings with it a high measurement uncertainty, causing some defects to be oversized or undersized. The purpose of this work is to analyze some parameters intrinsic to the MFL (Magnetic Flux Leakage) technique, such as: PIG (Pipeline Inspection Gauge) displacement speed, magnetization level and wave amplitude of the MFL signal, using the Box-Behnken statistical method to expose the factors that most influence the measurement uncertainty of the MFL tool. A performed-on site with 17 samples, using the ultrasound scan inspection technique (Fig. 1) to assess the real condition of the metal losses. It was observed that the parameter with the greatest influence on the measurement uncertainty is the wave amplitude (Fig. 2), however the combination of the three parameters mentioned above, provides a better answer in determining the measurement uncertainty. A significant factor is that the wave amplitude expresses different geometries for losses of thickness located in the body of the tube, if compared with losses located in the ZTA (Thermally Affected Zone). This can be explained by the modification of the crystalline structure of the material in the ZTA. In this way, pipeline monitoring and maintenance inspection routines, based on the combination of the three measurement parameters, will be able to prevent the spread of damage and improve the reliability of the entire pipeline and pipeline network.

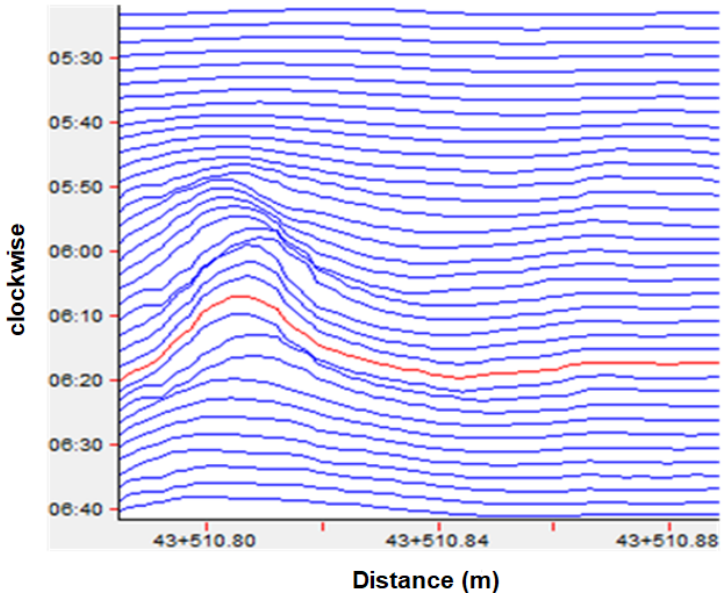

Fig. 1. MFL amplitude - Defect 1.

Fig. 2. Ultrasonic equipment fixed to the external wall of the pipe

REFERENCES

[1] Ramirez-Martinez, Antonio, et al. "Design and validation of an articulated sensor carrier to improve the automatic pipeline inspection." Sensors 19.6 (2019): 1394.
[2] Vanaei, H. R., A. Eslami, and A. Egbewande. "A review on pipeline corrosion, in-line inspection (ILI), and corrosion growth rate models." International Journal of Pressure Vessels and Piping 149 (2017): 43-54.

ACKNOWLEDGMENTS

Fatigue life prediction of S235 based on the strain energy model

Bruno Pedrosa[a*], José Correia[b], Carlos Rebelo[a], Grzegorz Lesiuk[c], Abílio Jesus[b], M. Veljkovic[d]

[a] *University of Coimbra, ISISE, Department of Civil Engineering, Coimbra, Portugal.*

[b] *INEGI & CONSTRUCT, Faculty of Engineering, University of Porto, Rua Dr. Roberto Frias, 4200-465 Porto, Portugal.*

[c] *Faculty of Mechanical Engineering, Department of Mechanics, Materials Science and Engineering, Wroclaw University of Science and Technology, PL-50370 Wrocław, Poland.*

[d] *Faculty of Civil Engineering and Geosciences, Delft University of Technology, Delft, Netherlands.*

**Corresponding author: bruno.pedrosa@uc.pt*

Keywords: Fatigue Life, S235, Strain Energy.

ABSTRACT

The traditional approach to model the fatigue phenomenon is to evaluate the initiation and propagation phases separately. However, recent scientific investigations were developed in which the FCG process is considered as successive crack re-initiations and, therefore, both initiation and propagation phases are physically similar. This methodology can be designated as a unified approach to fatigue [1–4].

In 1985, Glinka [2] introduced the use of strain-based fatigue local relations to model FCG processes. He developed the concept of discretization using elementary material blocks whose failure defines crack growth. Later on, new fatigue local models have been proposed. In 1999, Peeker and Niemi [3] proposed a model for fatigue crack propagation based on the superposition of the near-threshold and stable fatigue crack propagation regimes using cyclic elastoplastic stress-strain constants as well as strain-life constants. Then, Noroozi and Glinka [4–6] developed the UniGrow model based on the elastoplastic crack tip stress-strain history analysis in which the influence of the applied compressive stress is included. This model was developed using the Smith-Watson-Topper fatigue damage parameter. More recently, a crack propagation model based on residual stresses has been proposed by Correia et al [7], Hafezi et al [8], and Jesus et al [9] which considers the assumptions of the UniGrow model but the elastoplastic stress fields are obtained by finite element models. It is also important to refer that the implementation of probabilistic analysis to FCG models based on local approaches has been performed by Correia et al [7,10,11] and Bogdanov et al [12]. These FCG models have been also used in procedures to compute S-N curves of structural details. Correia et al [10,13,14] proposed a general procedure to obtain probabilistic fields for notched details.

In this paper, the fatigue life of S235 steel is analysed for the fatigue crack initiation phase considering the Huffman model [1]. It considers a damage parameter based on the strain energy density defined as:

$$\left(\frac{U_e}{U_d\rho_c}\right)\left(\frac{U_p^*}{U_d\rho_c}\right) = D = \frac{2N}{2N_f} \quad (1)$$

where U_e is the elastic strain energy density, U_p^* is the complementary strain energy density, ρ_c, is the critical dislocation density and U_d is the strain energy density.

The characterization of S235 concerning its cyclic elastoplastic stress-strain curve was previously studied by Carvalho *et al* [15]. This curve is defined with low-cycle fatigue tests performed under strain-controlled conditions following the ASTM E606 standard [16]. It was observed a good agreement between experimental data and Huffman model predictions. Concerning the value obtained for ρ_c, its mean value is in line with the expected values [13]. Frequentist inference is applied to find the optimum value.

In conclusion, it was observed that the application of the Huffman model to compute strain-life behaviour is reliable.

REFERENCES

[1] Huffman PJ. A strain energy based damage model for fatigue crack initiation and growth. Int J Fatigue 2016;88:197–204.

[2] Glinka G. A notch stress-strain analysis approach to fatigue crack growth. Eng Fract Mech 1985;21:245–61.

[3] Peeker E, Niemi E. Fatigue crack propagation model based on a local strain approach. J Constr Steel Res 1999;49:139–55.

[4] Noroozi A, Glinka G, Lambert S. A two parameter driving force for fatigue crack growth analysis. Int J Fatigue 2005;27:1277–96.

[5] Noroozi A, Glinka G, Lambert S. A study of the stress ratio effects on fatigue crack growth using the unified two-parameter fatigue crack growth driving force. Int J Fatigue 2007;29:1616–33.

[6] Noroozi A, Glinka G, Lambert S. Prediction of fatigue crack growth under constant amplitude loading and a single overload based on elasto-plastic crack tip stresses and strains. Eng Fract Mech 2008;75:188–206.

[7] Correia JAFO, de Jesus AMP, Fernández-Canteli A. A procedure to derive probabilistic fatigue crack propagation data. Int J Struct Integr 2012;3:158–83.

[8] Hadi Hafezi M, Nik Abdullah N, Correia JFO, De Jesus AMP. An assessment of a strain-life approach for fatigue crack growth. vol. 3. 2012.

[9] Jesus A, Correia J. Critical assessment of a local strain-based fatigue crack growth model using experimental data available for P355NL1 steel. J Press Vessel Technol 2013;135.

[10] Correia J. An Integral Probabilistic Approach for Fatigue Lifetime Prediction of Mechanical and Structural Components. PhD Thesis, Faculty of Engineering, University of Porto, Porto, 2014.

[11] Correia JAFO, de Jesus AMP, Fernández-Canteli A, Calçada RAB. Modelling probabilistic fatigue crack propagation rates for a mild structural steel. Frat Ed Integrita Strutt 2015;31:80–96.

[12] Bogdanov S, Mikheevskiy S, Glinka G. Probabilistic Analysis of the Fatigue Crack Growth Based on the Application of the Monte-Carlo Method to Unigrow Model. Mater Perform Charact 2014;3:20130066.

[13] Correia J, Huffman P, Jesus A, Cicero S, Fernández-Canteli A, Berto F, et al. Unified two-stage fatigue methodology based on a probabilistic damage model applied to structural details. Theor Appl Fract Mech 2017;92:252–65.

[14] Correia J, De Jesus A, Fernández-Canteli A. Local unified probabilistic model for fatigue crack initiation and propagation: Application to a notched geometry. Eng Struct 2013;52:394–407.

[15] Carvalho D, Silva A, De Jesus A, Fernandes A. Fatigue behaviour of structural steels. Comparison of Strain-life and Fatigue Crack propagation data. Mecânica Exp 2015;25:67–78.

[16] ASTM E 606. Standard Practice for Strain Controlled Fatigue Testing. Annual Book of ASTM Standards: American Society for Testing and Materials; 1998.

ACKNOWLEDGMENTS

The authors would like to acknowledge the Fundação para a Ciência e Tecnologia (FCT) for funding the Ph.D. scholarship SFRH/BD/145037/2019 and the researcher position (UIDB/04708/2020 and UIDP/04708/2020 - CONSTRUCT).

Design of Redundant Members for Latticed Steel Towers used in Power Transmission Lines

M.S. Rechtman[a], J.G. Santos da Silva[a*]

[a]*Civil Engineering Postgraduate (PGECIV), State University of Rio de Janeiro (UERJ), Brazil.*
**Corresponding author: jgss@uerj.br*

Keywords: latticed steel towers; power transmission lines; nonlinear analysis.

ABSTRACT

Lattice steel towers become essential elements to transmission systems are widely used as supports for these systems [1]. The lattice towers structural system is composed by primary and redundant members. The primary members (main members), baring the most of loads applied, carrying the loads from their application points to the foundation system. The redundant members are used to provide intermediate bracing points, resulting in a reduction of primary members unbraced lengths and also increasing capacity for compression [2].

In general, first-order elastic structural analysis is used to design lattice steel towers used in power transmission lines and the secondary effects (deflected structure) are ignored. Therefore, the forces in the redundant members are equal to zero; as a consequence, mostly of the projects do not be included redundant members in the finite element models [3]. In a second-order elastic structural analysis, secondary effects (structural displacement) could produce addition forces on the elements and may show redundant members are subjected to additional forces [4].

According to the standard ASCE 10 "Design of Latticed Steel Transmission Structures" [3] methodology, redundant members are subjected to forces between 1.5% to 2.5% of the forces acting on the primary member it supports. Three different analysis methods based on post buckling member behaviour models are described: method 1 assumes that the redundant member is capable of carrying compression forces on a geometrically buckled configuration; method 2 assumes that redundant members do not carry forces on a geometrically buckled configuration; and method 3 assumes that the redundant members are capable of carrying reduced forces on a geometrically buckled configuration.

Therefore, the main objective of this work is to develop an analysis methodology regarding the structural behaviour of lattice steel towers, evaluating the forces values acting on the redundant members and comparing with those calculated based on the ASCE 10 standard (Method 2) [3]. This way, several structural models of steel towers associated with a 500 kV transmission line, simple circuit, were analysed aiming to determine the forces acting on the redundant members based on a nonlinear structural analysis. The program PLS Tower R-14.2 was used for numerical modelling of the steel transmission towers based on the Finite Element Method (FEM). Thus, the forces values acting on the redundant member obtained in second-order elastic analysis were compared with those calculated according to the design standards (linear analysis).

The structural assessment consists of determine the redundant member of the investigated structural system that present the most relevant differences between the forces values calculated by the design standard recommendations and those determined based on the finite element numerical simulations (second-order elastic analysis). After that, having in mind its relevance to the system structural response (structural stability), the structural capacity of these elements was assessed according to the ASCE 10 [3], as well as primary members braced by them.

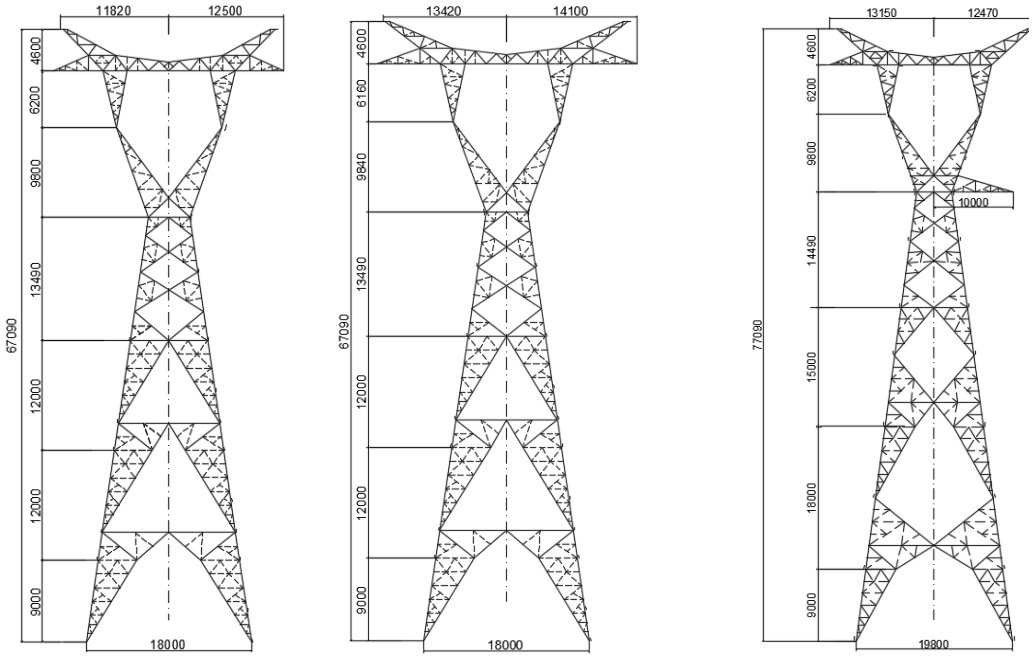

a) Light suspension tower (SL) b) Heavy suspension tower (SP) c) Transposition suspension tower (ST)

Fig. 1. Investigated steel towers.

The results obtained in this research work have indicated that the second-order elastic analysis is essential to understand the structural behaviour, distribution of loads, design and global stability of the structure. It is also recommended to avoid applying braces with small angles to the primary members so that they perform their function correctly. Finally, it must be emphasized that there is an interest of the authors in studying more deeply the behaviour of redundant members, analysing the components related to the absorption of forces, allowing optimizing the structures geometry for better knowledge of load distribution and structural behaviour.

REFERENCES

[1] Baran, E., Akis, T., Sen, G., Draisawi, A.: Experimental and numerical analysis of a bolted connection in steel transmission towers. Journal of Constructional Steel Research, n° 121, 253–260 (2016).
[2] Vazquez, J. C. V., Vazquez, I. R., Vazquez, A. H., et al.: Replacing steel members with composite members on transmission towers. Proceedings of the Institution of Civil Engineers - Energy, n° 172, 26–40 (2018).
[3] Design of Latticed Steel Transmission Structures Standards, ASCE 10, American Society of Civil Engineering, United States, 2015.
[4] Rao, N. P., Mohan, S. J., Lakshmanan, N.: A study on failure of cross arms in transmission line towers during prototype testing. International Journal of Structural Stability and Dynamics, vol. 5, n° 3, 435–455 (2005).
[5] Rao, P. N., Samuel, S. J., Mohan, et al.: Studies on failure of transmission line towers in testing. Engineering Structures, n° 35, 55–70 (2012).
[6] Design Criteria of Overhead Transmission Lines, IEC 60826, International Electrotechnical Commission, Switzerland, 2003.

ACKNOWLEDGMENTS

The authors gratefully acknowledge the financial support for this research work provided by the Brazilian Science Foundation’s CNPq, CAPES and FAPERJ.

Influence of the steel constitutive model in numerical analyses with shear connector applied on concrete-filled steel tubular columns

E. G. Silveira [a*], R. B. Caldas [b], H. S. Cardoso [c]

[a] *Eliane Gomes da Silveira- Department of Civil Engineering, Federal Institute of Education, Science and Technology of Southern Minas Gerais, Brazil.*
[b] *Rodrigo Barreto Caldas - Department of Structural Engineering, Federal University of Minas Gerais, Brazil.*
[c] *Hermano de Sousa Cardoso - ISISE – Department of Civil Engineering, University of Coimbra, Coimbra, Portugal.*
** Corresponding author: eliane.silveira@ifsuldeminas.edu.br*

Keywords: Composite structures of steel and concrete, concrete-filled steel tubular columns, shear connectors, numerical analysis, Crestbond.

ABSTRACT

Concrete-filled steel tubular columns (CFST) are an efficient and economical alternative, as they allow dispensing the use of formsworks, reduce the structures total weight and build more economical foundations. In addition, CFST have better toughness, ductility and bearing capacity when compared to traditional reinforced concrete columns. The shear connectors are applied when the adhesion between the filling concrete and the tubular profile is not sufficient to transmit the shear forces. In this work, experimental results are used with steel plate shear connectors *Crestbond* applied in rectangular tubular profiles, given the concrete confinement different behavior when compared to circular profiles. Numerical simulations were carried out in the ABAQUS program, changing the steel constitutive model applied to the connector and tubular profile, in order to obtain a model with satisfactory behavior against to the experimental results in terms of load *versus* relative slip. The proposed steel stress-strain relationships showed satisfactory for the representation of load transfer in PMPC with *Crestbond* connector, allowing future applications with the numerical model in behavior studies with parameters variation.

The main experimental results used in this article context are models I and J, executed with 320 x 250 x 8,2 mm tubular profiles (f_y = 363 MPa and f_u = 467 MPa) with two *Crestbond* connectors (f_y = 390 MPa and f_u = 508 MPa) filled with conventional concrete (f_{ck} = 25 MPa). Model I specimens did not contain reinforcement, while model J specimens had stirrups and longitudinal reinforcement.

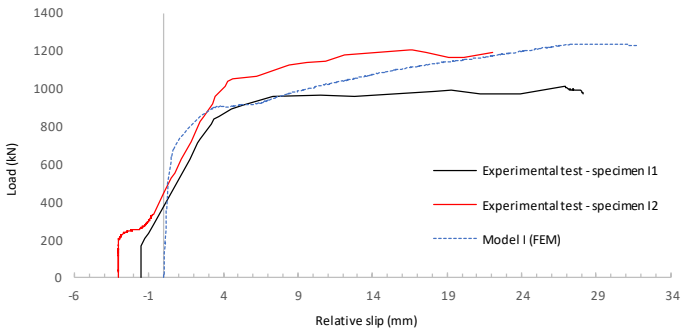

Fig. 1. Load versus relative slip curves for experimental and numerical results with model I [1].

The load versus relative slip curves with the experimental tests results and numerical results presented in [1] and [2] for CFST with rectangular profiles demonstrate that despite the good initial correspondence in terms of ultimate load and ultimate relative slip, the numerical curve always show an upward behavior

for the load (Fig. 1), unlike what is observed experimentally in which the load tends to stabilize as the relative slip grow up. In this article, some changes are proposed in the numerical model used by [1] for its adjustment, achieving results closer to the experimental tests.

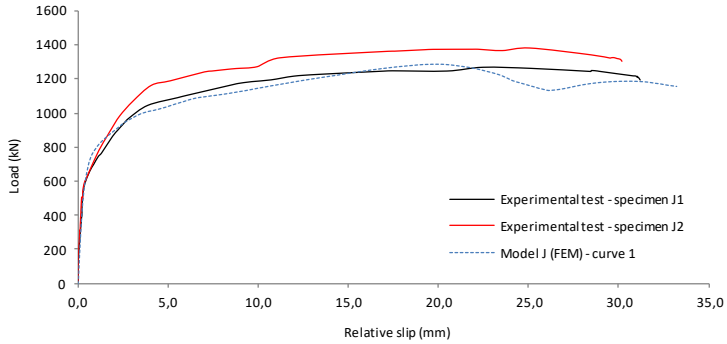

Fig. 2 Load versus relative slip with the proposed steel constitutive model applied (Curve 1).

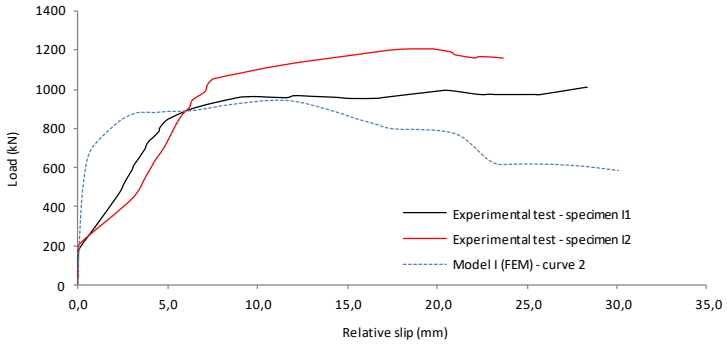

Fig. 3 Load versus relative slip with the proposed steel constitutive model applied (Curve 2).

The curves for the steel constitutive model of shear connector analyzed in this work showed good results in the numerical simulations when compared to the initial results presented by [1]. When compared to the experimental results they are more conservative with descending branches after reaching the maximum load capacity of the composite system. The elastoplastic curve with a descending branch (Curve 2 - Fig. 3) led to more conservative results than the first proposal (Curve 1 - Fig. 2), which makes it more reliable for application in parametric studies of composite dowels in CFST with rectangular profiles.

REFERENCES

[1] CARDOSO, H. S. Avaliação do comportamento de conectores constituídos por chapas de aço com recortes regulares - ênfase em conectores de geometria Crestbond aplicados em pilares mistos. Tese de Doutorado. Universidade Federal de Minas Gerais. Belo Horizonte. 2018.
[2] CARDOSO, H. S.; AGUIAR, O. P.; CALDAS, R. B.; FAKURY, R. H. Composite dowels as load introduction devices in concrete-filled steel tubular columns. Engineering Structures. v 2019. 2020.

ACKNOWLEDGMENTS

This work was funded by the brazilian research agencies CAPES, CNPq and FAPEMIG. The first author is also grateful for the support provided by IFSULDEMINAS.

Comparative study of steel-concrete composite beams for railway bridges

R. Santos[a*], H. Carvalho[b], R. B. Caldas[b], T. N. Bittencourt [a], R. F. Santos[c]

[a]*Department of Structural and Geotechnical Engineerings, University of São Paulo, Brazil*
[b]*Department of Structural Engineering, Federal University of Minas Gerais, Brazil*
[c]*Department of Civil Engineering, Federal University of Viçosa, Brazil*

**Corresponding author: ruanrichelly@usp.br*

Keywords: steel-concrete composite beams; railway bridges; composite dowels; Preflex beams.

ABSTRACT

Due to the growing demand for more economical, efficient, and sustainable bridges, constructive methods that provide such attributes become necessary. In this sense, steel-concrete composite bridges have been widely used worldwide for their remarkable structural performance, which combines the benefits of both steel and concrete elements. The shear connection in these structures allows the optimized use of both materials, improving stiffness and strength. For small and medium spans bridges, the typical solution of a concrete slab and stell I-girders (Fig. 1.a) often displays the most economical results. Nevertheless, other solutions, such as steel-concrete composite beams with composite dowels (Fig. 1.b) and pre-cambered composite beams (Preflex beams, Fig. 1.c), emerge as innovative alternatives for bridge construction.

The use of composite dowels in the girder web provides a way to overcome the inherent complexities regarding installing stud bolts and enables the steel top flange, commonly used only to fix the shear connectors, absence. These characteristics result in an economical, rationalized, and time-saving construction process. Furthermore, the oxy-cutting procedure adopted to obtain the composite dowels provides a system without welds, which increases the beam fatigue capacity [1]. On the other hand, the pre-cambered composite beam system consists of a pre-casted concrete bottom flange prestressed through the steel beam's pre-deflection. This particular configuration ensures gains in stiffness, flexural strength, and the increase of slenderness [2].

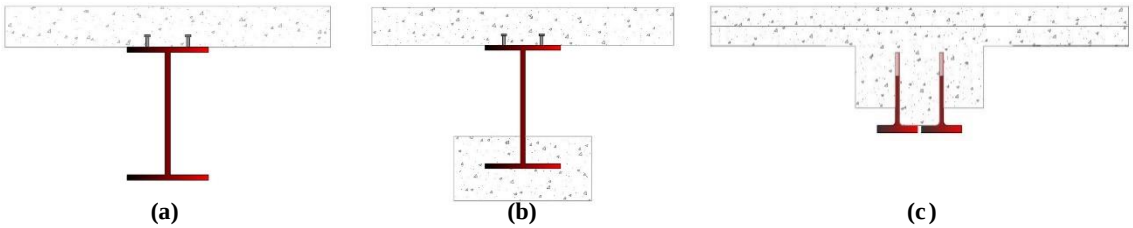

(a) **(b)** **(c)**

Fig.1: Cross-sections examples of a) traditional solution, b) pre-cambered beam, and c) beam with composite dowels

Given the benefits of these alternative constructive configurations, this work has aimed to develop a comparative study of the different solutions for composite beams to delimitate their efficiency and economy. Furthermore, developing guidelines for the design and execution of these systems [3] contribute to their dissemination in countries such as Brazil, in which their application is non-existent. Thus, case studies have been carried out according to the Eurocode design provisions [4]. Nevertheless, composite dowels design has been covered by the Z-26.4-56 [5] technical approval. Also, the procedures for calculating stresses and deflections due to creep and shrinkage effects for Preflex beams have been covered by Morano e Mannini's method [6].

The traditional beams and alternative solutions' performance were compared for the superstructure of a simply-supported railway bridge with 20 meters span and deck slenderness ratio (L/H) of 15, 20, and 25. The adopted cross-section configuration are shown in Fig. 1. Design spreadsheets were developed, and the indicators of performance were obtained for the optimized structural configurations. For the sake of simplicity, loads were transversally distributed according to Courbon's method [7]. Also, cost analysis has been developed accounting, for each material, the equivalent steel area based on their prices. Although strongly affected by uncertainties, the cost analysis provides valuable indications about these innovative structural solutions' economic relevance. Fig. 2.a displays the best slenderness range of use for the solutions, and Fig. 2.b shows the substantial savings provided by the alternative composite beams compared to the equally slender traditional solution.

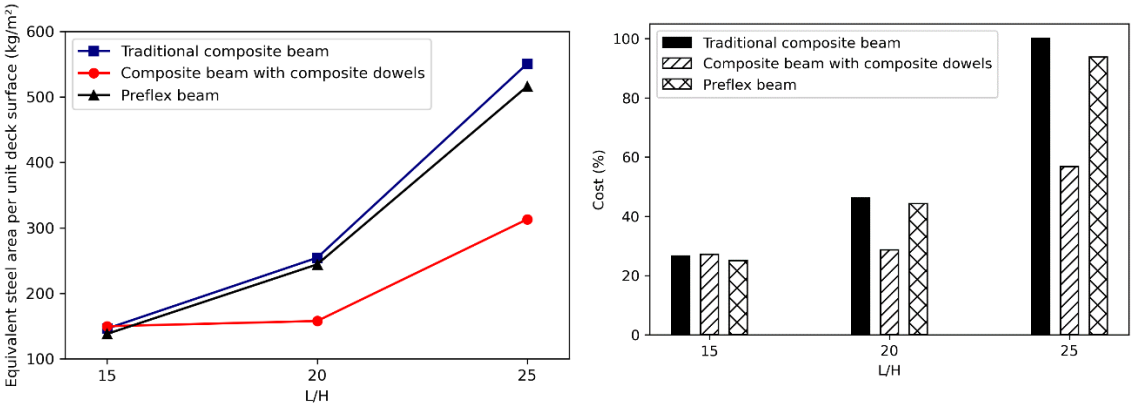

(a) **(b)**

Fig.2: Case studies results: a) equivalent steel area per deck to slenderness ratio graph, b) cost analysis.

REFERENCES

[1] Feldmann, M.; Kopp, M.; Pak, D.: Composite dowels as shear connector for composite beams - background to the German technical approval. Steel Construction 9(2), 80-88 (2016).

[2] Staquet, S.: Analyse et modelisation du comportment differe du beton. Application aux poutres mixtes, preflechies et precontraintes. Ph.D. Thesis. Universite Libre De Bruxelles. Brussels (2004).

[3] Santos, R.: Estudo comparativo de soluções para vigas mistas empregadas em obras de arte especiais. M.Sc. Thesis, Federal University of Minas Gerais. Belo Horizonte (2020).

[4] Comité Européen de Normalisation: EN 1994-2:2005. Eurocode 4: Design of composite steel and concrete structures – Part 2: General rules and rules for bridges. Brussels (2005).

[5] Deutsches Intitut für Bautechnik: Z-26.4-56. Allgemeine Bauartgenehmigung der Stahl-verbundträger mit Verbunddübelleisten in Klothoiden und Puzzleform. Berlin (2013).

[6] Morano, S. G.; Mannini, C.: Preflex Beams: a method of calculation of creep and shrinkage effects. Journal of Bridge Engineering 11(1), 48-58 (2006).

[7] Binjola, A.: Load distribution in girder bridges by different methods. M.Sc. thesis, University of Roorkee. Roorke (1988).

ACKNOWLEDGMENTS

The authors would like to acknowledge CNPq, CAPES, FAPEMIG, and FAPESP (grant nº 2020/02350-2) for providing an essential part of the financial support needed to develop this paper.

Numerical Modeling of Elliptical Concrete Filled Hollow Columns in case of Fire

Sérgio R. O. Q. Braga[a*], João Paulo C. Rodrigues[a], Fernando Pedro S. S. D. Simão[a] & António J. P. M. Correira[b]

[a]*Universidade de Coimbra, Portugal*
[b]*Instituto Politécnico de Coimbra, Portugal*
**Corresponding author: srobraga@gmail.com*

Keywords: Fire; Numerical modelling; Composite Column; Thermal Restraining

ABSTRACT

High costs and complexity limit the number of fire experiments on structural elements. Tubular steel columns filled with concrete have been assuming an increasing role in civil construction. Their excellent structural performance makes them particularly suitable for applications in tall buildings and bridges (Espinos et al.2013). Concrete filling offers an attractive practical solution to provide fire protection without the need of any external protection. Fire safety is one of the key aspects of structural design and the response of these columns when inserted in a building structure is different from when isolated. The restraining to thermal elongation of the column plays an important role in its stability, since it induces different forms of interaction between the heated column and the adjacent cold structure of the building (Rodrigues and Laím, 2017)

2 Numerical Model

The model was validated with results of tests accomplished by (Rodrigues and Laim, 2017). The experimental program comprised a large series of fire tests on circular, square, rectangular and elliptical concrete filled hollow columns. For the validation of the numerical models in this work was considered only the elliptical column tests. The elliptical column chosen had cross-section dimensions of 320 x 160 mm, thickness of 12,5mm and a length of 3.150mm. The column was filled with concrete of C25 / 30 class and was reinforced with 4 rebars of 20mm diameter, and longitudinal stirrups of 8 mm diameter spaced 150mm apart, both of B400 class. The support conditions of the columns were of the semi-rigid type and, during the experiment, the column was thermal restrained by a spatial restraining frame. In the validation of the model, a sequentially coupled thermal and mechanical analysis was adopted. A sensitivity analysis revealed that solid elements of C3D8R type of 20mm used in the concrete core and in the profile, led to a good response, with relative small processing time. The columns were entirely discretized. For the parameters that govern the heat transfer problem, the values recommended in EN 1991-1-2 were adopted. The thermal and mechanical properties of the concrete and steel at high temperatures were the ones obtained from EN 1992-1-2 and EN 1993-1-2, respectively.

3 Analysis and Conclusions

The imposition of restraining to the thermal elongation of the column, which strictly simulate the effects of the cold structure surrounding in case of fire, in general, mainly when the axial is much higher than the rotational restraining, reduces the critical time. The critical time (fire resistance) is defined in this work as the time elapsed between the start of heating and the return to the initial applied load, (Correia and Rodrigues, 2012). When comparing the critical times for the column without with the ones with thermal restraining, it can be seen that there was a reduction in critical time.

The initial applied load to the columns, in all the cases, was 30% of the design value of the buckling load of the columns at ambient temperature, according to the design procedures of EN-1994-1-1. The axial

restraining forces generated in the columns increased to a maximum and then decreased until the column failed, mainly due to the degradation of the mechanical properties of steel and concrete with the temperature. The higher the stiffness of the surrounding structure is, the higher the maximum restraining forces generated in the column are.

From the simulations it was also possible to observe that as the level of restraining increased, the time to reach the maximum load decreased. This doesn't mean that the critical times reduce, because the detrimental effect of the axial restraining that reduces critical times is contradicted by the rotational restraining that may increase them.

For the displacements, the higher the axial restraining imposed, the smaller the axial displacements. The displacements registered as a function of the restraining levels and time are consistent with those observed by (Rodrigues and Laim, 2017) in the experimental tests.

For lateral deformations, at half height of the column, they were increasingly greater after the maximum axial displacements were reached. Figure 1 shows the axial and lateral displacements of the columns when subjected to the ISO-834 fire for three axial restraining values of 30, 120 and 500 kN / mm.

Similar results were obtained for the columns subjected to the hydrocarbon fire curve simulations.

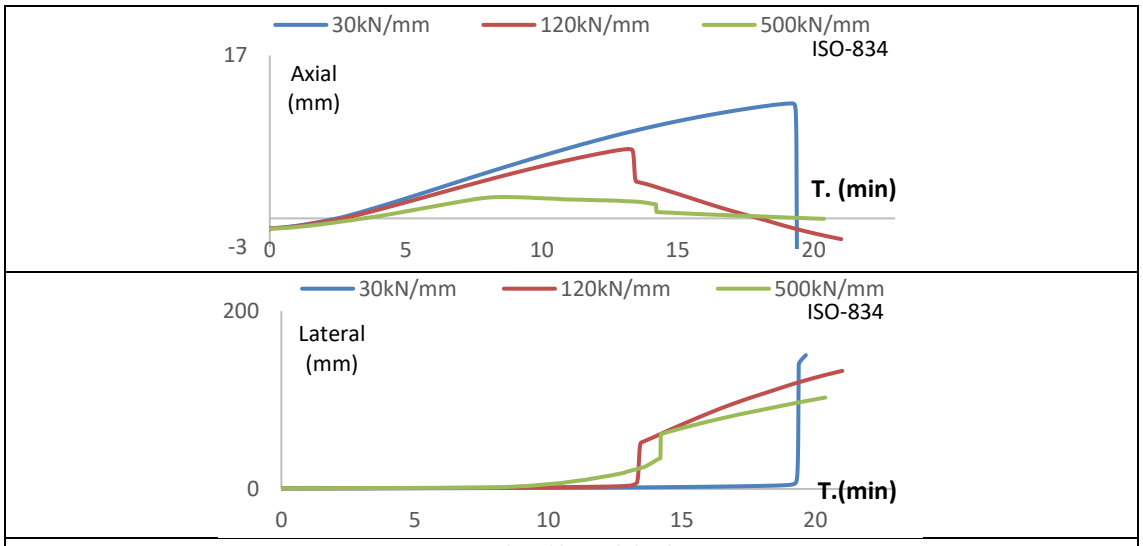

Figure 1: Axial and lateral displacements

References

[1] Espinos, A.; Romero, M. L. and Hospitaler, A.. "Fire Design Method for Bar-Reinforced Circular and Elliptical Concrete Filled Tubular Columns." Engineering Structures 56: 384–95 (2013).

[2] Rodrigues, J. P. C. and Laím, L.."Fire Resistance of Restrained Composite Columns Made of Concrete Filled Hollow Sections." Journal of Constructional Steel Research 133: 65–76 (2017).

[3] Rodrigues, J. P. C., and Laim, L.."Fire Response of Restrained Composite Columns Made with Concrete Filled Hollow Sections under Different End-Support Conditions." Engineering Structures 141: 83–96 (2017).

[4] Correia, A. J. P. M. and Rodrigues, J. P. C.. "Fire Resistance of Steel Columns with Restrained Thermal Elongation." Fire Safety Journal, vol. 50, pp. 1–11, (2012).

Ductility Of Bolted Steel Joints At High Temperatures

Fernando C. T. Gomes[a] & João Paulo C. Rodrigues[a]

[a]*Civil Engineering Department, Coimbra University*

1. Introduction

A beam-to-column steel joint is defined as partial-strength if the moment resistance of the joint is less than the moment resistance of the connected beam. In partial-strength joints, a plastic hinge may form at the joint and the rotation capacity of the joint must be checked. There is a need of a ductility rule, than can be used by design engineers, to check the rotation capacity of partial-strength joints.

In the case of bolted joints, premature failure of bolts in tension must be avoided, imposing that the failure of plates components (ex.: end-plate or column flange) will occur before the bolt failure.

Failure mechanisms of plates proposed in the literature usually underestimate the resistance of plate components. In this paper an upper bound of the plate resistance is evaluated which is necessary to prevent premature failure of bolts and ensure adequate rotation capacity of joints.

2. The Eurocode 3 ductility rule

According to the Eurocode 3 (EN 1993-1-8:2005) [1], the rotation capacity of a joint must be checked if the design moment resistance of the joint is less than 1.2 times the design plastic moment resistance of the cross section of the connected member. The following rule is given in EN 1993-1-8:2005, 6.4.2: "A joint with either a bolted end-plate or angle flange cleat connection may be assumed to have sufficient rotation capacity for plastic analysis, provided that both of the following conditions are satisfied: (a) the design moment resistance of the joint is governed by the design resistance of either the column flange in bending or the beam end-plate or tension flange cleat in bending; (b) the thickness t of either the column flange or the beam end-plate or tension flange cleat (not necessarily the same basic component as in (a)) satisfies:

$$t \leq 0.36\, d \sqrt{\frac{f_{ub}}{f_y}} \tag{1}$$

where d is the nominal diameter of the bolt, f_y is the yield strength of the relevant basic component and f_{ub} is the ultimate strength of the bolt".

3. Proposed ductility rule at ambient temperatures

Several failure mechanisms of plates are analyzed and compared with the resistance of bolts in tension, in order to avoid a brittle failure of the bolts. Using the results of Gomes and Rodrigues [2], the ductility rule at ambient temperatures becomes

$$t \leq \frac{0.14\, d f_{ub}}{f_u} \tag{2}$$

4. Proposed ductility rule at high temperatures

The ductility rule proposed for bolted joints at ambient temperature is modified for high temperatures, taking into account that the effect of temperature on the reduction of the bolt resistance is usually different of the effect of temperature on the resistance of plate components. At high temperatures the ductile rule becomes

$$t \leq \frac{0.14\, d k_{b,\theta}\, f_{ub}}{f_{u,\theta}} \tag{3}$$

where t is the plate thickness, d is the nominal diameter of the bolt, $f_{u,\theta}$ is given by

$$f_{u,\theta} = \begin{cases} 1.25\, k_{y,\theta}\, f_y & \text{for } \theta < 300\ ^\circ\text{C} \\ k_{y,\theta}\, f_y \left(2 - 0.0025\ \theta\right) & \text{for } 300\ ^\circ\text{C} \leq \theta < 400\ ^\circ\text{C} \\ k_{y,\theta}\, f_y & \text{for } \theta \geq 400\ ^\circ\text{C} \end{cases} \tag{4}$$

where θ is the steel temperature and the reduction factors $k_{y,\theta}$ and $k_{b,\theta}$ are defined in EN 1993-1-2:2005 [3].

5. Conclusions

In bolted steel joints, the resistance of bolts in tension should be greater than the resistance of the steel end-plate, cleat or column flange in tension. A detailed analysis of a circular plate demonstrates that it is necessary to evaluate correctly the resistance of the steel plate taking into account the actual dimension of the bolt head or nut, in order to avoid brittle failure of bolts in tension.

The Eurocode 3 ductility rule may lead to a brittle failure of the joint. In fact, the plate components resistance is underestimated by the Eurocode 3, which is safe for the resistance evaluation but is unsafe for ductility control.

As a conclusion, in order to avoid brittle failure of bolted beam-to-column joints, the currently possibilities are: (a) to prevent the formation of a plastic hinge in the joint by using full-strength joints, or (b) to use the proposed ductility rules at ambient and high temperatures.

References

[1] EN 1993-1-8:2005, *Eurocode 3: Design of steel structures - Part 1-8: Design of joints*, CEN, Brussels.

[2] Gomes, F.C.T., Rodrigues, J.P.C., *On the ductility of bolted steel joints at ambient and elevated temperatures*, Fire Research, 2017, vol. 1, pp 21-26.

[3] EN 1993-1-2:2005, *Eurocode 3: Design of steel structures - Part 1.2: Structural fire design*, CEN, Brussels.

Comparing the behavior of reinforced concrete columns embedded in walls and subjected to fire.

Bruno Matos[a] , Fernando Ferreira[a] , João Paulo C. Rodrigues[a] & Rodrigo B. Caldas[b]

[a]*Department of civil engineering, University of Coimbra, Portugal*
[b]*Department of civil engineering, Federal University of Minas Gerais, Brazil*

**Corresponding author: bruno00matos@yahoo.com.br*

Keywords: column; reinforced concrete; thermomechanical analysis; fire.

1.ABSTRACT

Fire is an exceptional action that may occur during the life of a building, so it must be considered in the design of its structure. Eurocode 1 part 1-2 [4] and Eurocode 2 part 1-2 [5] provide several types of design methods for that propose, namely: tabular methods, simplified calculation methods, advanced calculation methods and experimental methods. Also considered that the structure of the building can be analyzed by single elements, parts of structure or the structure as a whole.

The design of columns subjected to fire is important both for new buildings, as for buildings that will be refurbished and also for the verification of the residual resistance of columns after fire.

This article begins with a study on the behavior of the different types of building columns embedded in walls and subjected to fire. The paper presents also a benchmarking on comparing the studies made by different authors [6], [7] and [8] for different types of columns. After that a specific analysis on the behavior of reinforced concrete columns subjected to fire is carried out.

According to Kodur [1], the position of the column in the building structure leads to a different thermomechanical behavior. The position of the neutral axis of the element's cross section can rotate and (or) translate, according to the way of fire exposure.

Also according to Purkiss [2], for the verification of the compressive resistance of columns subjected to fire, the zone method was more conservative compared to the 500°C isotherm method, both prescribed in Eurocode 2 part 1-2 [5].

In this way, this paper analyzes numerically different ways of fire exposure and compare the results of the simplified calculation methods for designing the columns in case of fire and also the influence of the adjacent walls to a column in case of fire. The advanced calculations were performed with the finite element software, Abaqus CAE. Thermomechanical analysis of the columns subjected to fire, started with the temperature calculation in the cross-sections [3]. A thermal analysis of the cross sections of columns was carried out, for several cases of fire exposure. From the results, representative models of possible thermal behaviors, through the cross-section of the reinforced concrete columns subjected to fire, are obtained.

The numerical models in this work considered the column as isolated or embedded in the middle or the corner of a wall. The fire curve considered was the ISO 834, for a fire duration of 4 hours.

With this information, it was possible to perform the thermomechanical analysis of columns and present graphs with residual resistance of compression versus fire time. Considering varying the reinforcement rate, characteristic value of the compressive strength and the dimensions of the column cross section.

It was also possible, to compare the results of the advanced calculation methods with the simplified calculation ones them and verify which are more conservative.

It was also checked the walls effect on the behavior of the columns when subjected to fire. It was concluded that the walls prejudice when the column is at the corner and favorable when the column is at the middle. The protection effect promoted by the walls in some cases overlap the detrimental effect of the differential heating.

REFERENCES

[1] Raut, N., & Kodur, V. (2011). Response of reinforced concrete columns under fire-induced biaxial bending. *ACI Structural Journal*, *108*(5), 610–619.

[2] PURKISS, J. A. and LI, LONG-YUAN, Fire safety engineering design of structures, Third edition, CRC Press, 2007.

[3] Matos, B., Ferreira, F., Rodrigues J. P., Caldas R., Article S.: Thermal behavior of concrete columns embedded in walls subjected to a real fire curve. In: BRASILIAN CONFERENCE OF CONCRETE 2020,

[4] EUROPEAN STANDARD, Eurocode 1: Actions on structures - Part 1-2: General actions – Actions on structures exposed to fire. Portugal, 2010.

[5] EUROPEAN STANDARD, Eurocode 2: Design of concrete structures - Part 1-2: General rules – Structural fire design. Portugal, 2010.

[6] Correia, A. J. P.M.; Rodrigues, J. P. C. & Silva, V. P., V. (2009). Influence of brick walls on the temperature distribution in steel columns in fire. *Acta Polytechnica vol. 49*.

[7] Correia, A. M.; Rodrigues, J. P. C. & Silva, V. P., V. (2010). A simplified calculation method for temperature evaluation of steel columns embedded in walls. *Fire and materials. Fire mater:2011, 35:431-411*

[8] Correia, A. J. P.M.; Rodrigues, J. P. C. & Real, P. V. , V. (2010). A simplified calculation method for temperature evaluation of steel columns embedded in walls. *Fire safety journal 67 (2014) 53-69.*

Elastic Critical Moment of Lateral Distortional Buckling of Castellated Composite Beams Under Non-Uniform Hogging Moment

C. C. Silva[a*], R. B. Caldas[b], R. H. Fakury[c], J. V. F. Dias[d]

[a]*Department of Civil Engineering, Federal Institute of Minas Gerais, Campus Piumhi, Av. Severo Veloso, 1880, Piumhi, Brazil*
[b, c and d]*Department of Structural Engineering, Federal University of Minas Gerais, Av. Presidente Antônio Carlos, 6627, Belo Horizonte, Brazil*
**Corresponding author: carla.silva@ifmg.edu.br*

Keywords: Castellated composite beam; lateral distortional buckling; elastic critical moment; non-uniform moment.

ABSTRACT

Castellated steel beams are characterized by sequential openings in the web and designed in different types of structures. The manufacturing process, which simply consists of cutting, shifting and welding, increases the profile's height which results in greater inertia to the beam, increasing bending resistance and stiffness. These beams can be simply-supported, continuous and semicontinuous and can be designed as composite when there is a shear connection between the steel profile and the concrete slab.

Lateral distortional buckling (LDB), a global buckling mode, can occur in the hogging moment regions of continuous and semi-continuous castellated composite beams. This buckling mode is characterized by combined lateral displacement of the compressed flange and web distortion.

The European standard [1] presents no equation for the calculation of the elastic critical moment of regular I beams and the Brazilian standard [2] indicates a procedure for the assessment of this moment based on the inverted U frame mechanism. The elastic critical moment is adopted for the calculation of the resistant moment of these beams. This phenomenon also occurs in steel-concrete composite castellated beams, but there is no design procedure in current standards. Researchers [3] developed an analytical procedure to determine the critical moment of composite castellated beams under uniform hogging moment. This paper proposes an adjustment factor in the procedure presented in the literature [3] for composite castellated beams under non-uniform hogging moment.

Finite element simulations in the commercial code ANSYS [4] were performed and compared to the proposed procedure. Continuous composite beams with extreme spans and subjected to uniformly distributed load are present hogging moment in the central support region. To simplify the numerical models and allow an expressive number of analyses, in this paper, only the hogging moment regions were modelled. For the determination of the elastic critical moment of LDB of continuous composite beams, code prescriptions recommend that the concrete under tension should be ignored. Therefore, the concrete slab is replaced by a rotational spring of equivalent stiffness and only the steel section is simulated.

To assess the accuracy of the procedure with the previously explained simplifications, models with different cross-section dimensions and spans were adopted. Results indicate that this procedure is adequate and led to good agreement with numerical results, with an average deviation lower than 6.7%.

REFERENCES

[1] EN 1994-1-1. “Eurocode 4: Design of Composite Steel and Concrete Structures. Part 1-1: General Rules and Rules for Buildings.” Standard, Comite Europeen de Normalisation, Brussels, Belgium (2004).
[2] ABNT NBR 8800. “Projeto de Estruturas de Aço e de Estruturas Mistas de Aço e Concreto de Edifícios.” Standard, Associação Brasileira de Normas Técnicas, Rio de Janeiro, Brazil (2008).
[3] Silva, C. C., Caldas, R. B., Fakury, R. H., Dias, J. V. F. and Carvalho, H. “Elastic Critical Moment of Lateral Distortional Buckling of Castellated Composite Beams under Uniform Hogging Moment.” Pract. Period. Struct. Des. Constr. 25(4), (2020).
[4] Ansys Inc. Release 17.0 Documentation for Ansys (2016).

ACKNOWLEDGMENTS

The authors gratefully acknowledge the support provided by the Brazilian public agencies CAPES, CNPq, FAPEMIG, UFMG and IFMG campus Piumhi.

Lateral-torsional buckling resistance of cellular steel beams under fire situation

C. C. de Faria[a*], H. Carvalho[a], R. H. Fakury[a], L. F. Grilo[a]

[a] *Federal University of Minas Gerais, Brazil*
** Corresponding author: carolinecf@ufmg.br*

Keywords: lateral-torsional buckling; cellular beams; numerical study; fire situation.

ABSTRACT

The present study deals with the behavior of cellular steel beams under fire situation, focusing on the lateral-torsional buckling (LTB). This limit state, characterized by a lateral displacement and a torsion of the cross-section (**Fig. 1a**), has been extensively investigated at room temperature [1-4]. However, due to the lack of investigations at elevated temperatures [5], there is not a satisfactory procedure to assess the moment resistance. Therefore, the present research aims to provide new proposals to evaluate the LTB resistance ($M_{Rk,\theta}$) of cellular beams under fire situation.

In this study, a numerical model is developed using ABAQUS software (**Fig. 2b**) and validated by comparison with numerical and experimental results from [2-4, 6, 7]. Cellular beams simply supported, subjected to uniform bending, and exposed to fire from all sides [8] are investigated. The effects of elevated temperature are considered through a simplified model. Firstly, two different uniform temperatures for each time of fire exposure are calculated using the analytical procedure from [9], one for the web, and another for the flanges. Thereafter, these two temperatures are used to determine the material properties of the web and the flanges, respectively.

The validated numerical model is used for the parametric study, which assesses twenty hot-rolled parent sections, six groups of diameter and spacing of openings, values of non-dimensional slenderness between 1.0 and 4.0, seven flange temperatures, three load cases, and two structural materials, totaling 11,021 analyses. At the web-post width, the cross-sections of the resulting cellular members were Class 1, 2, or 3 for all temperatures investigated.

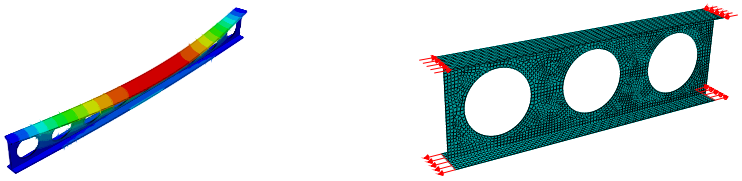

(a) Lateral-torsional buckling deformations (b) Numerical model

Fig. 1. Cellular steel beams bent about the major axis.

The numerical results are used to plot resistance curves for each temperature investigated. Based on the regression of the numerical curves, two methods to evaluate the LTB resistance of cellular beams are proposed. The proposed LTB reduction factor under fire situation, $\chi_{LT,\theta,Prop}$, is given by **Eq. (1)**, where $\Phi_{LT,\theta,Prop}$ is given by **Eq. (2)**, $\bar{\lambda}_{LT,\theta}$ is the non-dimensional slenderness, α_θ is the imperfection factor, as shown in **Table 1**, E is Young's modulus, f_y is the steel yield strength, θ is the flange temperature, and κ_0 is a correction factor for Proposal II, which provides better agreement with the numerical results.

$$\chi_{LT,\theta,Prop} = \left[\frac{1}{\Phi_{LT,\theta,Prop} + \sqrt{\Phi_{LT,\theta,Prop}^{\,2} - \bar{\lambda}_{LT,\theta}^{\,2}}} \leq \begin{cases} 1 \\ 1 \Big/ \bar{\lambda}_{LT,\theta}^{\,2} \end{cases} \right] \kappa_0 \tag{1}$$

$$\Phi_{LT,\theta,Prop} = 0.5 \left[1 + \alpha_\theta \, \bar{\lambda}_{LT,\theta} + \bar{\lambda}_{LT,\theta}^{\,1,9} \right] \tag{2}$$

Table 1. Proposed parameters under fire situation.

Method	θ	$\alpha_\theta / \sqrt{E/f_y}$	κ_0
Proposal I	200ºC to 800ºC	0.032	1.0
Proposal II	200ºC	0.008	$\begin{cases} \bar{\lambda}_{LT,\theta} \leq 1.700 \rightarrow \kappa_0 = 0.170\,\bar{\lambda}_{LT,\theta}^{\,2} - 0.289\,\bar{\lambda}_{LT,\theta} + 1.000 \\ \bar{\lambda}_{LT,\theta} > 1.700 \rightarrow \kappa_0 = 1.000 \end{cases}$
	300ºC	0.012	
	400ºC to 800ºC	0.021	

A comparison between numerical and analytical reduction factors is shown in **Fig. 2**, where W_y is the section modulus. As can be seen, Proposal I is more severe than the procedure from [9] and presented differences with the numerical results between -40% and 7%. Therefore, this procedure is indicated for fast and practical calculations since it leads to mostly conservative results. On the other hand, Proposal II provides a better agreement with all investigated models, with differences between -16% and 8%, but requires different imperfection factors and a correction factor for cellular beams with intermediate slenderness.

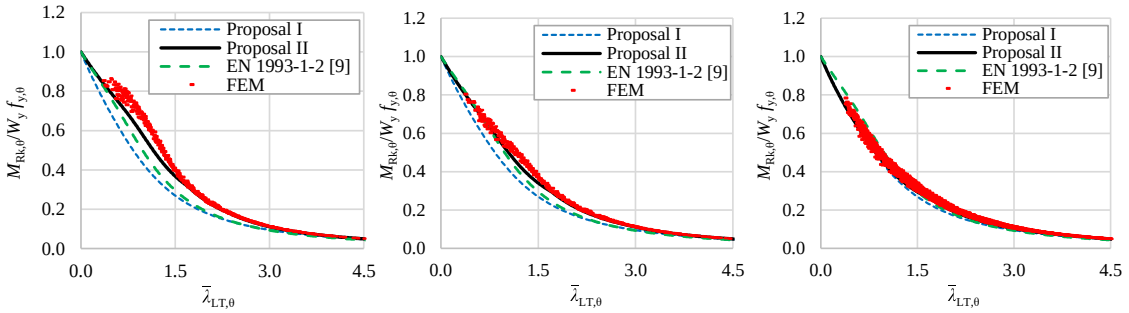

Fig. 2. Numerical and analytical resistance curves for the uniform bending case: (a) θ_f = 200ºC; (b) θ_f = 300ºC; and (c) θ_f from 400º to 800ºC

REFERENCES

[1] Sweedan, A. M. I.: Elastic lateral stability of I-shaped cellular steel beams. *J Constr Steel Res* 67, 151-163 (2011).
[2] Boissonnade, N, *et al*.: Design of cellular beams against lateral torsional buckling. *Proc Inst Civ Eng Struct Build* 167(SB7), 436-444 (2014).
[3] Sonck, D., Belis, J.: Lateral-torsional buckling resistance of cellular beams. *J Constr Steel Res* 105, 119–128 (2015).
[4] Panedpojaman, P., *et al*.: Cellular beam design for resistance to inelastic lateral-torsional buckling. *Thin-Walled Struct* 99, 182-194 (2016).
[5] Elsawaf, S., Hassan, M. M.: Behaviour of structural sub-assemblies of steel beams with openings in fire conditions. *J Constr Steel Res* 148, 627-638 (2018).
[6] Prachar, M., *et al*.: Experiments of Class 4 open section beams at elevated temperature. *Thin-Walled Struct* 98, 2-18 (2016).
[7] Wang, P., Wang, X., Liu, M.: Practical method for calculating the buckling temperature of the web-post in a cellular steel beam in fire. *Thin-Walled Struct* 85, 441-455 (2014).
[8] INTERNATIONAL ORGANIZATION FOR STANDARDIZATION. ISO 834: Fire resistance tests – Elements of building construction. Part 1: General requirements. Switzerland, 1999.
[9] EUROPEAN COMMITTEE FOR STANDARDIZATION. EN 1993-1-2: Design of steel structures. Part 1.2: General rules – Structural fire design. Brussels, 2005.

ACKNOWLEDGMENTS

The authors would like to acknowledge the support from the Brazilian agencies CAPES, CNPq, and FAPEMIG.

Comparative study of fracture mechanisms in 7050 and 7075 aluminium alloys

Douglas F. Galvão1, Ricardo Branco2, José Domingos Costa2, Ana Paula Amaro2, Ana Paula Piedade2, Luís Borrego3,2, Cândida Pereira3,4 and Artur Mateus3

1 Federal Technology Education Center of Minas Gerais, BH, MG 30480-000, Brazil
2 University of Coimbra, Coimbra. 3030-194, Portugal
3 Centre for Rapid and Sustainable Product Development, Polytechnic Institute of Leiria, Rua de Portugal, Marinha Grande, 2430-028, Portugal
4 Department of Mechanical Engineering, Coimbra Polytechnic - ISEC, Rua Pedro Nunes, Quinta da Nora, 3030-199 Coimbra, Portugal
douglasfilipe_cpm@hotmail.com

Keywords: 7000 series aluminium alloys, Low-cycle behaviour, Cyclic behaviour, Fracture mechanisms

Abstract

Aluminium alloys of the 7000 series widely utilized in the manufacturing of components within the aeronautical industry are often subjected to complex load cycles, which vary over time, causing the accumulation of plastic deformation. Thus, a solid knowledge of the cyclic elasto-plastic behavior of those components is crucial, in order to develop reliable fatigue life prediction models. This study aims at investigating the cyclic deformation behavior of two 7000 series aluminium alloys, namely 7050 and 7075. Low-cycle fatigue tests are conducted under strain-controlled conditions at a strain ratio equal to -1. After the tests, fracture surfaces are examined by scanning electron microscopy to identify the main fracture mechanisms. The results show that the 7050 aluminium alloy exhibits a cyclic softening behavior. As for the 7075 aluminium alloy, it was observed a mixed behavior, i.e. cyclic softening and cyclic hardening. The analysis of SEM fracture surfaces of the two aluminium alloys revealed that the main mechanisms were cleavage steps and micro-cavities.

Analysis and discussion on statistical evaluation of strain-life data of modern structural steels

A. Mourão[a*], José A.F.O. Correia[a], Túlio Bittencourt[b], Rui Calçada[a]

[a] *CONSTRUCT, Faculty of Engineering, University of Porto, 4200-465 Porto, Portugal*
[b] *Polytechnic School, São Paulo University, 05508-010 São Paulo, Brazil*
*
Corresponding author: amourao@fe.up.pt

Keywords: Coffin-Manson; modern steels; material properties; statistical analysis.

ABSTRACT

Modern structural steels, either by increased precision/regulation of fabrication processes or simply driven by rising demands of modern structural solutions in both size, load-bearing capacity, and quality requirements, have led to what is usually considered in the design environment to be a homogenous material.

Fatigue, per the definition of the American Society for Testing and Materials (ASTM) [1], is a progressive and permanent change in a material when subjected to fluctuating stresses/strains, which, even though these may occur within the scope of the material's elastic region, it does, more often than not, lead to a loss in structural load-bearing capacity or quite possibly the collapse of the same.

Usually characterized in standards as the graphical representation of a component's experimental resistance, fatigue results are highly influenced by a variety of factors which result in a considerable scatter in the measurable data. As such, and to be possible to generalize for any structural component geometry, localized approaches present in literature, such as the Coffin-Manson strain-life relation [2] presented in Eq. (1), employ material elastoplastic fatigue properties to portray the effect more accurately on the component.

$$\frac{\Delta\varepsilon}{2} = \frac{\Delta\varepsilon_e}{2} + \frac{\Delta\varepsilon_p}{2} = \frac{\sigma'_f}{E}\left(2N_f\right)^b + \varepsilon'_f\left(2N_f\right)^c \tag{1}$$

In the present work, the Coffin-Manson mean elastoplastic material properties for S235, S355, and S690, present in the EN 10025 [3], as well as the respective coefficient of variation for the Normal distribution, according to both ASTM E739 [4] and ISO 12107 [5] standards for fatigue testing of metallic materials are presented. Additionally, and with the same intention, the two-parameter Weibull distribution is used following the mindset of the previously mentioned testing standards. In Eqs. (2)-(3), the coefficient of variation (CoV) for both distributions is presented.

$$N(\sigma,\mu):\ CoV\ = \frac{\sigma}{\mu} \tag{2}$$

$$W(\alpha,\beta):\ CoV\ = \sqrt{\frac{\Gamma\left(1+\frac{1}{\beta}\right)}{\Gamma\left(1+\frac{1}{\beta}\right)^2} - 1} \tag{3}$$

By fitting the cumulative probability of the Weibull distribution with four distinct estimation methods, maximum likelihood method (MLM), linear least square method, the weighted linear least square method,

and the method of moments, the Weibull distribution two parameters, shape and scale, can be obtained and goodness-of-fit tests can be applied to determine the optimal outcome.

Finally, a comparison between the experimental data and values collected in the literature is presented with regards to the coefficient of variation of the strain-life parameters following both distributions.

REFERENCES

[1] ASTM E-1823. Standard Terminology Relating to Fatigue and Fracture Testing, American Society for Testing Material, USA, 2010.
[2] Coffin, LF.: A study of the effects of the cyclic thermal stresses on a ductile metal. Transactions ASME 76: 931–950 (1954).
[3] European Committee for Standardization (CEN). EN 10025: hot rolled products of structural steels. Brussels: European Standard; 2004.
[4] ASTM E-739, "Standard Practice for Statistical Analysis of Linear or Linearized Stress-Life and Strain-Life Fatigue Data, American Society for Testing Material, USA, 2004.
[5] International Organization for Standardization, Metallic materials—Fatigue testing—Statistical planning and analysis of data. Geneva, 2012.

ACKNOWLEDGMENTS

This work was financially supported by: Base Funding - UIDB/04708/2020 and Programmatic Funding - UIDP/04708/2020 of the CONSTRUCT - Instituto de I&D em Estruturas e Construções - funded by national funds through the FCT/MCTES (PIDDAC); Doctoral Grant PD/BD/15306/2019 funded by FCT/MCTES; FCT Doctoral Programme iRail - Innovation in Railway systems and technologies; and, FiberBridge project - Fatigue strengthening and assessment of railway metallic bridges using fiber-reinforced polymers (POCI-01-0145-FEDER-030103) through the FEDER funds provided by COMPETE2020 (POCI) and by national funds (PIDDAC) provided by the Portuguese Science Foundation (FCT/MCTES).

Mechanical characterization of the Desengano's iron bridge from the 19th century

I.G. Oliveira[a*], J. M. Pardal[a] , J. Correia[b], F. Berto[c]

[a]*Department of Mechanical Engineering, Fluminense Federal University, Brazil*

[b]*INEGI & CONSTRUCT, University of Porto, Portugal*

[c]*Department of Mechanical and Industrial Engineering, Norwegian University of Science and Technology, Norway*

**Corresponding author: iaragripp@id.uff.br*

Keywords: Puddled Iron; Mechanical Properties; Microstructure; Ancient Bridges.

ABSTRACT

Desengano's Bridge is a Brazilian bridge built in the 19th century over the river Paraíba do Sul and is used today as a road-rail bridge. This research study presents the results of chemical composition and microstructures analyses, monotonic tensile strength, hardness, and impact tests. The microstructural characterization by optical microscopy revealed that the samples analyzed have a ferritic matrix, coarse grain size, and a great number of slag inclusions, which are characteristics of puddled iron. In the tensile tests, high values of mechanical resistance and low ductility were observed, which was confirmed by the high hardness values obtained. In terms of impact toughness, low values of this property were obtained due to the high content of inclusions present in the material. Finally, the mechanical and microstructure properties of the bridge investigated were compared with different worldwide structures from the same historical period. It is known that this type of material under long-time operations and cyclic loading presents a degradation process, altering its mechanical properties, therefore, the information here presented is of great importance for structural safety.

REFERENCES

[1] Gordon, F.; Knopf, R.: Evaluation of Wrought Iron for Continued Service in Historic Bridges. Journal of Materials in Civil Engineering 17, 393-399 (2005).

[2] Raposo, P.; Correia, J.; Lesiuk, G.; Valente, I.; De Jesus, A.; Calçada, R.: Mechanical Characterization of Ancient Portuguese Riveted Bridges Steels. Engineering Structures and Technologies 9, 214-225 (2017).

[3] Mamani-Calcina, E. A.; Apaza-Huallpa, E.; Gonzalez-Diaz, D.; Vargas-Cardenas, H.; Guerra-Santander, E.; Andrade-Centeno, D. M.; Nacsa, B.; Alves, J.P.F; Landgraf, F.J.G.; Azevedo, C.R.F.: Microstructural and mechanical characterisation of the Simon Bolivar's iron bridge structure, 19th century, Arequipa, Peru. REM – International Engineering Journal 73, 523-530 (2020).

[4] Lesiuk, G.; Szata, M.; Bocian, M.: The mechanical properties and the microstructural degradation effect in an old low carbon steels after 100-years operating time. Arch. Civ. Mech. Eng. 15, 786–797 (2015).

ACKNOWLEDGMENTS

Authors acknowledge the Brazilian research agencies CAPES, CNPq and FAPERJ for the financial support.

Estimation of strain-life properties through the strain energy density-based Huffman model for various aluminium alloys

Victor H. Ribeiro[a*], José A.F.O. Correia[b], Peter Huffman[c], Grzegorz Lesiuk[d], Aparecido C. Gonçalves[a], Abílio De Jesus[b], Filippo Berto[e]

[a] *Mechanical Engineering Department, São Paulo State University (UNESP), School of Engineering, Ilha Solteira, São Paulo, Brazil.*

[b] *CONSTRUCT & INEGI, Faculty of Engineering, University of Porto, Campus FEUP, 4200-465 Porto, Portugal.*

[c] *Successful Failure Consulting Corp, USA.*

[d] *Faculty of Mechanical Engineering, Department of Mechanics, Materials Science and Engineering, Wroclaw U niversity of Science and Technology, PL-50370 Wrocław, Poland.*

[e] *Norwegian University of Science and Technology, Trondheim, Norway.*

**Corresponding author: victor.h.ribeiro@unesp.br*

Keywords: strain-life data; aluminium alloy; Morrow law; Huffman model; strain energy density

ABSTRACT

Fatigue crack initiation is traditionally described using empirical and/or deterministic models, usually in the form of single and double power law relationships for stress-life or strain-life. Fatigue crack growth is most often described as a power law relationship between the fatigue crack propagation rates and stress intensity factor ranges, in terms of fracture mechanics. Some models describe the initiation as being taken as the formation of the fatigue crack, and then propagation is the successive re-initiation locally at the crack tip [1-9].

The fatigue crack propagation modelling using strain-based fatigue local relation was first proposed by Glinka [1]. Others authors, as Peeker and Niemi [2], Noroozi et al. [3,4], Hurley and Evans [5], Correia et al. [6], Hafezi et al. [7], Jesus et al. [8] and Huffman [9], have used local fatigue local models based on strain and SWT relations to model the fatigue crack propagation curves.

The local damage parameter proposed by Huffman [9] uses the strain energy density approach from cyclic stress-strain properties to estimating the stress-life, strain-life, and fatigue crack growth. The Huffman local damage parameter is given by

$$\left(\frac{U_e}{U_d \rho_c}\right)\left(\frac{U_p^*}{U_d \rho_c}\right) = D = \frac{2N}{2N_f} \tag{1}$$

where $\boldsymbol{U_e}$ is the elastic strain energy density, $\boldsymbol{U_p^*}$ is the complementary plastic strain energy density, $\boldsymbol{U_d}$ is the strain energy density from dislocations, and $\boldsymbol{\rho_c}$ is the critical dislocation density. The strain energy from dislocations can be approximated by

$$U_d = \left(\frac{E}{2(1+\upsilon)}\right) \cdot \left|\vec{b}\right|^2 \tag{2}$$

where $\boldsymbol{\upsilon}$ is the Poisson's ratio and $\vec{\boldsymbol{b}}$ is the Burger's vector. The $\vec{\boldsymbol{b}}$ value for irons, steels or similar metals materials is equal to $\mathbf{2.52 \times 10^{-10}}$ m, as shown in reference [9]. Finding the strain energy density by integrating the Ramberg-Osgood stress-strain relationship give the damage equation in terms of materials parameters

$$\left(\frac{2}{U_d^2 \rho_c^2 E}\right)\left(\frac{n'}{1+n'}\right)\left(\frac{1}{K'}\right)^{(1/n\prime)} (\sigma_{max}{}^2)(\sigma_a)^{\frac{1+n\prime}{n\prime}}\left(\frac{1}{\mathrm{N}}\right) = D = \frac{1}{2N_f} \tag{3}$$

where $\boldsymbol{\sigma_{max}}$ is the maximum stress and $\boldsymbol{\sigma_a}$ is the stress amplitude.

Equation (3) can be used along with the elastic and plastic parts of the Ramberg-Osgood relationship separately to calculate the Strain life parameters, or Morrow parameters,

$$\sigma_f' = E\left(\frac{2}{U_d^2 \rho_c^2}\left(\frac{1}{K'}\right)^{1/n\prime}\left(\frac{n'}{1+n'}\right)E^{(1+2n\prime)/n\prime}\right)^{\frac{-n\prime}{1+3n\prime}} \tag{4}$$

where $\boldsymbol{\sigma_f'}$ is the fatigue strength coefficient, $\boldsymbol{E}$ is the elastic modulus, $\boldsymbol{K'}$ and $\boldsymbol{n'}$ are the cyclic Ramberg-Osgood parameters of the cyclic strength coefficient and cyclic strain hardening exponent respectively. The fatigue strength exponent is then

$$b = \frac{-n'}{1+3n'}. \tag{5}$$

The fatigue ductility coefficient is

$$\varepsilon_f' = E\left(\frac{2(K')^3}{U_d^2 \rho_c^2 E}\left(\frac{n'}{1+n'}\right)\right)^{\frac{-1}{1+3n\prime}}. \tag{6}$$

And the fatigue ductility exponent is

$$c = \frac{-1}{1+3n'}. \tag{7}$$

The value of $\boldsymbol{\rho_c}$ can be found by fitting the resultant strain-life curve to low-cycle strain-life data by solving the Equation (3), and, generally, has been found between $\mathbf{1 \times 10^{15} \leq \rho_c \leq 3 \times 10^{16}}$ m^{-2} [9]:

$$\rho_c = \sqrt{\left(\frac{2(2N_f)}{U_d^2 EN}\right)\left(\frac{n'}{1+n'}\right)\left(\frac{1}{K'}\right)^{(1/n\prime)} \times (\sigma_{max}{}^2)(\sigma_a)^{\left(\frac{1+n\prime}{n\prime}\right)}}. \tag{8}$$

This model was used to evaluating the strain-life parameters of the Al1050, 6061-T651, and AlMgSi0.8 metal alloys [10,11]. The mechanical properties, cyclic elastoplastic, and stress-strain parameters of the metal alloys under consideration are summarised in Table 1. These parameters were obtained based on experimental low-cycle fatigue tests of smooth specimens performed under strain controlled conditions. The Huffman model was applied to the metal alloys under consideration to predicting the Morrow constants using the strain energy based on fatigue crack initiation model. A good agreement for the strain-life constants between the Huffman model and the Morrow equation is verified (see Table 2 and Figure 1). The critical dislocation density, ρ_c, (Table 2) estimated for these materials are in line with the values recommended to the similar materials [9].

Table 1. Mechanical properties, cyclic elastoplastic and strain-life parameters based on Morrow relation for the various aluminium alloys under consideration [10,11].

Materials -	$\boldsymbol{R_{p,0.2}}$ [MPa]	$\boldsymbol{R_m}$ [MPa]	$\boldsymbol{E}$ [MPa]	$\boldsymbol{K'}$ [MPa]	$\boldsymbol{n'}$ [-]	$\boldsymbol{\sigma'_f}$ [MPa]	$\boldsymbol{b}$ [-]	$\boldsymbol{\varepsilon'_f}$ [-]	$\boldsymbol{c}$ [-]
Al 1050	19.0	73.5	70000	453.0	0.337	117	-0.1089	0.0167	-0.3147
6061-T651	289.9	328.5	68000	393.4	0.0567	394	-0.0453	0.8680	-0.7745
AlMgSi 0.8	157.0	260.0	66700	392.0	0.060	481	-0.0840	1.0945	-0.8671

Table 2. Strain-life parameters based on Huffman model for various metal alloys under consideration.

Materials -	ρ_c [m/m^3]	U_d [MPa]	σ'_f [MPa]	b [-]	ε'_f [-]	c [-]
Al 1050	1.20E+15	2.12E-15	208.20	-0.1676	0.0996	-0.4973
6061-T651	5.90E+15	2.06E-15	401.69	-0.0485	1.4445	-0.8546
AlMgSi 0.8	4.51E+15	2.02E-15	387.92	-0.0508	0.8398	-0.8475

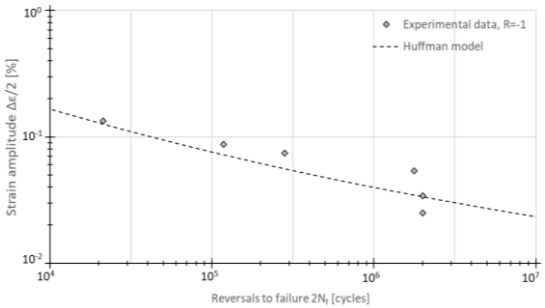

a) Al 1050

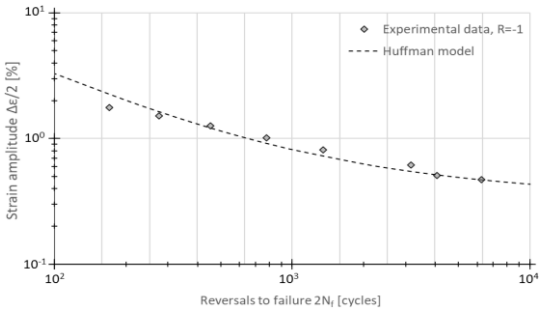

b) Al 6061-T651

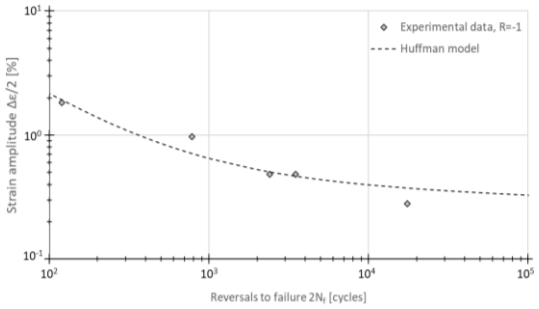

c) AlMgSi 0.8

Fig. 1. Strain-life curves – Experimental data vs. Huffman model.

REFERENCES

[1] Glinka, G. 1985, "A notch stress-strain analysis approach to fatigue crack growth", Engineering Fracture Mechanics, vol. 21, no. 2, pp. 245-261.

[2] Peeker, E. & Niemi, E. 1999, "Fatigue crack propagation model based on a local strain approach", Journal of Constructional Steel Research, vol. 49, no. 2, pp. 139-155.

[3] Noroozi, A.H., Glinka, G. & Lambert, S. 2005, "A two parameter driving force for fatigue crack growth analysis", International Journal of Fatigue, vol. 27, no. 10-12, pp. 1277-1296.

[4] Noroozi, A.H., Glinka, G. & Lambert, S. 2007, "A study of the stress ratio effects on fatigue crack growth using the unified two-parameter fatigue crack growth driving force", International Journal of Fatigue, vol. 29, no. 9-11, pp. 1616-1633.

[5] Hurley, P.J. & Evans, W.J. 2007, "A methodology for predicting fatigue crack propagation rates in titanium based on damage accumulation", Scripta Materialia, vol. 56, no. 8, pp. 681-684.

[6] Correia, J.A.F.O., Jesus, A.M.P.D. & Fernández-Canteli, A. 2012, "A procedure to derive probabilistic fatigue crack propagation data", International Journal of Structural Integrity, vol. 3, no. 2, pp. 158-183.

[7] Hafezi, M.H., Abdullah, N.N., Correia, J.F.O. & De Jesus, A.M.P. 2012, "An assessment of a strain-life approach for fatigue crack growth", International Journal of Structural Integrity, vol. 3, no. 4, pp. 344-376.

[8] De Jesus, A.M.P. & Correia, J.A.F.O. 2013, "Critical assessment of a local strain-based fatigue crack growth model using experimental data available for the P355NL1 steel", Journal of Pressure Vessel Technology, Transactions of the ASME, vol. 135, no. 1.

[9] Huffman, P.J. 2016, "A strain energy based damage model for fatigue crack initiation and growth", International Journal of Fatigue, vol. 88, pp. 197-204.
[10] Correia, J.A.F.O., De Jesus, A.M.P., Ribeiro, A.S. & Fernandes, A.A. "Strain-based approach for fatigue crack propagation simulation of the 6061-T651 aluminium alloy", International Journal of Materials and Structural Integrity, 2017, 11(1-3): 1-15.
[11] Boller C, Seeger T. Materials data for cyclic loading. Mater Sci Monogr, vol. 42E. Elsevier; 1987. Part D: Aluminium and titanium alloys.

ACKNOWLEDGMENTS

Thanks Coordenação de Aperfeiçoamento de Pessoal de Nível Superior - CAPES (Brazil) for the financial support.

This work was also financially supported by: Base Funding - UIDB/04708/2020 and Programmatic Funding - UIDP/04708/2020 of the CONSTRUCT - Instituto de I&D em Estruturas e Construções - funded by national funds through the FCT/MCTES (PIDDAC).

Fracture characterization of hybrid bonded joints for pure mode I

Rita Dantas[a,b*], Anis Mohabeddine[b], Marcelo Moura[a], Raul Moreira[a], Grzegorz Lesiuk[c], José Correia[a,b], Abílio De Jesus[a]

[a] *INEGI, Department of Mechanical Engineering, Faculty of Engineering of the University of Porto, Portugal*
[b] *CONSTRUCT, Department of Civil Engineering, University of Porto, Portugal*
c Faculty of Mechanical Engineering, Department of Mechanics, Materials Science and Engineering, Wroclaw University of Science and Technology, PL-50370 Wrocław, Poland
**Corresponding author: up201403351@fe.up.pt*

Keywords: fracture; S355 steel; CFRP; cohesive zone model; mode I.

ABSTRACT

At the end of the nineteenth century, several bridges were designed and built-in steel with the perspective of a certain service life, which is achieving its end. Since it is desired to maintain these structures and even extend their service life, the interest around different methodologies of maintenance and strengthening of steel bridges increased [1],[2]. One of the most popular methodologies is the application of carbon fibre reinforced Polymers (CFRP) locally in strategic points of the structures[3]–[5].

The CFRP are materials of high ultimate strength, low density, low weight and good resistance to fatigue, which are important characteristics for the rehabilitation of these structures [5]. Furthermore, since CFRP patches are connected through an structural adhesive, this strengthening method does not introduce defects or critical zones which can negatively affect the mechanical and fatigue properties, as in welded or drilled connections [3], [4]. Usually, the weakest point of these reinforced details is in the interface between CFRP patch and steel detail, sometimes, due to cohesive failures (in the adhesive) or adhesive failures (between adhesive- CFRP or adhesive-steel) [6]. This last mode of failure happens because of a deficient preparation of the adhesive joint, while the first one depends on the fracture properties of the adhesive. Therefore, to evaluate this methodology of reinforcement is essential to assess the fracture behaviour of the joint and structural adhesive. This work aims to characterize the fracture mechanics behaviour under pure mode I of hybrid joints, which combine CFRP with steel by means of a structural adhesive.

In order to determine mode I fracture energy (G_{IC}) and characterize the joint, an experimental campaign composed by asymmetric double cantilever beam (ADCB) tests was defined and performed. This type of test is performed on a specimen formed by two braces glued and with a pre-crack induced of a defined length (Fig.1). During this test a tensile load is applied to the specimen upper arm at the pre-crack side, leading to the crack propagation in mode I along the adhesive layer plane [7].

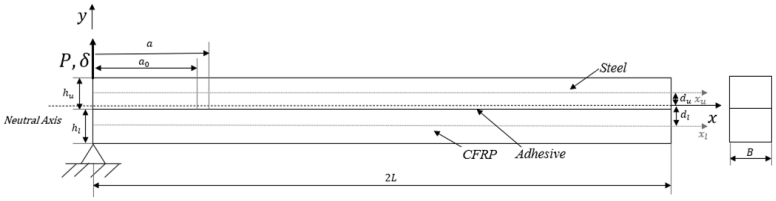

Fig. 1 Representation of ADCB test type (P: load; B: width; h_u: thickness of upper arm; h_u: thickness of lower arm)

The total strain energy release rate throughout the experimental test can be calculated by the following equation, which is based on the Irwin-Kies relation and the Castigliano theorem [7]–[9]:

$$G_T = \frac{P^2}{2B}\left(a_{eq}^2\left(\frac{1}{E_u I_u}+\frac{1}{E_l I_l}\right)+\frac{6}{5\,B}\left(\frac{1}{h_u G_{13(u)}}+\frac{1}{h_l G_{13(l)}}\right)\right) \quad (1)$$

where a_{eq} is the equivalent crack length, $E_u I_u$ is the bending stiffness of the upper arm (steel), $E_l I_l$ is the bending stiffness of the lower arm (CFRP), $G_{13(u)}$ is the shear modulus of the upper brace and $G_{13(l)}$ is the shear modulus 13 of the lower brace.

Thus, four specimens were tested in a MTS810 machine at 1mm/min speed. The setup of the experimental tests is portrayed in Fig.2. The results obtained were consistent and similar in all the four specimens tested: instead of a cohesive failure, it was observed the failure of the CFRP (Fig. 3). Hence, it was obtained the energy of fracture of the hybrid joint, which is around 0:3N/mm and the CFRP showed to be the weaker material of it under this mode of fracture. This experimental campaign was also supported by a numerical study based on a trapezoidal cohesive zone model.

Fig. 2. ADCB test setup

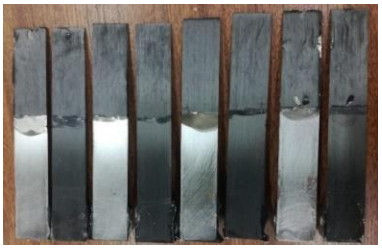

Fig. 3.ADCB specimens after experimental tests

REFERENCES

[1] S. S. . J. Moy and A. G. Bloodworth, "Strengthening a steel bridge with CFRP composites," *Proc. Inst. Civ. Eng. - Struct. Build.*, vol. 160, no. SB2, pp. 81–93, 2007.

[2] B. Pang, P. Yang, Y. Wang, A. Kendall, H. Xie, and Z. Yurong, "Life cycle environmental impact assessment of a bridge with different strengthening schemes," *Int. J. Life Cycle Assess.*, no. 20, pp. 1300–1311, 2015.

[3] S. C. Jones, S. A. Civjan, and M. Asce, "Application of Fiber Reinforced Polymer Overlays to Extend Steel Fatigue Life," *J. Compos. Constr. ASCE*, vol. 7, pp. 331–338, 2003.

[4] A. Mohabeddine, J. A. F. O. Correia, J. M. Castro, P. Montenegro, A. M. P. De Jesus, and R. A. B. Calçada, "Numerical investigation on the fatigue life of non- cracked metallic plates repaired with bonded CFRP," in *EUROSTEEL2021*, 2020.

[5] M. Heshmati, R. Haghani, and M. Al-emrani, "Durability of bonded FRP-to-steel joints : Effects of moisture , de-icing salt solution , temperature and FRP type," *Compos. Part B*, no. 119, pp. 153–167, 2017.

[6] M. Bocciarelli, P. Colombi, G. Fava, and C. Poggi, "Fatigue performance of tensile steel members strengthened with CFRP plates," *Compos. Struct.*, vol. 87, no. 4, pp. 334–343, 2009.

[7] R. D. F. Moreira, M. F. S. F. De Moura, and F. G. A. Silva, "A novel strategy to obtain the fracture envelope under mixed-mode I + II loading of composite bonded joints," *Eng. Fract. Mech.*, vol. 232, no. October 2019, p. 107032, 2020.

[8] Z. Liu *et al.*, "Global-local fatigue assessment of an ancient riveted metallic bridge based on submodelling of the critical detail," *Fatigue Fract. Eng. Mater. Struct.*, vol. 42, no. 2, pp. 546–560, 2019.

[9] M. F. S. F. De Moura, "Numerical simulation of the ENF test for the mode-II fracture characterization of bonded joints fracture characterization of bonded joints," *J. Adhes. Sci. Technol.*, vol. 20, no. 1, pp. 37–52, 2006.

ACKNOWLEDGMENTS

This work was financially supported by: Base Funding - UIDB/04708/2020 and Programmatic Funding - UIDP/04708/2020 of the CONSTRUCT - Instituto de I&D em Estruturas e Construções - funded by national funds through the FCT/MCTES (PIDDAC); MPP2030-FCT PhD Grants/02804649079 funded by FCT/MCTES and MIT Portugal; and, FiberBridge project - Fatigue strengthening and assessment of railway metallic bridges using fiber-reinforced polymers (POCI-01-0145-FEDER-030103) through the FEDER funds provided by COMPETE2020 (POCI) and by national funds (PIDDAC) provided by the Portuguese Science Foundation (FCT/MCTES).

Interlaminar fracture toughness determination in an inverse FML material under mode I loading condition

Sz. Duda[a*], G. Lesiuk[a], M. Smolnicki[a], T. Osiecki[b]

[a] *Faculty of Mechanical Engineering, Wroclaw University of Science and Technology, Department of Mechanics, Materials Science and Engineering, Poland*
[b] *Institute of Lightweight Structures, Chemnitz University of Technology, Germany*
**Corresponding author: szymon.duda@pwr.edu.pl*

Keywords: FML; Delamination; Fracture energy toughness; Fracture Mechanics; FEM.

ABSTRACT

The Europeans' concerns are going to the optimization of every produced part. Mostly, it consists of shape optimization, material changing, and technology process optimization. It is related to a couple of factors such as mass reduction, and strength increasing. At the time of modern technology, it is possible to design new materials with better properties. Hybrid laminates, the newest combination of different materials that are quickly developed by top universities in the European Union. These kinds of materials are using primarily in Aerospace Engineering, but gradually the automotive industry considers use them wide-reaching.

This paper focuses on one of the most important problems that occur during the use of composite materials, which is delamination. Such a process occurs predominantly between the layers especially along plastic and metal layers, and it is one of the most common reasons for the failure of those materials. In that, during the design process, the engineer has to check apart and find the weak regions. The intermediate solution for such a problem is a numerical analysis of delamination. This analysis so-called cohesive zone model (CZM) makes it possible. The fracture behavior of the material plays crucial role considering this analysis. The fracture toughness is one of the parameters that describe this behavior and needs to be implemented in this analysis.

Investigated fiber metal laminate (FML) consists of aluminum alloy AW-6061 T6 in the middle, carbon fibers reinforced and glass fibers reinforced thermoplastic layers. The material was developed by scientists at Chemnitz University of Technology (Germany) [1]. Because of its advantages such as high strength, low density, excellent corrosion and moisture resistance, high fatigue resistance, high energy absorbing capacity, and high impact resistance their application may be considered in the aerospace and automotive industry [2].

Interlaminar fracture energy toughness of the inverse fiber metal laminate with unidirectional fiber orientation was investigated by the combination of experiment and finite element method analysis. The Double Cantilever Beam test was used to predict the interlaminar fracture toughness of this laminate and was carried out according to the ASTM D5528 standard. Then the finite element analysis was carried out based on the cohesive zone model (CZM) to numerically estimate the interlaminar fracture energy according to the load-displacement curve obtained from the DCB test (Fig. 1).

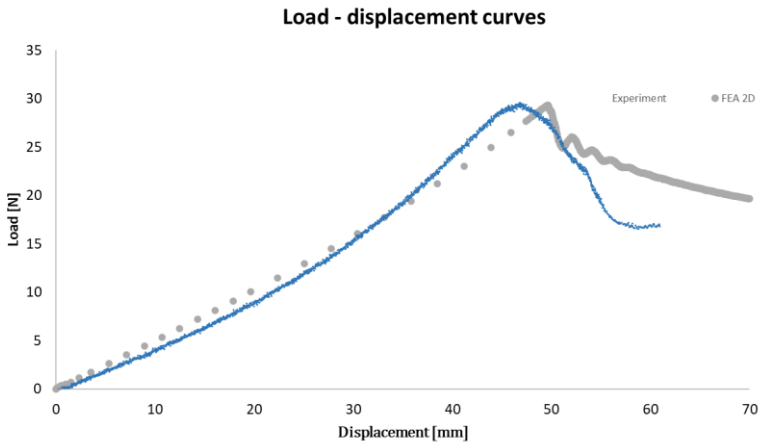

Fig. 1 DCB results, blue curve gives experimental data and grey curve the FEM results

Fig. 1 shows two curves that blue one follows the experimental results and the grey curve obtained by FEM. It is noticed that the fracture behavior represented by the numerical model is close enough in terms of max force, also the displacement at max force is an important parameter giving information once the delamination occurs. Table 1 compare these parameters for both approaches.

The approach shows that the interlaminar fracture toughness is equally approximately 0.88 kJ/m^2. The numerical results agreed with the experiments (Table 1). This approach may be used to determine the value of fracture energy for all these materials and configurations that are not covered by the normative approach. Obtaining such parameters let to apply them to models of structures and include analysis of the interface in case of such constructions.

Table 1 Results obtained from experiment and numerical approach

	Experiment	FEM
Max Force [N]	31.10	29.32
Displacement at max force [mm]	42.60	49.64
Normal Mode Fracture Energy (Mode I)	0.88 kJ/m^2	

REFERENCES

[1] T. Osiecki, C. Gerstenberger, A. Hackert, L. Kroll, and H. Seidlitz, 'THERMOPLASTIC FIBER REINFORCED/METAL-HYBRID LAMINATES FOR STRUCTURAL LIGHT-WEIGHT APPLICATIONS'.
[2] A. Salve, R. Kulkarni, and A. Mache, „A Review: Fiber Metal Laminates (FML's)-Manufacturing, Test methods, and Numerical modeling", Int. J. Eng. Technol. Sci., t. 6, nr 1, 2016.

ACKNOWLEDGMENTS

Calculations have been carried out using resources provided by Wroclaw Centre for Networking and Supercomputing (http://wcss.pl), grant No. 531.

The project was supported in part by the Polish National Agency for Academic Exchange grant number PPN/BUA/2019/1/00086

Mode I and mixed-mode (I+II and I+III) fatigue crack growth characterization of 42CrMo4 steel after heat treatment

M. Duda[a*], D. Rozumek[b], G. Lesiuk[a], M. Smolnicki[a]

[a]*Department of Mechanics, Materials and Biomedical Engineering, Wrocław University of Science and Technology, Smoluchowskiego 25, 50-370 Wrocław, Poland*
[b]*Department of Mechanics and Machine Design, Opole University of Technology, ul. Mikołajczyka 5, 45-271 Opole, Poland*
**Corresponding author: monika.duda@pwr.edu.pl*

Keywords: crack growth; fatigue; heat treatment; mixed-mode

ABSTRACT

The work contains results of experimental investigation on fatigue crack behaviour in 42CrMo4 steel after quenching and low tempering, which is one of most often heat treatments applied to the aforementioned structural material [1-3]. Tests were conducted for mixed-modes I+II and I+III, respectively on CTS and rectangular cross-section specimens (Fig. 1). CTS specimens were tested for 30 and 60 degrees loading angle, while rectangular specimens were tested for 30 and 45 degrees loading angle.

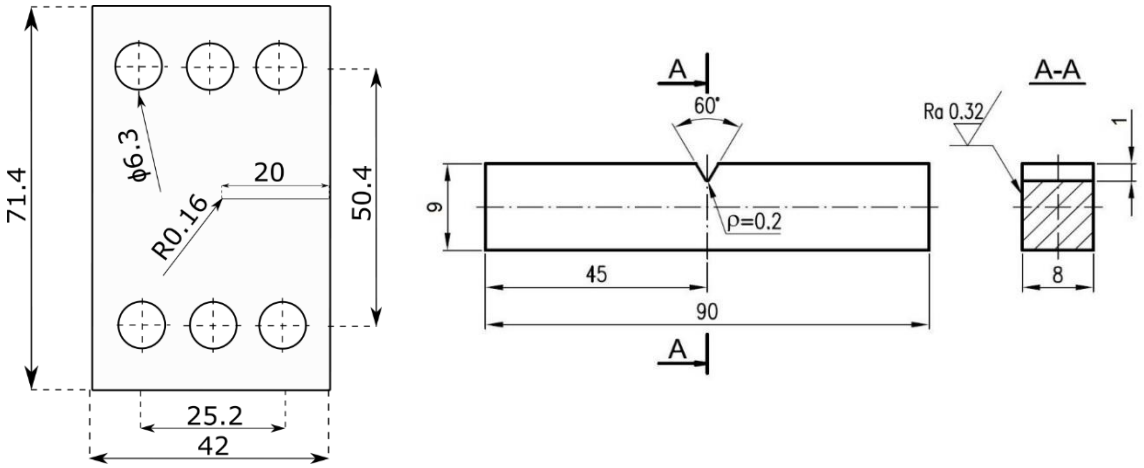

Fig. 1. Shape and dimensions of CTS and rectangular cross-section specimens; all dimensions given in mm.

Crack growth results show that greater durability of samples is observed for those which are tested under higher loading angle. The same observation was made in different study [1] for the same steel grade.

In order to calculate the mixed mode influence on crack development there were applied specific calculations. In case of CTS sample there was applied numerical solution based on Williams formula (Eq. 1-2) [4-5]. In order to construct da/dN – ΔK diagrams for mode I+III there were applied equations 3-4 [6-7].

$$K_I = \frac{F \cdot \sqrt{\pi a_0} \cdot \cos\alpha}{Wt\left(1-\frac{a_0}{W}\right)} \sqrt{\frac{0.26 + 2.65\left(\frac{a_0}{W-a_0}\right)}{1 + 0.55\left(\frac{a_0}{W-a_0}\right) - 0.08\left(\frac{a_0}{W-a_0}\right)^2}} \quad (1)$$

$$K_{II} = \frac{F \cdot \sqrt{\pi a_0} \cdot \sin\alpha}{Wt\left(1-\frac{a_0}{W}\right)} \sqrt{\frac{-0.23 + 1.4\left(\frac{a_0}{W-a}\right)}{1 - 0.67\left(\frac{a_0}{W-a_0}\right) - 2.08\left(\frac{a_0}{W-a_0}\right)^2}} \quad (2)$$

$$\Delta K_I = Y_1 \Delta\sigma \cos^2\alpha \sqrt{\pi(a_0 + a)} \quad (3)$$

$$\Delta K_{III} = Y_3 \Delta\sigma \sin\alpha \cos\alpha \sqrt{\pi(a_0 + a)} \quad (4)$$

Additionally, the results were checked in the domain of ΔK_{eq} as well as in case of mode I+II samples against MTS criterion. Moreover there was conducted fractographic investigation on all of the samples.

REFERENCES

[1] Lesiuk G, Duda MM, Correia J, de Jesus AMP, Calcada R. Fatigue crack growth of 42CrMo4 and 41Cr4 steels under different heat treatment conditions. International Journal of Structural Integrity, 2018, ISSN: 1757-9864

[2] Escalero, M., Blasón, S., Zabala, H., Torca, I., Urresti, I., Muniz-Calvente, M., & Fernández-Canteli, A. (2018). Study of alternatives and experimental validation for predictions of hole-edge fatigue crack growth in 42CrMo4 steel. Engineering Structures, 176, 621-631.

[3] Pandiyarajan, R., Arumugam, K., & Prabakaran, M. P. (2020). Fatigue life and fatigue crack growth rate analysis of high strength low alloy steel (42CrMo4). Materials Today: Proceedings.

[4] Paris P, Erdogan F (1963) A critical analysis of crack propagation laws. J Fluids Eng Trans ASME. https://doi.org/10.1115/1.3656900

[5] Lesiuk G, Smolnicki M, Mech R, et al (2020) Analysis of fatigue crack growth under mixed mode (I + II) loading conditions in rail steel using CTS specimen. Eng Fail Anal 109:104354. https://doi.org/10.1016/j.engfailanal.2019.104354

[6] Harris DO. Stress intensity factors for hollow circumferentially notched round bars. J Bas Engng 1967; 89.

[7] Chell GG, Girvan E. An experimental technique for fast fracture testing in mixed mode. Int J Fract 1978;14:81–4.

ACKNOWLEDGMENTS

This work was supported in part by grant number 2018/31/N/ST8/03590 financed by the Polish National Science Centre (Narodowe Centrum Nauki, NCN).

Experimental and numerical study of fatigue crack growth and crack closure phenomenon in constructional steel under mixed-mode loading conditions

Grzegorz LESIUK[1], Jose A.F.O. CORREIA[2], Dariusz ROZUMEK[3], Michał SMOLNICKI[1], Abilio M.P. De JESUS[2]

[a] *Wroclaw University of Science and Technology, Department of Mechanics, Materials and Biomedical Engineering, Smoluchowskiego 25 St, PL-50370 Wrocław, Poland*

[b] *University of Porto, Faculty of Engineering, Rua Dr. Roberto Frias, Campus FEUP, 4200-465 Porto, Portugal*

[c] *Opole University of Technology, Department of Mechanics and Machine Design, Mikołajczyka 5, 45-271 Opole, Poland*

**Corresponding author: Grzegorz.Lesiuk@pwr.edu.pl*

Keywords: S355 steel, 42CrMo4 steel, mixed-mode loading conditions, fatigue crack growth rate, crack closure phenomenon

ABSTRACT

The fatigue crack propagation process in metallic materials is an integral part of the fatigue lifetime assessment of structural joints. Due to different load conditions, the initiation of cracks does not always occur under mode I type of crack growth. In components subjected to complex stress state, fatigue cracks are initiated and propagate under curved trajectory following to the mixed-mode loading criteria. The object of Authors' interest is the description of the fatigue crack growth rate under complex stress state (I+II, I+III). An important factor in fatigue fracture mechanics for low, positive stress ratio R values is the fatigue crack closure phenomenon described by Elber. In literature, a lot of experimental results and theoretical models, including such effect are available only for mode I. In the case of the complex stress state, the number of researches is limited. This work is an attempt to fill the existing gap. An essential element of the presented experimental work is also an attempt to build fatigue crack growth models based on the cyclic strain energy parameter based on the J-integral - more precisely effective Jeff corrected for the effect of fatigue crack closure. In this case, the proposed equivalent J-integral for all three modes of fracture is the following:

$$\Delta J_{eq(eff)} = \Delta J_{Ieff} + \Delta J_{IIeff} + \Delta J_{IIIeff} \tag{1}$$

The cyclic J-integral was computed using numerical methods and directly calculated from an experiment using formula with corrected (effective) strain energy density U:

$$J_{eq} = -\frac{1}{2\pi L}\left(\frac{\partial U_{I+II/I+III}}{\partial a}\right)_{u,\alpha} \tag{2}$$

In Eq. (2) L represents ligament length (non-fractured specimen length measured along the crack path), u – displacement, α – load angle, U_{I+III}/ U_{I+II} – effective strain energy density for mode I+III/I+II.

The crucial part of the numerical analysis is the identification of the closure load level from the hysteresis loops. The algorithm for determination of closure point can be described in the following steps; registration of F-COD (Crack Opening Displacement) values during proper load cycles, splitting the F-COD line into two parts (i.e. nonlinear and linear) by fitting a first-order polynomial function (with two constants: A0, A1) for the linear part and a second-order polynomial function (with three different constants: B0, B1 and B2) for the nonlinear one, Adjustment of the constants of second-order function by minimising the sum of squared errors of prediction squares (or residual sum of squares - RSS). The value of expected closure load F_k corresponds to the smallest RSS (a measure of deviation from the point which

split F-COD curve into two parts). The presented method was also easily applied (with automation) in experimental campaign with the control system of the testing machine (Fig.1). Another important aspect was the comparison of the measured hysteresis loops from local approach (close to crack tip using DIC and tensometers) with the global hysteresis loops measured from clip-on gage (far-field displacement).

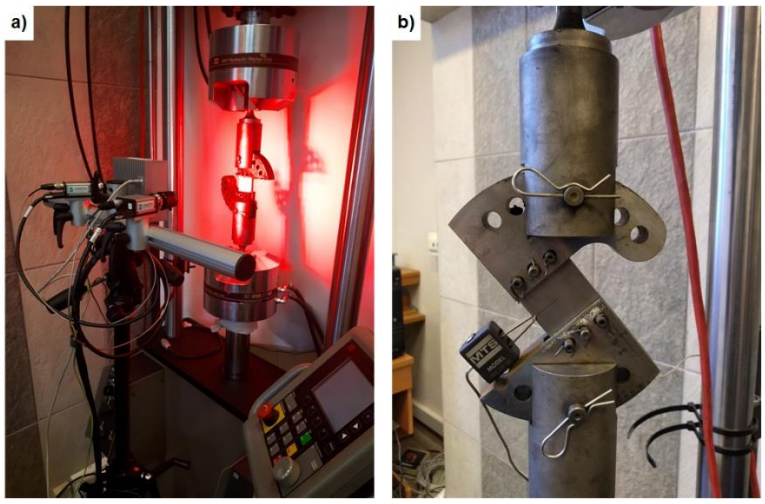

Fig. 1**.** Mixed-mode (I+II) fatigue crack growth rate testing and crack closure measurement system: a) using DIC – local, full-field strain analysis, b) using CMOD (Crack Mouth Opening Displacement) clip-gage

According to the experimental results, it is worth to note, that the applied measurement system allows separating mode I crack closure and mode II/III sliding-type crack closure. Obtained fatigue crack growth rate results for different mixity levels (and stress ratio) can be successfully analyzed using effective, equivalent stress intensity factors. Elber parameter U was lower for mixed-mode loading condition – compared with mode I data. However, for dominant shear mode (II, III) the roughness induced crack closure mechanism was dominant, RICC increase as a result of the crack surfaces contact (and sliding mode). This effect was observed in [3] for loading mode I+III (bending with torsion). On the other hand, for stabilized fatigue crack growth regime in CTS specimens, the Elber closure parameter for mixed-mode loading condition was close to mode I – U-Elber parameter.

ACKNOWLEDGMENTS

This work was supported by grant number 2018/02/X/ST8/02041 (02NA/0001/19) financed by the Polish National Science Centre (Narodowe Centrum Nauki, NCN).

Estimating Failure Mechanism of Steel Specimens using Stress-Corrosion-Cracking (SCC) Testing Methods: State and Development

Ericha Dwi Wahyu Syah Putri, Eko Surojo, Eko Prasetya Budiana, Triyono, Aditya Rio Prabowo*

Department of Mechanical Engineering, Universitas Sebelas Maret, Surakarta 57126
**Corresponding author: aditya@ft.uns.ac.id*

Keywords: Stress-corrosion-cracking; material failure; steel specimen; laboratory testing methods.

ABSTRACT

Stress Corrosion Cracking is the phenomenon of cracking in the material that occurs due to a combination of tensile stress, material sensitivity, and reactive environment [1]. Fig. 1 describes the parameters that cause stress corrosion cracking. SCC can cause material failure, so the phenomenon is hazardous for human life safety. It is caused by the crack propagation mechanisms in the SCC cannot be controlled and the failure time is unpredictable [2]. SCC susceptible experienced by structures operating in a reactive environment such as seawater environment. If the material structure is in a corrosive seawater environment and receives loads from continuous waves of seawater, the structure will experience failure caused by SCC [3]. Because of the dangerous effects caused by SCC, it is necessary to research these testing methods and standards. Previous studies have conducted SCC testing using several methods, including the U-Bend specimen [4], C-Ring specimen [5], tensile specimen [6], [7], and slow strain rate testing [8]. However, comprehensive information about these methods is still limited. Therefore, it is necessary to discuss how to analysis several SCC testing methods on a laboratory scale. This paper presents as a reference for students and future researchers who want to study the SCC phenomenon. Besides, determining the appropriate SCC testing method can help engineers consider selecting materials to be used in the design process using more advanced technology.

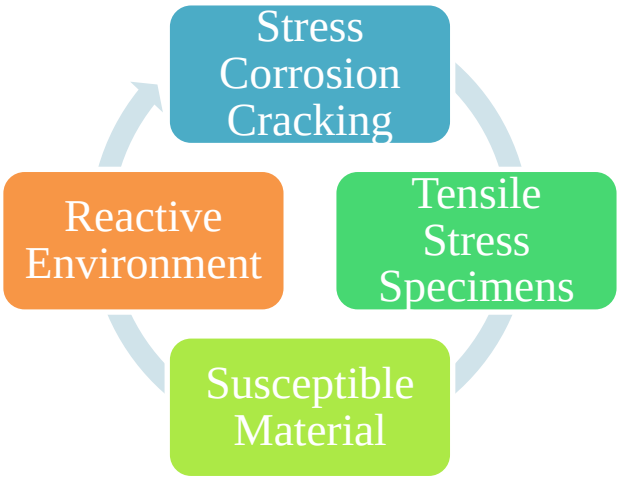

Fig. 1. The Parameters of Stress Corrosion Cracking [9]

REFERENCES

[1] Nishida, S.: Failure analysis in engineering applications. 1st Great Britain, Tokyo (1992).
[2] Fontana, M.G.: Corrosion engineering. 3rd McGraw- Hill Book Company, Singapore (1987).
[3] Scatigno, G. G., Dong, P., Ryan, M. P., Wenman, M.R.: The effect of salt loading on chloride-induced stress corrosion cracking of 304L austenitic stainless steel under atmospheric conditions. Materialia 8, 100509 (2019).

[4] Chu, T., Nuli, Y., Cui, H., Lu, F.: Pitting behavior of welded joint and the role of carbon ring in improving corrosion resistance. Material and Design 183, 108120 (2019).
[5] Prawoto, Y., Djuansjah, J. R. P., Wan Nik, W. B., Enemuoh, E.: Critical view on the usage of C-ring specimen for stress corrosion crack (SCC) test on orthopedic implant: Experimental, numerical and analytical approaches. Material Science and Engineering C 32, 1271-1279 (2012).
[6] Padekar, B. S., Raman, R. K. S., Raja, V. S., Paul, L.: Stress corrosion cracking of a recent rare-earth containing magnesium alloy, EV31A, and a common Al-containing alloy, AZ91E. Corrosion Science 71, 1-9 (2013).
[7] Bagchi, A., Gope, D. K., Chattopadhyaya, S., Wuriti, G.: A critical review on susceptibility of stress corrosion cracking in maraging steel weldments. Material Today: Proceedings 27, 2303-2307 (2020).
[8] Wang, Z., Xie, F., Wang, D., Liu, J.: Effect of Applied Potential on Stress Corrosion Cracking Behavior of X80 Steel in Alkaline Soil Simulated Solution with Sulfate-reducing Bacteria. Engineering Failure Analysis (2020).
[9] Jones, D. A.: Principles and Prevention of Corrosion. 2nd Prentice-Hall, Inc., USA (1996).

ACKNOWLEDGMENTS

This work was supported by the RKAT PTNBH Universitas Sebelas Maret, Surakarta under Scheme of Mandatory Research - Year 2021, with Grant/Contract No. 260/UN27.22/HK.07.00/2021. The support is gratefully acknowledged by the authors.

Long term Behaviour of Recycled Aggregate Concrete under sustained loading

B. Suguna Rao[1], Ampli Suresh[2], Srikanth M Naik[3]

1Faculty (Corresponding Author), Civil Engineering Department, Ramaiah Institute of Technology, Bangalore, Karnataka, India.
Address: C-406, Gowri Apartment, New BEL Road, Bangalore-560054
Telephone: 9611802797, E-mail: suguna_rao@yahoo.com
2M.Tech Student, Civil Engineering Department, Ramaiah Institute of Technology, Bangalore, Karnataka, India.
Address: # 23/1. Tejasnilaya, 5th cross, moodalapalya main road. Vijayanagar, Bangalore-560072,
Telephone: 9535938144, E-mail: sureshampili@yahoo.com
3Professor, Civil Engineering Department,
Ramaiah Institute of Technology, Bangalore, Karnataka, India.
Telephone: 9845879101, E-mail: srikanth_naik@yahoo.com

Keywords: recycled aggregate concrete, compressive strength, split tensile strength, flexural strength, and creep.

Abstract

Urbanization and Industrialization has increased the construction activities leading to huge generation of Construction and demolition waste. Construction wastes being bulky and heavy are unsuitable for disposing by incineration or compositing.

Central pollution board has estimated quantum of solid waste being generated in India to 48 million tons out of which 25% contributes to waste generated from construction industry. Reutilization or recycling is an important strategy for management of such waste. Hence this study is carried out to utilize the C & D waste developed from construction activities. Hence a study is carried out to replace natural aggregates by recycled aggregates partially to arrive at structural concrete of M60 grade for replacement ratio of 0%, 30%, 35%, 40%, 45% and 50%. When hydrated cement paste is subjected to sustained stress, depending upon magnitude of applied stress the C-S-H bond will lose large amount of physically absorbed water. This applied stress causes contraction in the system due to the hydrostatic tension in small capillaries of the hydrated cement paste. The non-linearity in the stress-strain relation in concrete at stress levels of about 30-40 % of the ultimate stress shows the interfacial transition zone micro cracks to crack. The bond between the cement and aggregate transfers the load to latter causing elastic deformation of aggregate that contributes to creep of Recycled aggregate concrete.

Parameter Optimization and Innovation Review of the Metal Matrix Composites: State and Development of the Manufacturing Process

Hammar Ilham Akbar, Eko Surojo*, Dody Ariawan, Aditya Rio Prabowo*

Department of Mechanical Engineering, Universitas Sebelas Maret, Surakarta 57126, Indonesia
**Corresponding author: esurojo@ft.uns.ac.id* (E.S.); *aditya@ft.uns.ac.id* (A.R.P.)

Keywords: Stir Casting Parameter; Metal Matrix Composite; Porosity; Optimization

ABSTRACT

Composite metal matrix is a concern for various industries, both automotive, aerospace, solar system and manufacturing due to its advanced properties of strength, stiffness, high temperature performance, wear resistance and low coefficient oh thermal expansion [1]. Aluminum matrix composites can be manufactured using a variety of techniques, such as squeeze casting, liquid metal infiltration, spray deposition and stir casting. Stir casting is the most commonly used technique because it is simple, flexible and the cheapest manufacturing process [2]. However, common technical problems during stir casting are the homogeneity of particle distribution, reinforcement wettability and porosity [3]. Its problem needs to be considered in order to obtain the desired material properties in the composite manufacturing process. Porosity plays an important role in the mechanical properties of AMC, several factors that influence porosity are: (a) the evolution of hydrogen gas (b) the phenomenon of shrinkage during solidification (c) trapping of air during the stirring process [4]. Fig. 1 describes the various parameters that cause porosity. The amount of porosity generally depends on process parameters such as agitation speed, stirrer position, blade angle and stirring time [5]. Researchers have studied various parameters of the stir casting process to obtain the desired mechanical properties of the material such as the geometry and position of the stirrer [6], fluid flow during stirring [7], particle drawdown [8]. In addition, various innovations have been carried out such as assisted stir casting and IoT to improve production performance and material properties [9, 10]. This paper presents the widespread study of parameters and innovations in the stir casting process.

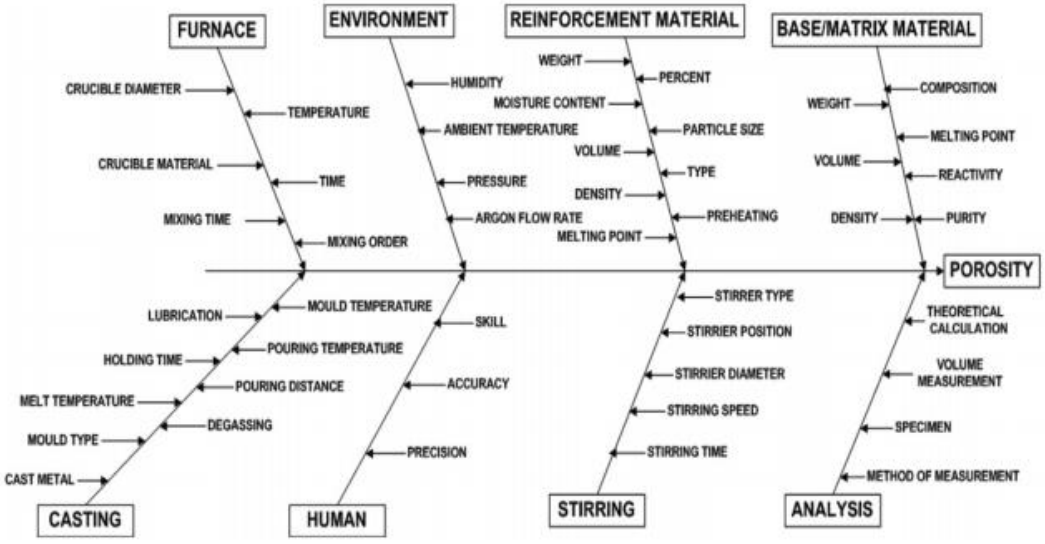

Fig. 1. Fish-bone diagram for porosity [11]

REFERENCES

1. Naher, S., Brabazon, D., Looney, L.: Simulation of the stir casting process. J. Mater. Process. Technol. 143–144, 567–571 (2003).
2. Su, H., Gao, W., Zhang, H., Liu, H., Lu, J., Lu, Z.: Optimization of stirring parameters through numerical simulation for the preparation of aluminum matrix composite by stir casting process. J. Manuf. Sci. Eng. Trans. ASME. 132, 0610071–0610077 (2010).
3. Vishnu Prasad, K., Jayadevan, K.R.: Simulation of Stirring in Stir Casting. Procedia Technol. 24, 356–363 (2016).
4. Hashim, J., Looney, L., Hashmi, M.S.J.: The wettability of SiC particles by molten aluminium alloy. J. Mater. Process. Technol. 119, 324–328 (2001).
5. Moses, J.J., Dinaharan, I., Sekhar, S.J.: Prediction of influence of process parameters on tensile strength of AA6061/TiC aluminum matrix composites produced using stir casting. Trans. Nonferrous Met. Soc. China (English Ed. 26, 1498–1511 (2016).
6. Rangrej, S., Mehta, V., Ayar, V., Sutaria, M.: Effects of stir casting process parameters on dispersion of reinforcement particles during preparation of metal composites. Mater. Today Proc. (2021).
7. Kumar, M.S., Begum, S.R., Vasumathi, M., Ross, K.N.S.: Applying visualization techniques to study the fluid flow pattern and the particle distribution in the casting of metal matrix composites. J. Manuf. Process. 58, 668–676 (2020).
8. Tran, T.T., Vo, T.T., Cho, S.C., Lee, D.H., Hwang, W.R.: A stir casting system for drawdown of light particles in manufacturing of metal matrix composites. J. Mater. Process. Technol. 257, 123–131 (2018).
9. Chaubey, A., Dwivedi, R., Purohit, R., Rana, R.S., Choudhary, K.: Experimental inspection of aluminium matrix composites reinforced with SiC particles fabricated through ultrasonic assisted stir casting process. Mater. Today Proc. 26, 3054–3057 (2019).
10. Raj, P.A.C., Kavitha, P., Sophia, S., Thilagam, K., Devi, V., Khan, J.M.F.: IoT based stir casting system of aluminium MMC. Mater. Today Proc. 10–12 (2021).
11. Suthar, J., Patel, K.: Identification, screening and optimization of significant parameters for stir cast hybrid aluminium metal matrix composite. Heliyon. 4, (2018).

ACKNOWLEDGMENTS

This work is funded by the Ministry of Research and Technology of the Republic of Indonesia (National Research and Innovation Agency), through the doctoral dissertation research program in 2021.

Microstructural analysis and radial compression behaviour of GFRP/CFRP composite bars

Lesiuk G.[a], Duda Sz.[a], Barcikowski M. [a], Ziółkowski G. [a], Żołyńska K. [a], Zielonka P. [a], Warycha J. [a], Stabla P. [a], Lubecki M. [a], Filipiak-Kaczmarek A. [a] , Błażejewski W.[a]

[a] *Faculty of Mechanical Engineering, Wroclaw University of Science and Technology, Poland*
**Corresponding author: Grzegorz.Lesiuk@pwr.edu.pl*

Keywords: composite rods; defects; radial compression test; failure analysis, computer tomography

ABSTRACT

Composite reinforcing rebars (CRBs) are becoming more and more popular in construction applications due to several advantages over steel rebars. This also applies to similar structures, such as composite mining and construction anchors, mining nets, carbon reinforcements of building structures, etc. The main driver is the resistance to chemically aggressive environments, such as seawater, corrosive environment in mines and concrete structures, and open-air conditions [1-2]. One aspect that hinders the development of the CRB application is the lack of standards for assessing performance quality. Often, CRB producers advertise their products, calling them corrosion-proof, which is not true because they have not been age tested, and it is not known will the reinforcing effect will be after, for example, one hundred years of exploitation of the building structure.

The experimental campaign designed four different types of hybrid CFRP/GFRP composite bars subjected to microstructural and strength analysis. Longitudinal cross-sections of round bars are shown in Fig.1. The test specimens were produced by pultrusion and filament winding methods based on epoxy resin and glass fibers (bright area) and carbon fibers (dark area).

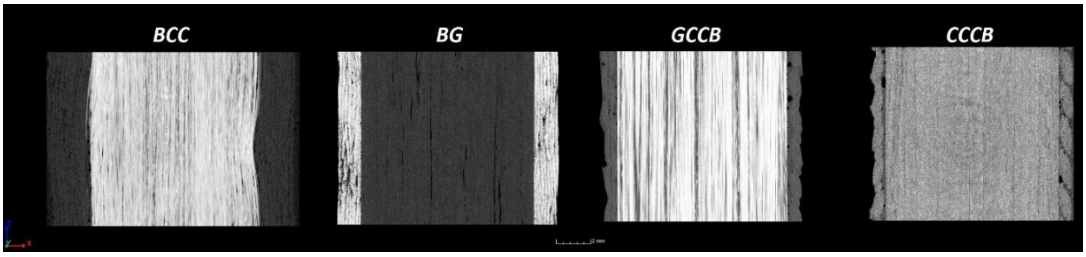

Fig. 1 Longitudinal cross-section of the designed hybrid composite rods

In order to assess the size of possible technology-induced microstructure defects, a detailed analysis was performed using computer tomography(CT). CT scans were performed using a GE Phoenix v|tome|x m 300/180 technical tomography system and phoenix datos|x2.7.2 software (GE Sensing & Inspection Technologies GmbH, Wunstorf, Germany). A resolution (voxel size) of 8 µm was achieved for the tested samples. The lamp voltage and current at the time of measurement were 120kV and 240 µA, respectively. A total of 3000 projections were collected with an integration time of 400 ms per projection. The data analysis, which resulted in the volume of the composites and the determination of the pore size (Figure 2), was carried out using VG Studio MAX 3.3 (Volume Graphics GmbH, Heidelberg, Germany).

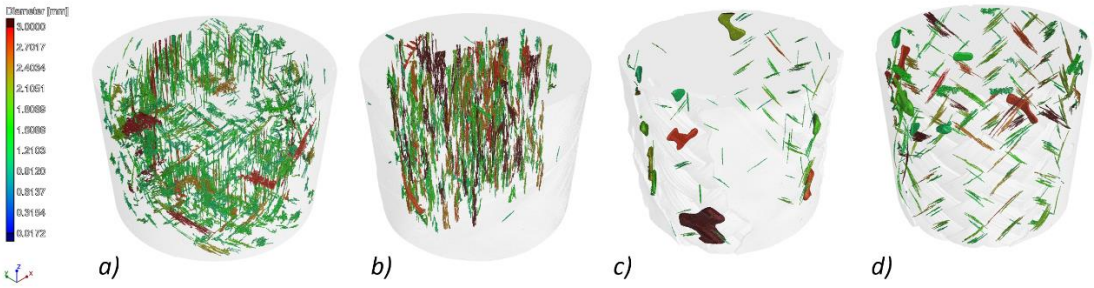

Fig. 2. Defects distribution with a diameter larger than 1 mm for structures a) BCC, b) BG, c)GCCB, d) CCCB

In the next phase of the experimental campaign, radial compression test was carried out to evaluate the potential influence of the defects distribution and hybridization influence on the mechanical response of fiber-matrix during the radial compression test. Selected results are shown in Fig. 3.

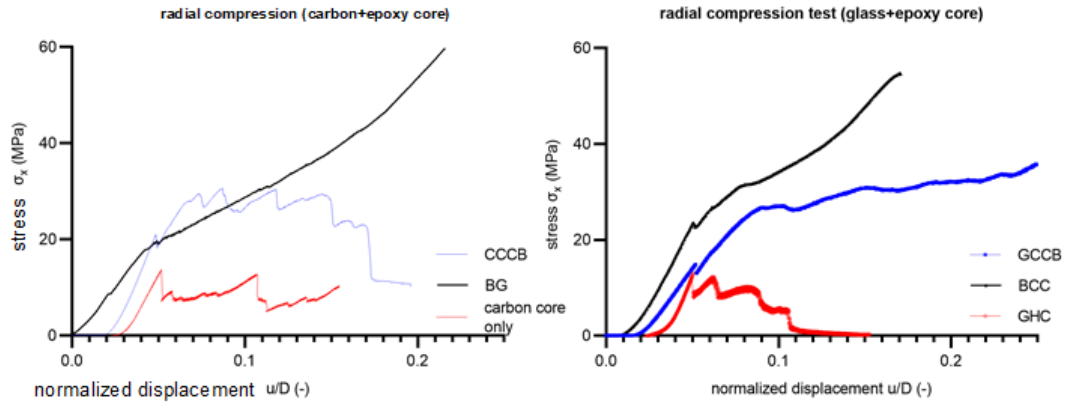

Fig. 3. Radial compression results for glass+epoxy core and carbon+epoxy core compared with monolithic bar (glass – GHC, carbon core)

As may be noted, each time an improvement in compressive strength was obtained - with respect to monolithic bars - manufactured by pultrusion and winding methods containing two different types of fibers.

REFERENCES

[1] Claure, De Caso y Basalo, F., Nanni, A., GFRP hollow-core bars as internal reinforcement for concrete slabs. Civil, Architectural & Environmental Engineering, pp. 68-74, 2015.

[2] S. Spagnuolo, A. Meda, Z. Rinaldi, A. Nanni., Curvilinear GFRP bars for tunnel segments applications, Civil, Arch. & Environmental Eng., pp. 137-147, Composites B: V.141, 2018.

ACKNOWLEDGMENTS

The research was financed by the National Centre for Research and Development of Poland (NCBiR) grant number LIDER/40/0219/L-10/18/NCBR/2019.

Review of Polypropylene in Fused Deposition Modelling (FDM): Optimizing The Potential As a 3D Printing Filament

Ruben Bayu Kristiawan, Aditya Rio Prabowo*, Fitrian Imaduddin, Dody Ariawan

Department of Mechanical Engineering, Universitas Sebelas Maret, Surakarta 57126, Indonesia
**Corresponding author: aditya@ft.uns.ac.id*

Keywords: Additive Manufacturing; Fused Deposition Modeling; Filament Polypropylene; Filament Engineering; Mechanical Properties

ABSTRACT

Fused Deposition Modeling (FDM) is an Additive Manufacturing technology that generally uses polymer filaments as the material. Polymers of the Polypropylene (PP) type are an alternative filament material[1, 2]. However, this type of filament has several properties that make it less popular than Acrylonitrile Butadiene Styrene (ABS), Polylactic Acid (PLA), or other types of filaments. Pure PP filament has mechanical strength below ABS, PLA, Nylon, and PETG, as shown in the diagram shown in Fig. 1 [3–5]. Due to shrinkage and warping properties, it is difficult to adhere to the platform due to the lack of adhesion to standard platform materials and the high risk of welding on PP-based platform materials, making PP material has several drawbacks; to be used in the FDM method [6].

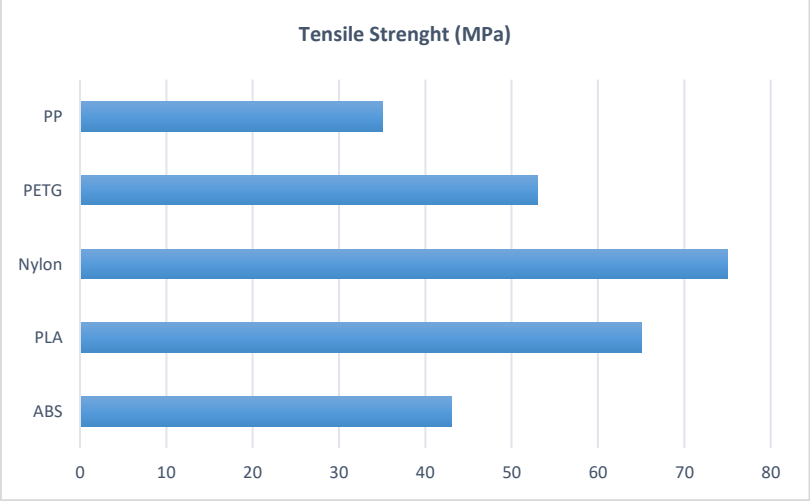

Fig. 1. Filament tensile strength diagram[2–5, 7–10].

In this study, a literature review on PP filament engineering has been carried out to improve its mechanical properties and place literature on the relationship between the FDM method's processing parameters to get PP filament printing results with maximum conditions. Increasing the mechanical properties of PP can be done by engineering it into a composite PP filament by adding an additive that acts as a reinforcement. In addition, additives in the form of high volume filler fractions can reduce shrinkage and warping properties. Several types of reinforcement that can increase the mechanical strength of the PP filament can be seen in fig.2 [10–12]. The difficulty of the extrusion results adhere to the platform can be overcome by optimizing a comprehensive parametric study. A higher adhesion force is obtained by increasing several parameters such as platform temperature, extrusion temperature, increasing the flow rate, and decreasing the first layer's thickness [13]. And for the risk of welding on PP-based platform materials, you can use several choices of types of platforms that have been specially designed as PP filament platforms [14].

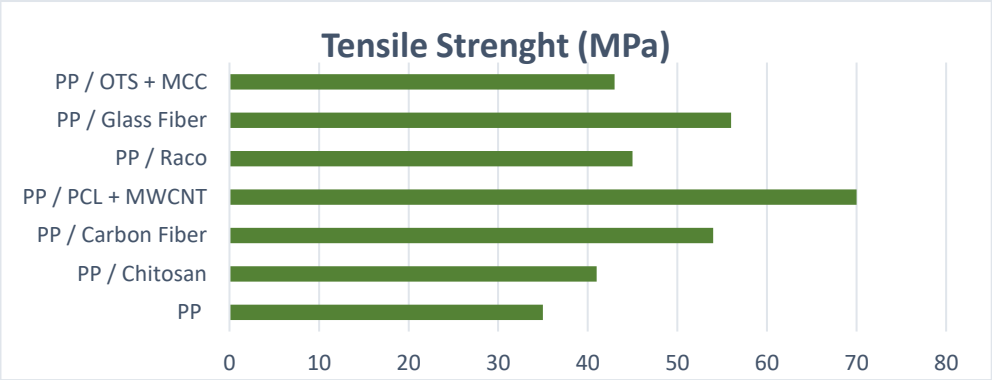

Fig. 2. Composite PP Filament tensile strength diagram [12, 15–19]

REFERENCES

[1] Sodeifian G, Ghaseminejad S, Yousefi AA. Preparation of polypropylene/short glass fiber composite as Fused Deposition Modeling (FDM) filament. *Results Phys* 2019; 12: 205–222.

[2] Carneiro OS, Silva AF, Gomes R. Fused deposition modeling with polypropylene. *Mater Des* 2015; 83: 768–776.

[3] Peterson AM. Review of acrylonitrile butadiene styrene in fused filament fabrication: A plastics engineering-focused perspective. *Addit Manuf* 2019; 27: 363–371.

[4] Lay M, Thajudin NLN, Hamid ZAA, et al. Comparison of physical and mechanical properties of PLA, ABS and nylon 6 fabricated using fused deposition modeling and injection molding. *Compos Part B Eng* 2019; 176: 107341.

[5] Szykiedans K, Credo W, Osiński D. Selected Mechanical Properties of PETG 3-D Prints. *Procedia Eng* 2017; 177: 455–461.

[6] Milosevic M, And DS, * KLP. Characterizing the Mechanical Properties of Fused Deposition Modelling Natural Fiber Recycled Polypropylene Composites. *J Compos Sci* 2017; 1: 7.

[7] Chacón JM, Caminero MA, García-Plaza E, et al. Additive manufacturing of PLA structures using fused deposition modelling: Effect of process parameters on mechanical properties and their optimal selection. *Mater Des* 2017; 124: 143–157.

[8] Weng Z, Wang J, Senthil T, et al. Mechanical and thermal properties of ABS/montmorillonite nanocomposites for fused deposition modeling 3D printing. *Mater Des* 2016; 102: 276–283.

[9] Kaynak C, Varsavas SD. Performance comparison of the 3D-printed and injection-molded PLA and its elastomer blend and fiber composites. *J Thermoplast Compos Mater* 2019; 32: 501–520.

[10] Hertle S, Drexler M, Drummer D. Additive Manufacturing of Poly(propylene) by Means of Melt Extrusion. *Macromol Mater Eng* 2016; 301: 1482–1493.

[11] Sodeifian G, Ghaseminejad S, Yousefi AA. Preparation of polypropylene/short glass fiber composite as Fused Deposition Modeling (FDM) filament. *Results Phys* 2019; 12: 205–222.

[12] Spoerk M, Savandaiah C, Arbeiter F, et al. Optimization of mechanical properties of glass-spheres-filled polypropylene composites for extrusion-based additive manufacturing. *Polym Compos* 2019; 40: 638–651.

[13] Tlegenov Y, Lu WF, Hong GS. A dynamic model for current-based nozzle condition monitoring in fused deposition modelling. *Prog Addit Manuf* 2019; 4: 211–223.

[14] Spoerk M, Gonzalez-Gutierrez J, Lichal C, et al. Optimisation of the adhesion of polypropylene-based materials during extrusion-based additive manufacturing. *Polymers (Basel)*; 10. Epub ahead of print 2018. DOI: 10.3390/polym10050490.

[15] Cayla A, Campagne C, Rochery M, et al. Melt spun multifilament yarns of carbon nanotubes-based polymeric blends: Electrical, mechanical and thermal properties. *Synth Met* 2012; 162: 759–767.

[16] Rathnayake WSM, Karunanayake L, Samarasekara AMPB, et al. Fabrication and Characterization of Polypropylene - Microcrystalline Cellulose Based Composites with Enhanced Compatibility. *MERCon 2019 - Proceedings, 5th Int Multidiscip Moratuwa Eng Res Conf* 2019; 354–359.

[17] Spoerk M, Savandaiah C, Arbeiter F, et al. Anisotropic properties of oriented short carbon fibre filled polypropylene parts fabricated by extrusion-based additive manufacturing. *Compos Part A Appl Sci Manuf* 2018; 113: 95–104.

[18] Salmah H, Amri F, Kamarudin H. Properties of Chitosan-Filled Polypropylene (PP) Composites: The Effect of Acetic Acid. *Polym - Plast Technol Eng* 2012; 51: 86–91.

[19] Jin M, Neuber C, Schmidt HW. Tailoring polypropylene for extrusion-based additive manufacturing. *Addit Manuf* 2020; 33: 101101.

Cyclic analysis of isotropic damage models under the nonlocal approach

B. C. Campos [a*], L. R. S. Pereira [a], S. S. Penna [a]

[a] *Department of Structural Engineering, Federal University of Minas Gerais, Brazil*
**Corresponding author: bu_caroline@hotmail.com*

Keywords: cyclic analysis; isotropic damage models; nonlocal models.

ABSTRACT

The study of appropriate models for representing quasi brittle materials such as concrete has been addressed over the past years, and various approaches have been presented and discussed in literature. Isotropic damage models, for instance, are examples of formulations that consider the material degradation over a damage parameter and its correspondent evolution law. From other perspective, the nonlocal approach presents itself as a valuable method to deal with strain localization and mesh dependence that might occur in local models.

In this paper, both isotropic damage models and the nonlocal formulation are considered so that numerical simulations are in consonance with experimental data. Furthermore, the analyses consider a cyclic loading of the structure, feasible due to the adaptation of cyclic stress-strain laws to continuum damage mechanics framework [1]. For the numerical simulations herein presented, the adopted damage constitutive model is based on a standard isotropic damage model with Mazars' equivalent strain, considering an exponential damage law.

The model was implemented in the INSANE (Interactive Structural Analysis Environment) platform, an open-source software developed at the Department of Structural Engineering of the Federal University of Minas Gerais [2].

The damage mechanics framework for isotropic damage models considers the following stress-strain relationship [3]:

$$\sigma_{ij} = (1 - \omega) D^{e}_{ijkl} \varepsilon_{kl}, \tag{1}$$

where σ_{ij} represents the stress tensor components, ε_{kl} represents the strain tensor components, D^{e}_{ijkl} represents the elastic stiffness tensor components and ω is the damage variable. The stress-strain relationship is complemented by a damage loading function $f = f(\tilde{\varepsilon}, \kappa)$, being $\tilde{\varepsilon}$ the equivalent strain and κ a history variable indicating the highest value of $\tilde{\varepsilon}$ assumed during the loading.

Since the damage evolution is related to the strain, it is possible to stablish a connection between it and the stress-strain law. Hence, it is noteworthy that the parameters of the damage law must be parametrized to correspond to the material properties and adequately represent the material behaviour.

Regarding the nonlocal approach, it considers the state variables in the neighbourhood of a point so that the stress in such point is computed [4]. The variable to be considered on the nonlocal approach is arbitrary, although a few requirements should be accomplished. For instance, the maximum value of the equivalent strain is a commonly adopted variable for isotropic damage models, since it has a monotonic behaviour and therefore adequately represents the structure response under loading.

To validate the proposed coupled approach, a four-point bending beam [5] was simulated, as depicted in Fig. 1. Firstly, it was necessary to adequately define the parameters of the aforementioned simplified Mazars isotropic damage model [6] so that the material representation accorded with experimental tests. Then, the nonlocal model was employed, and the cyclic analysis was performed. As illustrated in Fig. 2, the equilibrium path obtained by the isotropic model is in great agreement with the experimental curve.

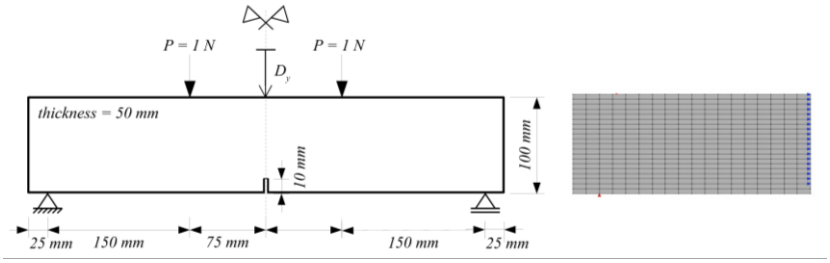

Fig. 1**.** Configuration and mesh for the beam [5].

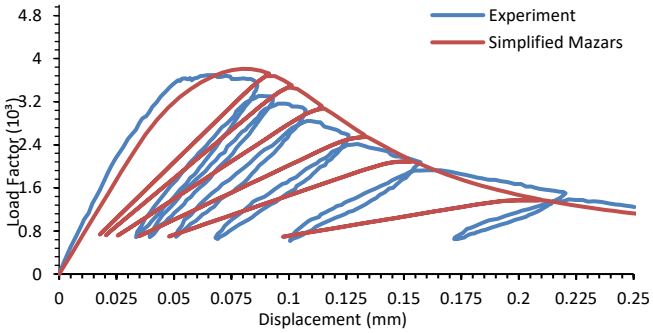

Fig. 2**.** Equilibrium paths for cyclic loading considering the nonlocal model.

The association of the different approaches herein mentioned provided consistent results. Therefore, it is highlighted the importance and utility of aggregating such methodologies so that the simulations have a more realistic characteristic especially when compared to experimental tests.

REFERENCES

[1] Pereira, L. R. S.: Formulação de modelos de dano tensorial para análise fisicamente não linear de estruturas de concreto submetidas a carregamentos monotônicos e cíclicos. Masters Dissertation, Federal University de Minas Gerais, Belo Horizonte (2020).

[2] Fonseca, F., Pitangueira, R.: An object-oriented class organization for dynamic geomet-rically nonlinear FEM analysis. Iberian Latin American Congress on Computational Methods in Engineering – CILAMCE, Belém, Brazil (2007).

[3] de Borst, R.: Fracture in quasi brittle materials: a review of continuum damage-based approaches. Engineering Fracture Mechanics (69), 95-112 (2002).

[4] Jirasék, M.: Non-local damage mechanics with application to concrete. Révue Française de Génie Civil (8), 683-707 (2004).

[5] Hordijk, D. A.: Local approach to fatigue of concrete. Doctorate Thesis, Delft University of Technology, Netherlands (1991).

[6] de Borst, R., Gutiérrez, M. A.: A unified framework for concrete damage and fracture models including size effects. International Journal of Fracture (95), 261-277 (1999).

ACKNOWLEDGMENTS

The authors gratefully acknowledge the important support of the Brazilian research agency CNPq (in Portuguese “Conselho Nacional de Desenvolvimento Científico e Tecnológico”) – grant 311663/2017-6.

Isotropic damage models for physically nonlinear cyclic analysis using the secant operator

Lívia Ramos Santos Pereira[a*], Bruna Caroline Campos[a], Samuel Silva Penna[a]

[a]*Department of Structural Engineering, Federal University of Minas Gerais, Belo Horizonte, Brazil*
**Corresponding author: lrsp@ufmg.br*

Keywords: Isotropic Damage Models; Cyclic Secant Operator; Cyclic Analyses.

ABSTRACT

The description of the concrete nonlinear behavior has been an important issue in structural engineering since the 1960s decade. Despite the diversity of constitutive models for concrete, it is noteworthy that most of those are restricted to the envelope function and only a few models include cyclic regimes. Aiming to couple some well-established models with cyclic analysis, the present work proposes the adaptation of the damage formulation to include unloading and reloading paths.

In this paper, three models of isotropic damage are presented. The model proposed by Lemaitre and Chaboche [1], with the equivalent strain $\bar{\varepsilon}$ defined based on energy criteria; the model by de Vree et al. [2], which deals with strain tensor invariants; and Mazars model [3], based on principal strains.

These models are in agreement with the unified framework proposed by [4] and extended by [5], developed to describe elastic degradation and damage models based on the concept of loading function. The loading function is given by $F[\bar{\varepsilon}, D] = \bar{\varepsilon} - \bar{r}[D]$, where $\bar{r}$ is the history variable, that is related with the maximum damage.

The strategy adopted to make cyclical analyses feasible was the cyclic secant operator (E^{cs}), based on [6]. This operator (Eq. 1) is responsible for mapping the cycle, relating equivalent strain to equivalent stress. It comes from the initial elasticity modulus (E^0) and a damage law, which provides the current damage variable D.

$$\tilde{\sigma} = E^{cs}\tilde{\varepsilon}; \qquad E^{cs} = (1 - D)E^0. \tag{1(a, b)}$$

Using E^{cs} is possible to obtain the tangential stiffness (E^t_{ijkl}) during the cyclic regimes

$$E^t_{ijkl} = E^{cs} + \frac{1}{\bar{H}}\bar{m}_{ij}\,\bar{n}_{kl}, \qquad \bar{m}_{ij} = -E^0_{ijkl}\varepsilon_{kl};\ \bar{n}_{kl} = \frac{\partial F}{\partial \bar{\varepsilon}} = \frac{\partial \bar{\varepsilon}}{\partial \varepsilon_{kl}};\ \bar{H} = -\frac{\partial F}{\partial \bar{r}}\frac{\partial \bar{r}}{\partial D} = \frac{\partial \bar{r}}{\partial D}, \tag{2(a, b, c, d)}$$

where $\bar{m}_{ij}$ is the degradation direction; $\bar{n}_{kl}$ is the direction normal to the loading surface and $\bar{H}$ is the hardening-softening modulus.

For the unloading and reloading regimes, the elastic degradation (ED) and the elastoplastic (EP) proposals were reformulated from the damage laws and the equivalent strain definitions. The linear law based on focal point was also considered. This approach is similar to ED, with the difference that the cycles are directed to a pole, allowing the analysis to reproduce both the stiffness degradation and the appearance of permanent strain.

To validate the proposed methodology, numerical simulations of direct tension and three-point bending [7] were performed, as illustrated in Fig. 1 and Fig. 2. The model was implemented in the open-source software INteractive Structural Analysis Environment (INSANE), developed at the Department of Structural Engineering of the Federal University of Minas Gerais.

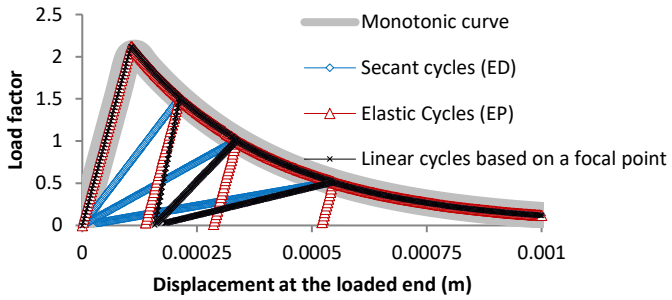

Fig. 1. Direct tension simulation – model by [2].

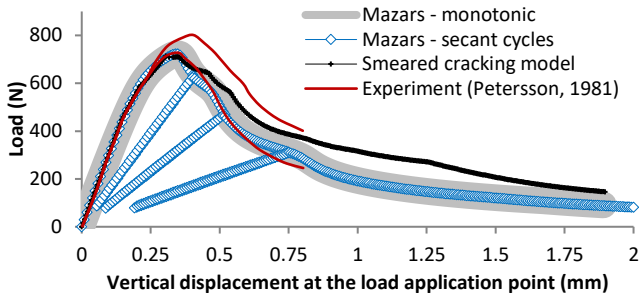

Fig. 2. Three-point bending simulation.

The proposed methodology for adapting isotropic damage models to cyclic analysis proved to be suitable for describing simple stress/strain states. The simulations were carried out for different constitutive models, damage laws and unloading/reloading paths, leading to consistent results.

REFERENCES

[1]Lemaitre, J.; Chaboche, J. L.: Mechanics of Solid Materials. CUP, Cambridge (1990).

[2]de Vree, J. H.; Brekelmans, W. A. M.; van Gils, M. A. J.: Comparison of nonlocal approaches in continuum damage mechanics. Comp. & Structures 55(4), 581-588 (1995).

[3]Mazars, J. Application de la mécanique de l'endommagement au comportement non lineaire et à la rupture du béton de structure. PhD thesis, Université Paris. Paris, (1984).

[4] Carol, I.; Rizzi, E.; Willam, K.: A unified theory of elastic degradation and damage based on a loading surface. Int. Journal of Solids and Structures 31(20), 2835-2865 (1994).

[5] Penna, S. S.: Formulação multipontecial para modelos de degradação elástica – Unificação teórica, proposta de novo modelo, implementação computacional e modelagem de estruturas de concreto. PhD thesis, Federal University of Minas Gerais. Belo Horizonte (2011).

[6] Pereira, L. R. S.: Formulação de modelos de dano tensorial para análise fisicamente não linear de estruturas de concreto submetidas a carregamentos monotônicos e cíclicos. Masters dissertation, Federal University de Minas Gerais. Belo Horizonte (2020).

[7] Petersson, P. E.: Crack growth and development of fracture zones in plain concrete and similar materials. Division of building materials, Lund Institute of Technology, Lund Sweden, 28 TVBM-1006 (1981).

ACKNOWLEDGMENTS

The authors are grateful for financial support from the Brazilian agency CNPq, in Portuguese "Conselho Nacional de Desenvolvimento Científico e Tecnológico" – (CNPq - grant nº 311663/2017-6).

Calibration of Water Distribution Systems Hydraulic Models Using Nature Inspired Algorithm

J. Jafari-Asl[a], M. Ben Seghier[b,c*], S. Ohadi[a], Hermes Carvalho[d], Jose A. F. O. Correia[e]

[a]*Department of Civil Engineering, University of Sistan and Baluchestan, Zahedan, Iran.*
[b]*Department, University, Country Division of Computational Mathematics and Engineering, Institute for Computational Science, Ton Duc Thang University, Ho Chi Minh City, Vietnam*
[c] *Faculty of Civil Engineering, Ton Duc Thang University, Ho Chi Minh City, Vietnam*
[d] *Department of Structural Engineering, Federal University of Minas Gerais, Belo Horizonte, Brazil*
[e]*INEGI, Faculty of Engineering, University of Porto, Rua Dr. Roberto Frias, 4200-465 Porto, Portugal*
**Corresponding author: benseghier@tdtu.edu.vn*

Keywords: Water distribution systems; Calibration; Hydraulic models; Meta Heuristic methods

ABSTRACT

Today, the use of computer models for the hydraulic simulating of flow in the water distribution systems is widely used and plays an effective role in the evaluation and management of the water distribution systems. The success of this hydraulic modeling of water distribution networks is associated with the ability of these models to represent real systems accurately. Therefore, in order to improve the performance of the model and reduce the effect of uncertainties on different conditions of consumption in water distribution systems, the practice of the calibration of the model is essential. In this research, the calibration process was performed by optimizing an objective function and considering some of the constraints. To solve this problem, an optimization-simulation model based on nature-inspired algorithm is utilized. Thus, the meta-heuristic optimization algorithm was integrated into the MATLAB environment and coupled with the EPANET model's hydraulic simulator. The Hazen-Williams coefficients are considered as decision variables, in different consumption scenarios, the model was calibrated to minimize the error between the observed and calculated pressure values. The results showed the efficiency of the proposed method based on several comparative criteria.

Experimental calibration and validation of a freight wagon numerical model under real operating conditions

C. Bragança[a*], J. Neto[b], N. Pinto[b], D. Ribeiro[c], H. Carvalho[a], R. Calçada[b]

a Department of Structural Engineering, Federal University of Minas Gerais, Belo Horizonte, Brazil
b CONSTRUCT - LESE, Faculty of Engineering, University of Porto, Porto, Portugal
c CONSTRUCT - LESE, School of Engineering, Polytechnic of Porto, Porto, Portugal
**Corresponding author: cassioscb@ufmg.br*

Keywords: freight wagon, dynamic tests, model updating, train-track interaction, validation.

ABSTRACT

This article presents the calibration and validation of a numerical model of a freight wagon based on a dynamic test under real operation conditions. The dynamic test takes place during a regular journey of the train and involved the installation of an on-board monitoring system consisting of a set of accelerometers and LVDTs. The data derived from the dynamic test was used, first, for the identification of the modal parameters of the carbody, namely the frequencies, mode shapes and damping coefficients, and second, to extract the time-histories of accelerations and displacements under operation conditions. A FE numerical model of the freight wagon was developed and calibrated using an iterative methodology by means of a genetic algorithm and based on modal parameters. The methodology proves efficiency and robustness in precisely estimating three numerical parameters, besides a significant upgrade in relation to the numerical model before calibration. Model validation involved the comparison between numerically simulated results, based on a train-track dynamic interaction analysis in the vertical direction, and the experimental observations. An excellent agreement between experimental and numerical after updating time-histories was obtained, especially for the carbody responses, since the dynamic behaviour of this component is governed by lower frequencies (below 3.5 Hz), in which the model calibration process was focused.

Analysis of the influence of the wind models in the train running safety against crosswinds

P.A. Montenegro[a*], R. Heleno[b], H. Carvalho[b], R. Calçada [a]

[a] *CONSTRUCT - LESE, Faculty of Engineering, University of Porto, Rua Dr. Roberto Frias s/n, 4200 465 Porto, Portugal*
[b] *Department of Structural Engineering, Federal University of Minas Gerais, Av. Pres. Antônio Carlos, 6627 - Pampulha, 31270-901, Belo Horizonte, Brazil*
**Corresponding author: paires@fe.up.pt*

Keywords: train running safety; stochastic turbulent mode; discrete gust model; high-speed railways; vehicle-structure interaction.

ABSTRACT

The present paper analyzes the influence of different wind models in the running safety of trains subjected to earthquakes. The analyses are carried out with a vehicle-structure interaction tool, which allows the application of wind loads to moving trains and the evaluation of the contact forces that arise from the contact between wheel and rail. From those forces, it is possible to evaluate the derailment indexes associated with the Nadal, Prud'homme and unloading criteria. The two wind models studied in this article consist of a turbulent wind model, based on stochastically generated wind fields, and the discrete gust model defined in the European Norm called Chinese Hat or European Committee for Standardization (CEN) model. The calculations are carried out taking into consideration bridges with decks located at different heights to understand the accuracy of both models in the analysis of the running safety of trains moving over bridges. Since previous studies showed that the influence of the bridge flexibility in the values of the derailment indexes was low, a simplified model that only takes into account the flexibility of the track is adopted. The results show that the CEN discrete gust model is inaccurate when compared to the more realistic turbulent model as the height above the ground increases, since the former is based on a fixed turbulence intensity corresponding to the ground level, while the latter considers the correct turbulence intensity dependent on the deck elevation. To overcome this drawback present in the normative wind model, an alternative discrete gust model is proposed in order to take into account the deck elevation and the correct turbulence intensity.

ACKNOWLEDGMENTS

This work was financially supported by: Base Funding - UIDB/04708/2020 and Programmatic Funding - UIDP/04708/2020 of the CONSTRUCT - Instituto de I&D em Estruturas e Construções funded by national funds through the FCT/MCTES (PIDDAC); and CAPES - Coordenação de Aperfeiçoamento de Pessoal de Nível Superior - Brazil. The authors would also like to express their gratitude to the FiberBridge – Fatigue strengthening and assessment of railway metallic bridges using fiber-reinforced polymers (POCI-01-0145-FEDER-030103) by FEDER funds through COMPETE2020 (POCI) and by national funds (PIDDAC) through the Portuguese Science Foundation (FCT/MCTES).

Vibration Analysis of Highway Bridges Based on a Progressive Pavement Deterioration Model

A.C. Soares da Silva[a], J.G. Santos da Silva[a*]

[a]*Civil Engineering Postgraduate Programme (PGECIV), State University of Rio de Janeiro (UERJ), Brazil.*
**Corresponding author: jgss@uerj.br*

Keywords: dynamic structural analysis; highway bridges; progressive pavement deterioration.

ABSTRACT

Highway bridges are usually subjected to random dynamic actions of variable magnitude due to vehicles convoys crossing on the bridge pavement deck along their service life. These dynamic actions can generate the nucleation of fractures or even their propagation on the bridge deck structure. In this context, the deteriorated road surface condition of the asphalt pavement represents a key issue to the significant increase of the displacements and stresses values on the highway bridge decks [1].

Having in mind that approaches based on the use of a unique road-roughness level for the entire bridge lifecycle can lead to unrealistic results or over-conservative lifecycles, it is necessary and more realistic to consider the influence of the progressive degradation of the road surface roughness based on the use of a vehicle-bridge interaction model [2, 3]. Considering this fact, the aim of this research work is to develop an analysis methodology to evaluate the displacement and stress values of a steel-concrete composite highway bridge, including the dynamic actions due to vehicles convoy and also the effect of the progressive deterioration of the pavement. The investigated structural model corresponds to a typical steel-concrete composite highway bridge deck, with straight axis, simple supported, and spanning 13.0 m by 40.0 m. The structural system is constituted by four composite girders and a 0.225 m thick concrete slab, see Fig. 1(a). The truck used in this work is presented in Fig. 1(b), being one of the most common vehicles in the roads of Brazil.

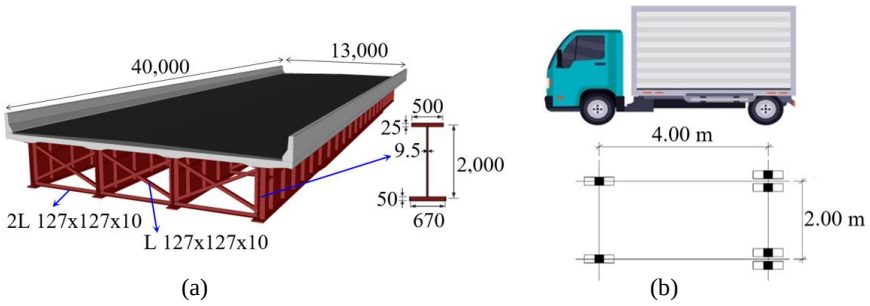

Fig. 1. Investigated simply supported steel-concrete highway bridge and the two axle truck prototype model.

Aiming to study the dynamic behaviour of the bridge, based on the analysis of displacement spectra, see Fig. 2, the vehicles convoys were positioned based on three different positions, the velocity varies from 20 to 80 km/h, and three levels of traffic increase were considered (α = 0%, α = 3%, α = 5%). This way, the main conclusions of this investigation have indicated that the road-roughness condition influences directly the dynamic structural response of the bridge, and along the time the more deteriorated road condition induces a larger vertical translational displacement which leads to a bigger stress values. Based on the increase of the traffic rates (α = 0% to 5%), it must be emphasized that the vertical translational displacement were considerably higher, representing a relevant increase up to four times.

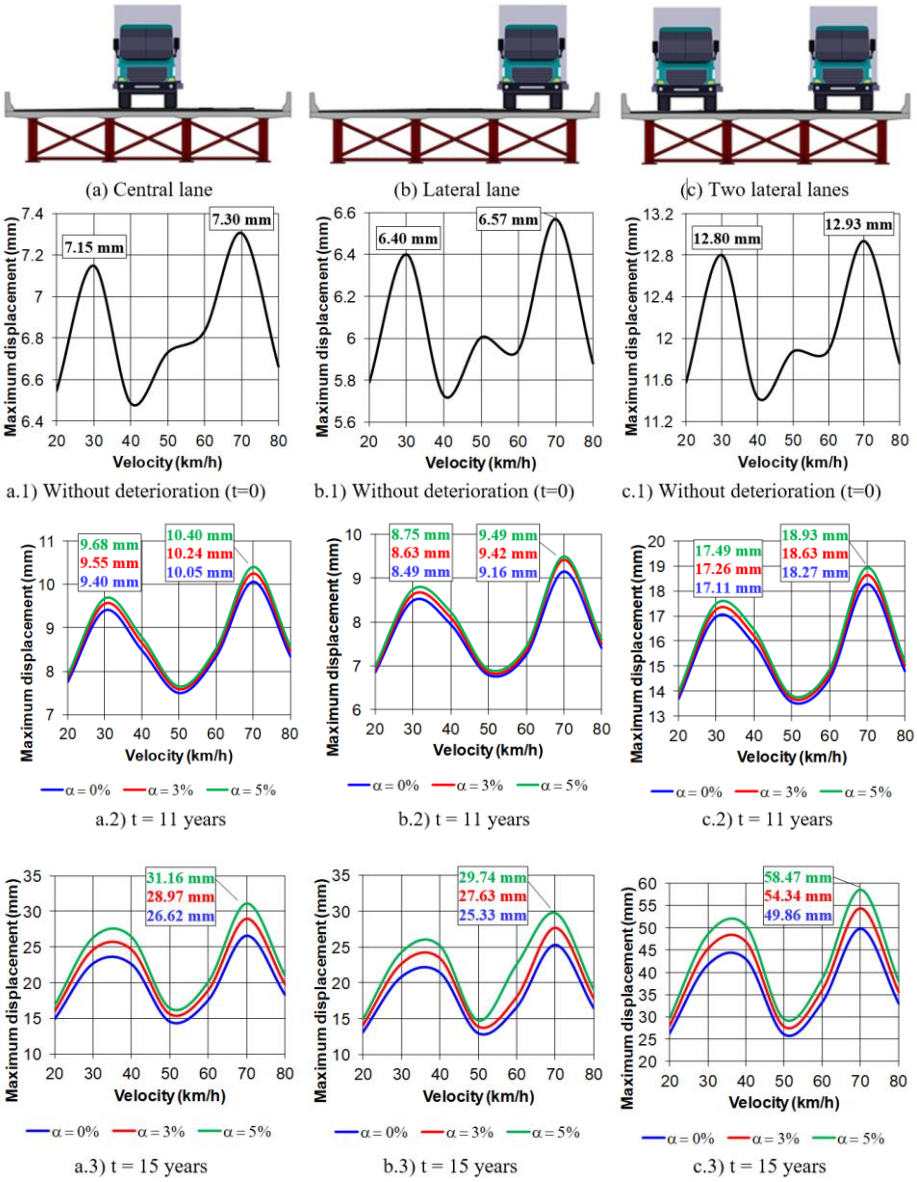

Fig. 2. Response spectra: translational vertical displacement values.

REFERENCES

[1] Silva, A.C.S.: Dynamic analysis of steel-concrete composite highway bridge decks considering the effect of the progressive degradation of the road surface roughness. MSc. Dissertation (In Portuguese), State University of Rio de Janeiro (2020).

[2] Zhang, W., Cai, C.S.: Fatigue reliability assessment for existing bridges considering vehicle speed and road surface conditions. Journal of Bridge Engineering 17(3), 443–453 (2012).

[3] Zhang, W., Cai, C.S.: Reliability-based dynamic amplification factor on stress ranges for fatigue design of existing bridges. Journal of Bridge Engineering 18(6), 538–552 (2013).

ACKNOWLEDGMENTS

The authors gratefully acknowledge the financial support for this research work provided by the Brazilian Science Foundation's CNPq, CAPES and FAPERJ.

Crashworthiness performance simulation of additively manufactured thin-walled tubular impact absorbers filled with lattice structures.

Vinícius Veloso[a]

[a]*olytechnic Institute, Mechanical Engineering Department, Centro Universitário UNA, Brazil*
vinivel@hotmail.com

Keywords: impact absorption; filled tube; lattice material; additive manufacturing; crashworthiness.

ABSTRACT

Impact absorbers are structural members dedicated to reduce the effects of impact loads on structures, protecting occupants and/or loads. Thin-walled tubes are largely used as impact absorbers in a wide range of applications, like road vehicles, rail and aerospace applications. Lightweight, compact size and highly energy absorption efficiency are some of the advantages of this type of structural members. The impact energy is dissipated by the progressive buckling of the tube, and the efficiency is generally correlated to shape, material properties and impact load nature [1]. The use of fillers, like Foams, cellular structures, lattice metamaterials, is widely investigated, as a way to improve energy absorption efficiency of tubular absorbers [2,3]. Lattice structures are constituted by connected unit cells forming a space structure. The dimensions of unit cells can vary from small scale (foams) to large scale cells used in structural infills. This type of structure is very customizable, and can be tuned to provide enhanced energy absorption characteristics, with lightweight design [4,5]. In other hand, lattice structures also involve complex geometries that are hard (or even impossible) to obtain by use of conventional manufacture procedures. Additive manufacturing techniques, otherwise, can be used to obtain complex lattice structures due the increased control of geometry during layer-by-layer construction. In other hand, material characteristics are affected by the parameters used during additive manufacturing process, and the material models may also consider the adopted manufacture process.

In this study, the effects of the inclusion of squared lattice material inside of a tubular energy absorber was evaluated using finite element analysis simulation. The lattice cell size of the infill was varied and crashworthiness efficiency of the absorbers was compared to an empty tube version (figure 1).

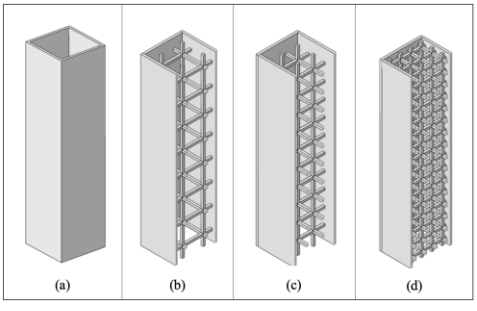

Fig. 1**.** Tube configurations tested (empty tube (a) and filled, 10mm cell (b), 7.5mm cell (c) and 5mm cell (d)).

The tubes were positioned between a fixed rigid plate and a moving rigid wall. A 250kg mass was associated to the rigid wall, that impacted longitudinally the tube at 10m/s velocity.

The analysis was accomplished using Abaqus Explicit, and the material adopted to impact absorber was a literature-based addictive manufactured (Selective Laser Melting) AlSi10Mg alloy [6]. Johnson Cook material model was used to predict material response during plastic deformation, considering material hardening, strain rate sensitivity and thermal effects. Johnson Cook damage model was also applied to the model. Initial geometric imperfections are also a factor that can interfere in the buckling behaviour of the tube, and they were also considered in the model [7].

The results pointed to an increase in crashworthiness efficiency with the inclusion of lattice structured infill. The infill density affected crushing mode (figure 2) and directly influenced energy absorption efficiency of tubes. A comparison between empty tube and 7.5mm cell

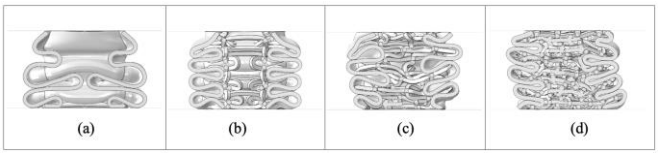

Fig. 2. Crushed tubes after 6ms impact load (empty tube (a), 10mm cell (b), 7.5mm cell (c) and 5mm cell (d)).

All lattice filled samples presented superior energy absorption capacity before densification (EA) than empty tube. The denser infill presented higher total energy absorption before densification occurs. Infill density directly affected peak crush force (PDF) and mean crush force (MCF) during crushing. These results are presented in table 1.

Table 1. Crashworthiness parameters of simulated impact absorbers.

1. Configuration	Lattice cell size (mm)	PCF (kN)	MCF (kN)	EA (kJ)
empty	N/A	27.2	12.1	0.57
C5	5	34,3	21.6	0.97
C75	7.5	29,9	17.2	0.96
C10	10	28.4	15.0	0.74

REFERENCES

[1] Baykasoglu,C., Cetin, M.T.: Energy absorption of circular aluminium tubes with functionally graded thickness under axial impact loading. International Journal of Crashworthiness, 20(1), 95-106 (2015).
[2] Zarei, H., Kröger, M.: Optimum honeycomb filled crash absorber design. Materials & Design, 29(1), 193-204 (2008).
[3] Chen, Y., Li, T., Scarpa, F., Wang, L.. Lattice Metamaterials with Mechanically Tunable Poisson's Ratio for Vibration Control. Physical Review Applied, 7(2), 02412 (2017).
[4] Cetin, M.T., Baykasoglu,C.,: Crashworthiness of graded lattice structure filled thin-walled tubes under multiple impact loadings. Thin-walled structures, 154, 10684 (2020).
[5] Pan, C.; Han, Y.; Lu, J. Design and Optimization of Lattice Structures: A Review. Applied Sciences, 10, 6794 (2020).
[6] Racholsan Raj Nirmal, B. S. V. Patnaik, R. Jayaganthan. Numerical Simulation on Deformation Behaviour of Additively Manufactured AlSi10Mg Alloy. International Journal of Mechanical and Materials Engineering, 14(10), 445-450 (2020).
[7] Nagel, G.M., Thambiratnam, D. P. Dynamic simulation and energy absorption of tapered thin-walled tubes under oblique impact loading. International Journal of Impact Engineering, 32 (10), 1595-1620 (2006).

Dynamic Structural Response of Buildings under Longitudinal and Transversal Wind Actions

L. de S. Bastos[a], J.C. Mota Silva[a] and J.G. Santos da Silva[a*]

[a]*Civil Engineering Postgraduate (PGECIV), State University of Rio de Janeiro (UERJ), Brazil.*
**jgss@uerj.br*

Keywords: tall buildings; modified spectral representation; wind dynamic actions; human comfort.

ABSTRACT

In the last few decades, Brazilian cities have presented substantial growth in relation to the design and construction of tall and slender buildings. However, this architectural trend has produced flexible structural systems, with low natural frequency values and, therefore, more susceptible to problems of excessive vibration, arising from the dynamic action of the wind [1-5].

On the other hand, it is important to emphasize that in addition the longitudinal dynamic action of the wind (along-wind), the dynamic actions on the structure in relation to the transversal direction (across-wind), induced by the appearance of vortices should be considered relevant as well. Recent studies have demonstrated that the across-wind action may produce a higher dynamic structural response when compared to the along-wind, which may be determinant for the assessments of service limit state [1-5].

Therefore, this research work aims the assessment of the Modified Spectral Representation Method (SRM-M) developed by Bastos [1], for the evaluation of the dynamic response of buildings when the transversal and longitudinal directions are considered. This analysis methodology simulated the action of the longitudinal (FL) and transversal (FT) wind loadings using the traditional SRM formulation [5], increasing the final dynamic loads based on the coefficients (γ1, γ2, γ3 and γ4), see Fig.1, determined by data obtained through experimental tests in wind tunnels provided by the Tokyo Polytechnic University (TPU-DB) [6].

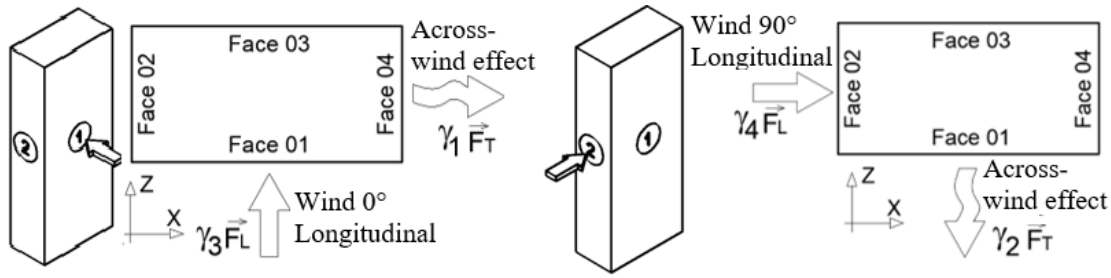

a) Longitudinal wind (wind 0º): largest facade. b) Longitudinal wind (wind 90º): smallest facade

Fig. 1. Dynamic wind load directions and definition of γ coefficients (MRE-M) [1].

This way, eight reinforced concrete buildings (see Fig. 2) are considered in this investigation to evaluate the structures dynamic response having in mind a comparison between the results associated to the longitudinal and transversal accelerations, obtained by the Modified Spectral Representation Method (MRE-M [1]) with those determined by traditional methodologies described in DEDM-HR [7], TPU-DB [6] and MRE [5]. The forced vibration analysis of the investigated buildings will be performed using the eight structural models, see Fig. 2, based on the Finite Element Method (FEM) numerical simulations.

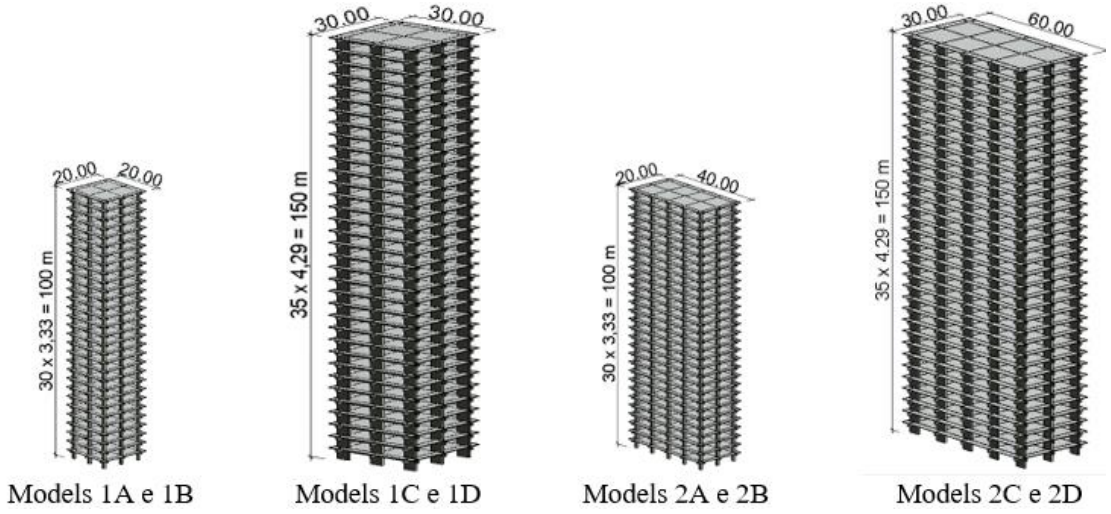

Fig. 2. Investigated reinforced concrete buildings [Group 1 (1A to 1D) and Group 2 (2A to 2D)].

It is important to note that the peak accelerations values determined by the investigated analyses methodologies, based on the use of data from wind tunnels (DEDM-HR and TPU-DB) are quantitatively divergent, revealing the complexity of the assessment. According to the results presented in this research work, it appears that the developed methodology MRE-M [1], qualitatively, presents good results with regard the peak accelerations, both longitudinal and transversal accelerations. It may also be emphasized that in most design situations, the transversal peak accelerations have presented higher values, thus representing a determining factor for the analysis and verification of human comfort in tall buildings.

REFERENCES

[1] Bastos, L. S.: Assessment of the nondeterministic dynamic structural behaviour of tall buildings considering the across-wind effect and the modelling of the soil-structure interaction. PhD Thesis (In Portuguese). In: Civil Engineering Post-Graduate Programme, PGECIV, State University of Rio de Janeiro, UERJ, Rio de Janeiro/RJ, Brazil (2020).
[2] Silva, J. C. M.: Study of nondeterministic dynamic structural behaviour and assessment of human comfort in tall buildings. PhD Thesis (In Portuguese. In development). In: Civil Engineering Post-Graduate Programme, PGECIV, State University of Rio de Janeiro, UERJ, Rio de Janeiro/RJ, Brazil (2020).
[3] Ferrareto, J. A.: Human comfort in tall buildings subjected to wind-induced motion. PhD Thesis (In Portuguese). In: University of São Paulo, USP, São Paulo/SP, Brazil (2017).
[4] Tozan, S., Guler, K., Erkus, B.: Wind comfort assessment of a tall building according to various structural codes. Second Conference on Smart Monitoring, Assessment and Rehabilitation of Civil Structures, 1-8 (2013).
[5] Santos, V. H.: Comparison between the Discrete Method NBR 6123 (ABNT-1988) and the Synthetic Wind Method (FRANCO-1993), for multi-storey reinforced concrete buildings. MSc Dissertation (In Portuguese). In: Civil Engineering Post-Graduate Programme, Federal Technological University of Paraná, UFPR, Curitiba/PR, Brazil (2018).
[6] Aerodynamic Database of High-rise Buildings. [http://www.wind.arch.t-kougei.ac.jp/info_center/windpressure/highrise/Homepage/homepageHDF.htm]. Accessed in 02/24/20221.
[7] Vortex-Winds [http://evovw.ce.nd.edu/dadm_INT/VW_design6_INT1_noauth1.html]. Accessed in 02/24/20221.

ACKNOWLEDGMENTS

The authors gratefully acknowledge the financial support for this investigation provided by Brazilian Science Foundation's CAPES, CNPq and FAPERJ.

Human Comfort Analysis of Steel-Concrete Composite Floors Subjected to Rhythmic Loadings

N.A.C. Branco[a], F.A. de Sousa[a], J.G. Santos da Silva[a*]

[a]*Civil Engineering Postgraduate (PGECIV), State University of Rio de Janeiro (UERJ), Brazil.*
**Corresponding author: jgss@uerj.br*

Keywords: steel-concrete composite floors; dynamic structural analysis; human comfort.

ABSTRACT

Over the last few years, a lot of structural problems associated to excessive vibration of building floor systems when induced by human rhythmic activities have occurred in places such as fitness centres, event halls and offices [1-3]. The resonance phenomenon can occur due to equality (or proximity) between one of the excitation frequencies and the structure natural frequencies.

Having this though in mind, this paper investigated the dynamic structural behaviour of a steel-concrete composite floor when subjected to loadings induced by human rhythmic activities. This work aims to evaluate the human comfort of a structural system that consists on a health club which presents an area used for aerobics activities. The structural system has the dimensions 22.5 m by 14 m and a total area of 315 m². In this study, the dynamic loadings were obtained through dynamic load models such as AISC [4], SCI [5], Faisca [6], and also based on the use of biodynamic systems [7], incorporating the human-structure interaction dynamic effect.

The composite floor numerical model was generated based on usual modelling techniques adopting the mesh refinement present in the Finite Element Method (FEM) and implemented in the ANSYS [8] program. The dynamic response [a_p: peak acceleration; $a_{w,rms}$: RMS acceleration; VDV: vibration dose values], calculated through the consideration of 20 people practicing rhythmic activities on the specified area (see Fig. 1) were compared to the recommended limits presents in the design standards.

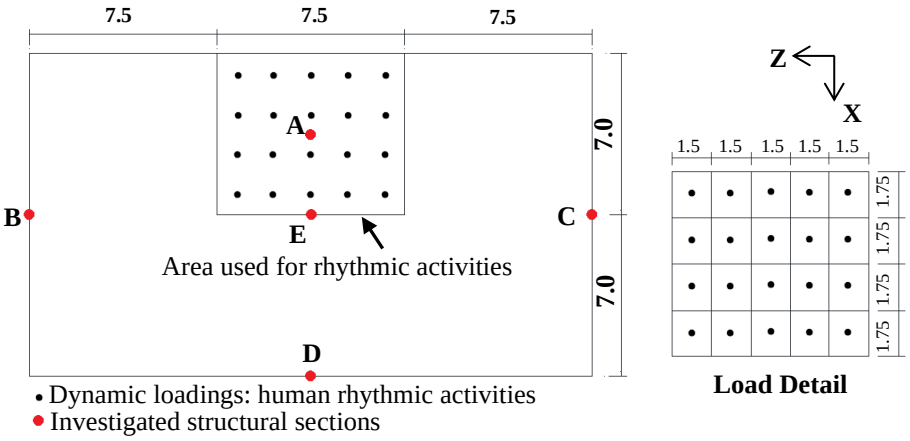

Fig. 1. Dynamic loads of 20 people on the steel-concrete composite floor (units in metres).

This way, after the evaluation of the floor dynamic structural response, considering each loading model [4-7], it was possible to identify the critical sections of the investigated floor and compare the dynamic effects with the design criteria limits developed for ensuring human comfort.

Thus, after the analysis (time and frequency domain), the structural section E presented the higher values when the floor dynamic response was investigated. This way, the accelerations in frequency domain for this critical section (Section E) can be seen in Fig. 2. It must be emphasized that the "only force" loading models [4-6] presents the highest energy peak transfer on the floor dynamic response, due to the direct

impact of the loads on the concrete slab. On the other hand, the biodynamic models [7] considered the dynamic characteristics of the people and the damping contribution of each person, determined experimentally, and this way have produced lower levels of energy transfer to the slab.

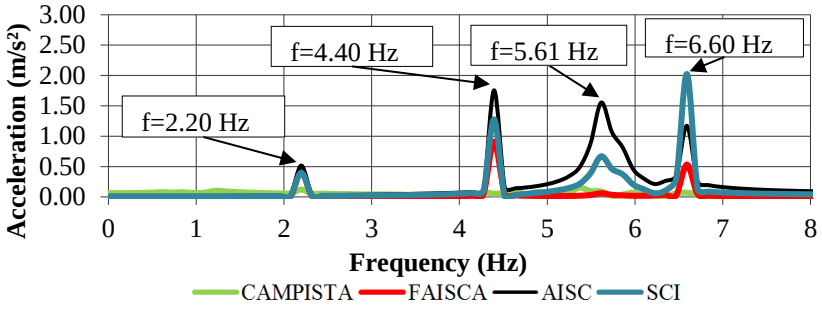

Fig. 2. Accelerations in the frequency domain to the critical section (Structural section E).

On the other hand, the peak accelerations values calculated in the time domain analysis and considering the floor critical section (Section E) is equal to 7.22m/s² (AISC model [4]), 3.92 m/s² (SCI model [5]), 1.24 m/s² (Faisca model [6]), and 0.68 m/s² (Campista model [7]). It is important to mention that all dynamic loading models led to peak accelerations values higher than the recommended tolerance ($a_p \leq 0.50$ m/s²). Nevertheless, based on the human comfort criteria, the investigated steel-concrete composite floor presents excessive vibration and user's discomfort.

REFERENCES

[1] Sousa, F. A.: Analysis of the dynamic structural response of building floors subjected to rhythmic human activities based on the use of biodynamic systems (In Portuguese. In development). PhD Thesis. In: Civil Engineering Post-Graduate Programme, PGECIV, State University of Rio de Janeiro, UERJ, Rio de Janeiro/RJ, Brazil (2021).

[2] Sousa, F. A., Aguiar, J. V., Branco, N. A. C., Silva, J. G. S.: Dynamic experimental monitoring and numerical analysis of floors subjected to human activities. In: Congress on Computational Methods in Engineering, ISSN 2675-6269, Foz do Iguaçu/PR, Brazil (2020).

[3] Lee, K., et al.: Global vertical resonance phenomenon between steel building and human rhythmic excitations. Journal of Constructional Steel Research, v. 92, p. 164–174 (2014).

[4] Murray, T. M., et al, T.: Vibrations of Steel-Framed Structural Systems Due to Human Activity. 2nd Edition. DG11. Chicago, USA (2016).

[5] Smith, A. L., Hicks, S. J, Devine, P.J.: Design of floors for vibrations: A new approach, p354. In: The Steel Construction Institute (SCI), Ascot (2009).

[6] Faisca, R. G.: Characterization of Dynamic Loads due to Human Activities (in Portuguese), pp. 1-240. PhD Thesis. In: COPPE/UFRJ, Rio de Janeiro, RJ, Brazil (2003).

[7] Campista, F. F.: Modelling of biodynamic systems for evaluation of the dynamic structural behaviour of steel concrete composite building floors subjected to human rhythmic activities (in Portuguese). PhD Thesis Civil Engineering Post-Graduate Programme, PGECIV. State University of Rio de Janeiro, UERJ. Rio de Janeiro/RJ, Brazil (2019).

[8] Ansys. Swanson Analysis Systems, Inc., P.O. Box 65, Johnson Road, 15342-0065, Version 10.0, Basic analysis procedures, Second edition, Houston, PA (2010).

ACKNOWLEDGMENTS

The authors gratefully acknowledge the financial support for this research work provided by the Brazilian Science Foundation's CNPq, CAPES and FAPERJ.

Human comfort assessment of steel-concrete composite floors of buildings

B. Ferreira[a*], H. Carvalho[b], J. Silva[c], R. Caldas[b], J. Aguiar[c], T. Bittencourt

[a]*Departamento de Engenharia Civil, Universidade de São Paulo, Brazil*
[b]*Departamento de Engenharia de Estruturas, Universidade Federal de Minas Gerais, Brazil*
[c]*Faculdade de Engenharia, Universidade do Estado do Rio de Janeiro, Brazil*
[d]*Departamento de Estruturas e Geotecnia, Universidade de São Paulo, Brazil*
**Corresponding author: barbara.elisaf@usp.br*

Keywords: human comfort assessment; experimental dynamic analysis; numerical modelling; composite floor.

ABSTRACT

Steel and concrete composite structures have been consolidated as a strong technological alternative in the Brazilian civil construction scenario, being increasingly adopted in commercial, parking, and residential buildings. On the other hand, with the emergence of materials with greater resistance, it has become increasingly feasible to reduce the total height of a composite floor system, seeking useful space improvement. However, this trend implies in reducing the system's stiffness, making these structures increasingly susceptible to the effects of dynamic loads induced by human activities, causing discomfort to users or even structural problems [1-2]. This research work aims to investigate the dynamic structural response of steel-concrete composite floors, from the point of view of human comfort, when subjected to human walking. The analysed structural model corresponds to a steel-concrete composite floors system, used for school occupancy, presenting a total area of 1300 m², being supported by composite columns, with a ceiling height of 3.40m [3]. The numerical model (Fig. 1) developed for the dynamic analysis of the floor adopts usual mesh refinement techniques present in the FEM and implemented in the ANSYS program. Next, free vibration tests were carried out to obtain the modal parameters of the structure. Forced vibration tests with excitation caused by a person walking at different step frequencies and directions were performed to determine de maximum structure's response (Fig. 2). Grounded on the developed analysis methodology, the dynamic experimental response values of the floors were compared with the results obtained through the numerical model, with the results obtained based on the analytical formulation (Table 1) and with the limits proposed by AISC practical design guide, aiming at the structure's performance evaluation with regard to human comfort (Table 2).

Through Table 1 it is noted that the experimental results obtained for the floors show a satisfactory agreement when compared to the numerical results, with differences between 0.15% and 3.33%, which indicates that the structural model under study is well calibrated and able to represent the structure behaviour. However, when the experimental and numerical results were compared to the analytical ones, larger differences in the order of 41% to 50% were observed. This fact can be perfectly explained by the fact that the analytical expressions of AISC DG 11 [4] assumes that each floor slab panel behaves, in a simplified way, as a system with one degree of freedom, which does not correspond exactly the reality. Analysing Table 2 it can be noted that the proposed human comfort criteria AISC DG 11 [4] was met considering a person action over the studied floors. This way, this investigation emphasizes the importance of the structural engineers to be knowledgeable about the activities performed on the structural system, aiming the development of a rational and optimized project, according to current procedures foreseen in the standards and design recommendations based on human comfort criteria.

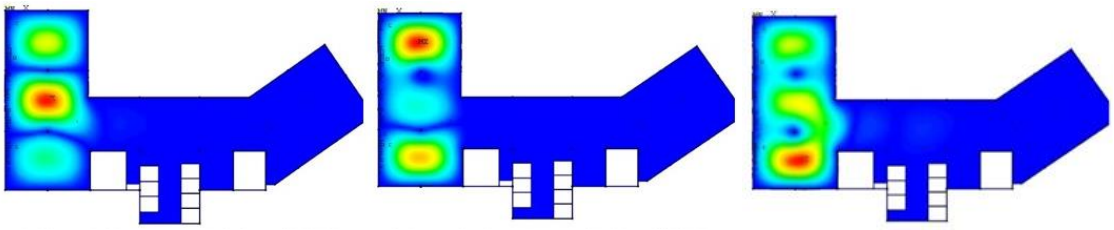

a) f_{01} = 5,71 Hz b) f_{02} = 6,49 Hz c) f_{03} = 6,87 Hz

Fig. 1. Threes first vertical bending vibration modes of the floors under study.

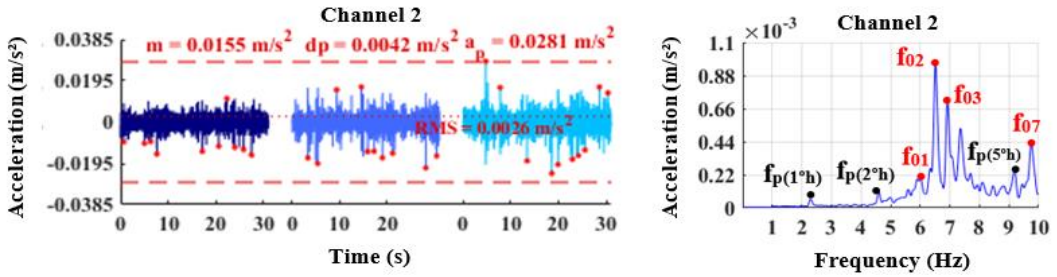

Fig. 2. Example of dynamic response from floor for normal walking on a random trajectory (floor 1).

Table 1. Comparison between the natural frequency values obtained.

Mode	Natural Frequency (Hz)			Difference (%)		
	Numerical (Ansys)	Experimental Test	Analytical (AISC)	Numerical x Experimental	Numerical x Analytical	Experimental x Analytical
1º	5.71	5.90	3.36	3.33	41.16	43.05
2º	6.49	6.50	3.31	0.15	49.00	49.08
3º	6.87	6.97	3.48	1.46	49.34	50.07

Table 2. Human comfort analysis through experimental acceleration analysis.

Experimental test	Peak Acceleration (m/s²)	Human comfort AISC [7]
Floor 1 test: normal walking	0.028	Acceptable
Floor 2 test: normal walking	0.031	Acceptable
Floor 3 test: normal walking	0.024	Acceptable

REFERENCES

[1] Nguyen, H. A. T., “Walking induced floor vibration design and control,” Ph.D. thesis, Fac. Eng. Ind. Scienc. Swinburne Univ. Tec., Melbourne, Australia, 2013.

[2] Berczynsky, S., Wroblewski, T., "Experimental verification of natural vibration models of steel-concrete composite beams," J. Vib. Control, vol. 16, pp. 2057–2081, 2010. http://dx.doi.org/10.1177/1077546309350552.

[3] Ferreira, B. E., “Análise numérico-experimental de vibrações induzidas pelo caminhar humano sobre pisos mistos (aço-concreto),” M.S. thesis, Univ. Fed. Minas Gerais, Belo Horizonte, Brasil, 2020.

[4] Murray, T. M., Allen, D. E., Ungar, E. E., Davis, D. B., Vibrations of Steel-Framed Structural Systems Due to Human Activity, 2nd ed. USA: AISC, 2016.

ACKNOWLEDGMENTS

The authors thank for the financial support provided by the country's research funding agencies, CAPES and FAPERJ, which make this study possible.

Application of Sandwich Panels in Steel Structures

Aditya Vidwans[1,*], José A.F.O. Correia[1,2]

[1] *Department of Civil Engineering and Geosciences, Delft University of Technology, Netherlands*
[2] *CONSTRUCT, Faculty of Engineering, University of Porto, 4200-465 Porto, Portugal*
** Corresponding author: aditya.vidwans94@gmail.com*

Keywords: Sandwich Panel; FEM; Lightweight Structure; Extra High Strength Steel; Material Models.

ABSTRACT

In steel structures, a lot of attention is paid to lightweight structures, i.e. reduction of dead load without compromising structural safety, integrity, and performance as well as cost-effectiveness. Thanks to modern steel aluminium sandwich panel manufacturing technology a new possibility became available for lightweight structural design. The most simple type of sandwich panel consists of two strong, stiff, thin plates/sheets of highly dense material separated by a thick layer of low-density material that can be much less strong and stiff [1]. Figure 1 shows an idea of a sandwich panel. Some advantages of sandwich panel are high bending stiffness, high load carrying capacity and high strength to weight ratios, reduction in the cost of formwork & foundation, and high structural efficiency [2].

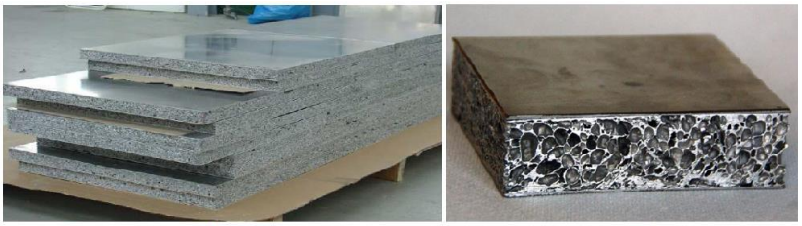

Figure 1. Steel aluminium foam sandwich panel [3][4].

The objective of this study is to evaluate the application of sandwich panels in the construction of steel structures with the aim of weight reduction without affecting other parameters like safety, performance, cost, etc. In this study, both column and plate buckling theories are considered and applied to the sandwich panel to evaluate its behaviour under in-plane compressive load. Effects of various material models and imperfections on buckling strength of sandwich panel are evaluated. Material models used in this study for steel are bilinear material mode which is option 'c' and the true stress-strain curve which is option 'd_1' in Figure 2. For aluminium foam, bilinear material model with no strain hardening is considered. Option 'a', Figure 2, gives an idea of the material. Both local and global imperfections, modelled by ANSYS software [5], are considered in this study, as shown in Figure 3 and Figure 4, respectively.

In this study, stiffened plate and sandwich panel are compared in terms of buckling resistance and self-weight. Three different sandwich panels made from faceplates of steel grade, S355, S690 & S1100, are used for the replacement of the S355 stiffened plate. Efforts were made to understand the effect of various physical parameters on buckling resistance of sandwich panel in both column and plate buckling theories. Finally, as a case study, sandwich panel technology is used to redesign the Huisman structure [6]. The objective is to investigate whether applying sandwich panels in redesign makes it possible to obtain a sufficient weight reduction without losing its performance. For this case study, sandwich panels with faceplates of steel grade S355, S690, and S1100 are used. The static and buckling strength of the new design is evaluated. Also, the cost of the new design and original design is evaluated and results are compared. Cost analysis is done to evaluate whether a sandwich panel is an economical solution. The findings of this study are that in the future it is possible to use sandwich panels in steel structures to save a significant amount of weight while taking considerations into account. Sandwich panels can be successfully used to replace stiffened plates. Sandwich panels with faceplates made from extra high strength steel can give significant weight reduction. But the use of sandwich panels also increases the overall cost of the structure. So in terms of costs, it is questioned whether or not using sandwich panels is economically beneficial.

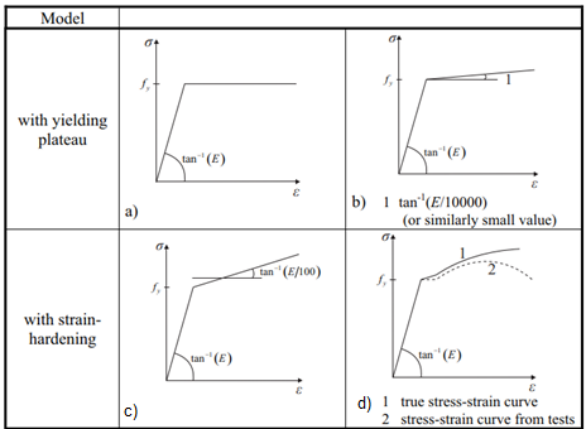

Figure 2. Modelling of material behaviour (from EN 1993-1-5) [7][8].

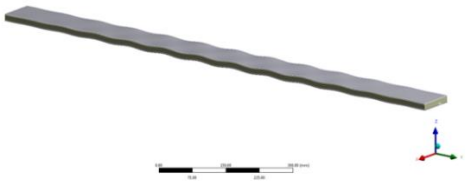

Figure 3. Local geometric imperfection

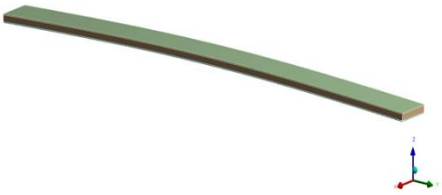

Figure 4. Global geometric imperfection

REFERENCES

[1] ANALYSIS AND DESIGN OF STRUCTURAL SANDWICH PANELS by HOWARD G. ALLEN Senior Lecturer, Dept. of Civil Engineering, University, Southampton.
[2] S. Belouettar, A. Abbadi, Z. Azari, R. Belouettar, P. Freres, "Experimental investigation of static and fatigue behaviour of composite honeycomb materials using four point bending tests", Composite Structures, vol. 87, no. 3, pp. 265-273,2008.
[3] Local buckling strength of steel foam sandwich panels by S Szyniszewski, BH Smith, JF Hajjar, SR Arwade, BW Schafer, Hopkins University, University of Massachusetts, Northeastern University.
[4] Innovative lightweight constructions of aluminum foam, Havel Metal Foam, Germany.
[5] ANSYS Theory Reference release 5.6.
[6] Huisman Design Report of Huisman Structure.
[7] Baumeister, J. Verfahren zur Herstellung poroser Metallkorper, German Patent DE 4018360 Cl (1991).
[8] Baumeister, J., v. Hagen, H., Hatzfeld D., Paschen, M., Weber, M.: Werkstoffpriifung an neuartigen Sandwich-Verbundwerkstoffen aus Stahldeckblechen mit Aluminiumschaum-kern, Proceedings 11. Aachener Stahlkolloquium, 20.-21.6.1996, Aachen, p. 169/176.

ACKNOWLEDGMENTS

This study was supported by Delft University of Technology (TUDelft) and Huisman Equipment. Many thanks to Prof. Dr. Milan Veljkovic, Dr. Henk den Besten, Haohui Xin, Ir. Eric Romeijn and Jaap Overal for their guidance and support. Also, thanks to Ben van de Geer, Alexander Richter & Havel Metal Foams for providing all the information related to the sandwich panel which was required for this study as well as giving me an opportunity to visit their production facility which was an enriching experience.